MARMARA UNIVERSITY
INSTITUTE FOR GRADUATE STUDIES
IN PURE AND APPLIED SCIENCES

USE OF ENGINEERED NANOPARTICLES IN NITROGEN AND PHOSPHORUS RECOVERY FROM AQUEOUS SOLUTIONS

BÜŞRA KARA

MASTER THESIS

Department of Environmental Engineering

Thesis Supervisor

Assoc. Prof. Dr. Neslihan SEMERCİ

ISTANBUL, 2023

MARMARA UNIVERSITY

INSTITUTE FOR GRADUATE STUDIES IN PURE AND APPLIED SCIENCES

USE OF ENGINEERED NANOPARTICLES IN NITROGEN AND PHOSPHORUS RECOVERY FROM AQUEOUS SOLUTIONS

BÜŞRA KARA

(524318007)

MASTER THESIS

Department of Environmental Engineering

Thesis Supervisor

Assoc. Prof. Dr. Neslihan SEMERCİ

ISTANBUL, 2023

ACKNOWLEDGEMENT

Firstly, I would like to express my appreciation to my supervisor Assoc. Prof. Dr. Neslihan SEMERCİ, who showed me an interesting, new and rarely known research topic that I gained lots of knowledge and experience. I am thankful for her to guide and support me, moreover share her knowledge.

I would like to express my thanks to Assist. Prof. Dr. Seval GENÇ to help in the synthesis and characterization of magnetic activated nanoparticles. I am thankful to Prof. Dr. Zehra Semra CAN, who shared her vast knowledge with me while conducting laboratory experiments.

I would like to thank members of thesis committee, Prof. Dr. Zehra Semra CAN and Prof. Dr. Erkan ŞAHİNKAYA for their valuable contributions.

Last but not least, I would like to express my endless thanks to my entire KARA and TERZİEROL family members for their support, guidance and love. And a very special thanks to my husband Güvenç TERZİEROL and my cat OSMAN for not allowing me to give up when the going gets tough. They have always been with me.

January 2023 **Büşra KARA**

TABLE OF CONTENTS

ACKNOWLEDGEMENT i
TABLE OF CONTENTS ii
ABSTRACT iv
ÖZET vi
SYMBOLS viii
ABBREVIATIONS x
LIST OF FIGURES xi
LIST OF TABLES xiv
1. INTRODUCTION 1
1.1. Nitrogen and Phosphorus: As Essential Nutrients to Life 1
1.1.1. Nitrogen cycle 1
1.1.2. Phosphorus cycle 3
1.2. Impacts of Heavy Nitrogen and Phosphorus Loads in Water Bodies 5
1.2.1. Eutrophication 5
1.3. Controlling the Water Contamination Caused by Heavy Nutrient Loads 6
1.3.1. Ammonia and phosphate removal techniques 7
1.3.2. Current phosphate removal techniques 9
1.3.3. Simultaneous ammonia and phosphate recovery 10
1.4. Adsorption Theory 12
1.5. Types of Adsorptions 14
1.5.1. Physisorption 14
1.5.2. Chemisorption 14
1.5.3. Ion (exchange) adsorption 16
1.6. Factors Affecting Adsorption 17
1.7. Engineered Nanoparticles 19
1.7.1. Engineered magnetic iron oxide nanoparticles 22
1.7.2. Engineered magnetite nanoparticles 24
1.7.3. Engineered magnetic activated carbon (PAC-MNP) composite nanoparticles 25
1.8. Importance of Crucial Nitrogen and Phosphorus Nutrients' Recovery 29
2. MATERIALS AND METHODS 31
2.1. Materials 31
2.1.1. Preparation of synthetic wastewater 31
2.2. Methods 31

2.2.1. Synthesis of bare and composite magnetic nanoparticles 31
2.2.2. Physicochemical characterization of PAC-MNPs 33
2.2.3. Adsorption experiments 35
2.2.4. Desorption experiments 37
2.2.5. Analytical - experimental measurements 38
2.2.6. Conducting the studies of kinetics and isotherm models 38
3. RESULTS AND DISCUSSION 41
3.1. Characterization of The PAC-MNPs 41
3.1.2. BET results 43
3.1.3. FT-IR results 44
3.1.4. SEM results 46
3.1.5. EDX results 47
3.2. Adsorption Performance 49
3.2.1. Adsorption isotherm experiment – equilibrium tests 49
3.2.2. Adsorption kinetics tests 51
3.2.3. Effect of pH 53
3.2.4. Effect of adsorbent dosage 55
3.2.5. Comparing the adsorption performance of Functionalized$_{HCl}$-PAC and PAC-MNPs 56
3.3. Desorption Experiments 57
3.3.1. Desorption of N and P 57
4. CONCLUSIONS 63
REFERENCES 66
CURRICULUM VITAE 84

ABSTRACT

USE OF ENGINEERED NANOPARTICLES IN NITROGEN AND PHOSPHORUS RECOVERY FROM AQUEOUS SOLUTIONS

Nitrogen and phosphorus are important elements for all living things and also play a critical role in fertilizers used in agriculture. On the other hand, due to the threat of eutrophication as a result of the uncontrolled access/discharge of nitrogen and phosphorus to natural water resources above the limit values, they also play an extremely important role in the fight against environmental pollution and wastewater management. When considered the necessity of the nutrients to living species as well as their excessive amounts somehow occurring in water bodies are considered, the control and management of these nutrients, especially in wastewater, should be evaluated in a more sustainable way. As these nutrients are inevitably found in wastewater, it would be wiser to conceive them as fertilizer "raw material" and recycle them, rather than evaluating as "waste" and disposing them. Especially since phosphorus is a non-renewable and limited resource, it is extremely valuable beyond characterizing it as waste. In this respect, phosphorus minerals (phosphate rocks) are included in the critical raw material list published by the European Commission. On the other hand, ammonia, as the most important form of nitrogen, is required for the production of nitrogen-based fertilizer as the second most produced industrial chemical in the world, although it is not included in this list. As a result, studies to be carried out for the recovery of both ammonia and phosphate rather than their disposal should be considered in this regard.

This study was conducted to investigate the effectiveness of using modified activated carbon magnetic nanoparticles (composite PAC-MNPs) in ammonia-nitrogen and phosphorus recovery. From this point, it was intended to recover the secondary ammonia and phosphorus sources by simulating the effluents obtained from B-stage of High Rate Activated Sludge (HRAS) systems. In the scope of the study, batch experiments were carried out for adsorption studies within the initial concentration range of 50 to 1000 mg/L from an aqueous solution (N-P solution). Powdered activated carbon was modified with strong hydrochloric acid (functionalized$_{HCl}$ – PAC) and then impregnated with magnetite

nanoparticles (MNPs) by “co-precipitation” method. For PAC-MNP characterization, Potentiometric Titration, Zeta Potential, SEM, EDX, FTIR, and BET measurements were performed. These experiments proved that Composite PAC-MNP is effective in simultaneous adsorption of ammonia-nitrogen and phosphate species.

Equilibrium studies showed that the synthetically prepared N-P solution was consistent with the Freundlich isotherm model for ammonia-nitrogen and Redlich-Peterson for phosphate ions. As a result of the kinetic studies of the synthetic N-P solution, it was determined that ammonia was consistent with the Psedou-Second Order and Phosphate was consistent with the Elovich models. The highest adsorption capacity was achieved to be 21.74 mg/g for phosphate, 15.05 mg/g for ammonia at pH 10 by employing 0.3 g PAC-MNPs to N-P solution prepared as 1000 mg/L. For the desorption experiment of N and P species from the surface of PAC-MNP for 1-hour and until four cycles, different electrolyte solutions were tried, but it was determined that the most appropriate solution was 1 M NaOH.

According to the results of the study, it is considered that the adsorption method is a sustainable and effective method for the control of ammonia and phosphate in wastewater as well as their conversion to struvite as nutrient source.

Keywords: Activated carbon, Magnetic composite nanoparticles, Ammonia removal, Ammonia recovery, Phosphate removal, Phosphate recovery, Adsorption, Zeta potential

ÖZET

SULU ÇÖZELTİLERDEN AZOT VE FOSFOR GERİ KAZANIMINDA TASARIMLANMIŞ NANOPARÇACIKLARIN KULLANIMI

Azot ve fosfor tüm canlılar için önemli elementlerdir ve aynı zamanda tarımda kullanılan gübreler açısından da kritik role sahiptir. Buna karşın azot ve fosforun sınır değerlerinin üzerinde doğal su kaynaklarına kontrolsüzce erişmesi/deşarj edilmesi sonucu ötrofikasyon tehdidi nedeniyle çevre kirliliği ile mücadele ve atıksu yönetiminde de rolleri son derece büyüktür. Dolayısıyla hem canlıların ihtiyaç duyması sebebiyle hem de gereğinden fazlasının yine canlıya ve doğaya zarar vermesi açısından ele alındığında bu besin elementlerinin özellikle atıksulardaki kontrolü ve yönetimi daha sürdürülebilir bir boyutta değerlendirilmelidir. Bu besin elementleri kaçınılmaz olarak atık sularda bulunduğundan, "atık" statüsü ile değerlendirerek bertarafına yoğunlaşmak yerine, gübre "hammaddesi" olarak ele alıp onları geri kazanmak çok daha akıllıca olacaktır. Özellikle fosfor yenilenemez ve sınırlı bir kaynak olduğundan atık olarak nitelendirmenin ötesinde son derece değerlidir. Bu bakımdan fosfor mineralleri (fosfat kayaçları) Avrupa Komisyonu tarafından da yayınlanan kritik hammadde listesinde yer almaktadır. Öte yandan azotun en önemli formu olarak amonyak ise, bu listede yer almasa da dünya genelinde en çok üretilen ikinci endüstriyel kimyasal olarak azot bazlı gübre üretimi için gereklidir. Sonuç olarak hem amonyak hem de fosfat için bertaraflarının yanı sıra geri kazanımlarına yönelik yapılacak çalışmalar bu bakımdan dikkate alınmalıdır.

Bu çalışma, amonyak ve fosfor geri kazanımında modifiye edilmiş aktif karbon manyetik nanoparçacıkların (kompozit PAC-MNP) kullanılmasının etkinliğini araştırmak için yapılmıştır. Bu noktadan hareketle, Yüksek Hızlı Aktif Çamur (YHAÇ) sistemlerinin B aşamasından elde edilen atıksuların simülasyonu yapılarak ikincil amonyak ve fosfor kaynaklarının geri kazanılması amaçlanmıştır. Çalışma kapsamında sulu çözeltiden 50 ila 1000 mg/L başlangıç konsantrasyon aralığında kesikli adsorpsiyon deneyleri yapılmıştır. Toz aktif karbon, güçlü hidroklorik asit ile modifiye edilmiş (fonksiyonel$_{HCl}$ – PAC) ve daha sonra "birlikte çökeltme" sentez yöntemi ile manyetit nanoparçacıkları ile emprenye edilmiştir. PAC-MNP karakterizasyonu için, Potentiyometrik Titrasyon, Zeta Potansiyel,

SEM, EDX, Fourier Transform Infrared Spektroskopi (FT-IR), ve BET ölçümleri yapılmıştır. Bu deneyler Kompozit PAC-MNP'nin amonyak ve fosfat simultane adsorpsiyonunda etkili olduğunu kanıtlamıştır.

Denge çalışmaları, sentetik olarak hazırlanan N-P çözeltisinin, amonyak için Fre undlich izoterm modeli ve fosfat iyonları için Redlich-Peterson modeli ile uyumlu olduğunu göstermiştir. Ayrıca, sentetik N-P çözeltisinin kinetik çalışmaları sonucunda amonyak-azotun Psedou-İkinci Derece ile, fosfatın Elovich modelleriyle uyumlu olduğu belirlenmiştir. En yüksek adsorpsiyon kapasitesi, 1000 mg/L olarak hazırlanan N-P çözeltisi ile pH 10 da, 0,3 g PAC-MNP kullanılarak fosfat için 21,74 mg/g, amonyak için 15,05 mg/g elde edilmiştir. Amonyak ve fosfatın PAC-MNP'nin yüzeyinden 1 saat ve 4 döngü boyunca gerçekleştirilen desorpsiyon deneyi için farklı elektrolit çözeltiler denenmiş, ancak optimum çözeltinin 1 M NaOH çözeltisi olduğu tespit edilmiştir.

Araştırma sonuçlarına göre, adsorpsiyon yönteminin atıksulardaki amonyak ve fosfatın kontrolü ve besin kaynağı olarak Strüvit'e dönüştürülmelerinde sürdürülebilir ve etkili bir yöntem olduğu düşünülmektedir.

Anahtar kelimeler: Aktif karbon, Manyetik kompozit nanoparçacık, Amonyak giderimi, Amonyak geri kazanmı, Fosfar giderimi, Fosfat geri kazanımı, Adsorpsiyon, Zeta potansiyeli

SYMBOLS

C_0 : Initial concentration of adsorption (mg/L)

C_e : Equilibrium concentration (mg/L)

Ci : Initial concentration (mg/L)

Ct : Concentration at time, t (mg/L)

D_{des} : Desorption rates (%)

k_1 : Rate constant of Pseudo-first order model (1/min)

k_2 : Rate constant of Pseudo-second order model (g/mg.min)

K_F : Freunlic constant $((mg/g)/(mg/L)^n)$

K_L : Langmuir constant (L/mg)

K_R : Redlich-Peterson constant

K_s : Sips equilibrium constant $(mg/L^{)-1/nS}$

m : Mass of adsorbent (g)

n : Freundlich intensity

q_a : Initially adsorbed NH_3 and PO_4^{3-} (mg/g) (mg/g)

q_{calc} : Calculated amount of adsorbate uptake (mg/g)

q_d : Amount of desorbed uptake (mg/g)

q_e : Amount of adsorbate uptake at equilibrium (mg/g)

q_{exp} : Amount of adsorbate uptake in experiment (mg/g)

q_{max} : Maximum adsorption capacity calculated from Langmuir model (mg/g)

q^s_{max} : Maximum adsorption capacity calculated from Sips model (mg/g)

q_t : Amount of adsorbate uptake at time, t (mg/g)

R^2 : Correlation coffecient

T : Temperature (°C)

t : Time (min)

V **:** Volume (L)

W **:** Weight (g)

χ^2 **:** Non-linear chi-square

α **:** Initial sorption rate constant (mg/g.min)

β **:** Elovich constant (g/mg)

ABBREVIATIONS

ATP **:** Adenosine triphosphate

BET **:** Bruneuer–Emmett–Teller

EBPR **:** Enhanced biological phosphate removal

DI **:** Deionized water

EDX **:** Energy dispersive X-ray

FT-IR **:** Fourier transform infrared spectroscopy

HRAS **:** High rate activated sludge system

IEP **:** Isoelectronic point

IONPs **:** Iron oxide nanoparticles

MAP **:** Magnesium Ammonia Phosphate

MNPs **:** Magnetic activated carbon nanoparticles

MNPs **:** Magnetic nanoparticles

NPs **:** Nanoparticles

NRMSE **:** Normalized root mean square error

P **:** Phosphorus

PAC **:** Powdered activated carbon

PAC-MNPs: Powdered activated carbon – Magnetic nanoparticles (Composite)

PAOs **:** Polyphosphate accumulating organisms

PFO **:** Pseudo-first order

pH_{PZC} **:** Point of zero charge

PSO **:** Pseudo-second order

RO **:** Reverse osmosis

SEM **:** Scanning electron microscopy

UCT **:** University of Cape Town

LIST OF FIGURES

Figure 1. 1. Various ways of nitrogen fixation 2

Figure 1. 2. Phosphorus Cycle 4

Figure 1. 3. Various pathways of nutrient deposition linked between hydrology, anthropogenic nutrient inputs, eutrophication (Paerl, 2006) 5

Figure 1. 4. Fundamentals terms of adsorption theory (Worch, 2012) 12

Figure 1. 5. Steps of adsorption process (adapted from Benmahdi et al., 2019) 13

Figure 1. 6. Demonstration of differences between physisorption and chemisorption (Sarkar and Paul, 2016) 15

Figure 1. 7. Various water pollutants and nanostructured materials used for the removal of pollutants (Choi and Lee, 2022) 20

Figure 1. 8. The crystal structure of (a) hematite, (b) magnetite ve (c) maghemite kristal (the black ball is Fe^{2+}, the green ball is Fe^{3+}, and the red ball is O^{2-}) (Wu et al., 2015) 23

Figure 2. 1. PAC-MNPs synthesis 32

Figure 2. 2. Drying process of the composite nanoparticles 32

Figure 2. 3. Grinding process of dried composite nanoparticles 33

Figure 2. 4. FT-IR (left) and SEM (right) 35

Figure 2. 5. Batch experiments (Gulyás et al., 2021) 35

Figure 2. 6. Flow diagram of adsorption experiments 36

Figure 2. 7. Flow diagram of the cycles of adsorption-desorption experiments 38

Figure 3. 1. a) pHpzc value of PAC-MNPs b) IEP value of PAC-MNPs 42

Figure 3. 2. IR spektrum of 1) functionalized$_{HCl}$-PAC, 2) PAC-MNP (HCl modification) 45

Figure 3. 3. IR spektrum of 1) Raw PAC-MNP 2) PAC-MNP after Adsorption at pH=10 45

Figure 3. 4. SEM images of 1) functionalized$_{HCl}$-PAC, 2) PAC-MNP (before adsorption) 47

Figure 3. 5. SEM image of PAC-MNP (after adsorption) 47

Figure 3. 6. The EDX results obtained from FunctionalizedHCl -PAC 48

Figure 3. 7. The EDX results obtained from of PAC-MNPs (before adsorption) 48

Figure 3. 8. The EDX results obtained from of PAC-MNPs (after adsorption) 49

Figure 3. 9. The EDX results A) obtained from PAC-MNPs (before adsorption) as weight percentage B) PAC-MNPs (after adsorption) as weight percentage 49

Figure 3. 10. Kinetic model plots for NH_3 (1) and PO_4^{-3} (2) adsorption (Adsorption conditions: N-P solution, 500 mg/L, pH ~9). 51

Figure 3. 11. Effect of solution pH on NH_3 (1) and PO_4^{3-} (2) adsorption and the zeta potential of PAC-MNPs (adsorption conditions: N-P simultaneous solution, 500 mg/L; PAC-MNPS dosage; temperature, 20 °C). 54

Figure 3. 12. Effect of solution pH on NH_3 (1) and PO_4^{-3} (2) adsorption (adsorption conditions: N-P simultaneous solution, 1000 mg/L; PAC-MNPS dosage; temperature, 20 °C)..... 55

Figure 3. 13. Effect of adsorbent dosage on NH_3 (1) and PO_4^{-3} (2) adsorption (adsorption conditions: N-P simultaneous solution, 1000 mg/L; PAC-MNPS dosage; temperature, 20 °C)..... 56

Figure 3. 14. Effect of adsorbent dosage on NH_3 (1) and PO_4^{-3} (2) adsorption, respectively shown on graphs (adsorption conditions: N-P simultaneous solution, 500 mg/L; PAC-MNPS dosage; temperature, 20 °C) 57

Figure 3. 15. Reusability of magnetic nanoparticles for phosphate recovery from synthetic N-P solution (Experimental conditions for desorption; distille water, 1 h contact time. Experimental conditions for adsorption; for synthetic N-P solution: 15 g/L MNP, initial N-P: ~500 mg/L) 58

Figure 3. 16. Adsorption performance of PAC-MNPs for ammonia species recovery from synthetic NH_3 solution (Experimental conditions for desorption; distille water, 1 h contact time. Experimental conditions for adsorption; for synthetic N solution: 15 g/L MNP, initial pH = 10, initial N: ~500 mg/L) 59

Figure 3. 17. Reusability of magnetic nanoparticles for ammonia recovery from synthetic N-P solution through 0.1 M HCl, 0.5 M HCl, 1 M HCl, 1 M NaOH desporption solutions (Experimental conditions for desorption; distille water, 1 h contact time. Experimental conditions for adsorption; for synthetic N-P solution: 15 g/L MNP, initial pH = 10, initial N-P: ~500 mg/L). 60

Figure 3. 18. Reusability of magnetic nanoparticles for phpsphorus recovery from synthetic N-P solution through 0.1 M HCl, 0.5 M HCl, 1 M HCl, 1 M NaOH desporption solutions (Experimental conditions for desorption; distille water, 1 h contact time. Experimental conditions for adsorption; for synthetic N-P solution: 15 g/L MNP, initial pH = 10, initial N-P: ~500 mg/L) 61

Figure 3. 19. Color changing during the adsorption-desorption cycles..... 62

Figure 3. 20. Effect of 0.5 M and 1 M HCl desorption solutions on the PAC-MNPs (changing color)..... 62

LIST OF TABLES

Table 1.1. Comparison of physical and chemical adsorption 16

Table 2. 1. Isotherms parameters used for model determination (Gulyás et al., 2021) . 40

Table 3. 1. Theoretical parameters of kinetic and isotherm studies..... 50

Table 3. 2. Kinetic model parameters for NH_3 and PO_4^{-3} adsorption on PAC-MNPs at pH 10 52

1. INTRODUCTION

1.1. Nitrogen and Phosphorus: As Essential Nutrients to Life

Life of living beings cannot last long in case of deficiency of crucial Nitrogen (N) and Phosphorus (P) elements. After hydrogen (H), carbon (C), and oxygen (O), nitrogen is one of the rich-in-content elements in biomass that is the fourth one by moles (Howarth, 2022). Nitrogen refers to the building block of chlorophyll that is such an important pigment responsible for photosynthesis (Maathuis and Diatloff, 2013). Moreover, it's rich in the structure of amino acids which make up proteins of all living species. As for the phosphorus, it's great essential in making of either proteins or carbohydrate polymers, by means of complex nucleic acids (DNA, RNA) and phospholipids (Mackey et al., 2019). In ecosystem these essential nutrients have an excellent accordance and circulate in natural pathways/routes. This is mostly associated with biogeochemical cycles of nutrients, and referred biological, geological, and chemical aspects of each nutrient cycle (Falkowski, 2001).

The nutrient elements through the biogeochemical cycles flow in different forms between abiotic and biotic systems. The nutrients must be recycled or harvested continuously from abiotic systems (i.e., atmosphere, soil, and water) because they make up living cells, then their travel will be somehow over in biotic systems (i.e., plants, animals, microbes). For instance, the heterotrophs (i.e., consumers) eat plant tissues containing proteins thereby they could provide animal-based tissues. After plants and animals die, the remaining decompose so that the nutrients are let out to the environment as mostly in the organic forms. Although the impacts of both elements on living things are equally critical, there are differences in their existing forms. In other words, in order for producers and consumers to exist together in ecological system, the availability of both organic and inorganic forms of N and P are required in the environment (Nieder et al., 2018).

1.1.1. Nitrogen cycle

Nitrogen is abundantly present in gas phase corresponding to 78% of the atmosphere (Widdison and Burt, 2008), however no gaseous phase is available for phosphorus in natural environment (Jahnke, 1992). The most important atmospheric forms of the nitrogen cycle are inert dinitrogen (g) and ammonia (g). In particular, the nitrogen cycle

occurs with the movement of nitrogen in the Earth's various reservoirs (Holland, 1998) such as atmosphere, biosphere, hydrosphere and lithosphere. When it comes to the availability to use of tightly bound gas form of nitrogen (N_2) for primary producers (plants), it is only possible when it is converted to ammonium (NH_4^+) or nitrate (NO_3^-) ionic forms by lightning or relevant biotic or industrial nitrogen fixation (Figure 1.1). These inorganic nitrogen forms that plants mostly use can be also known as mineral nitrogen.

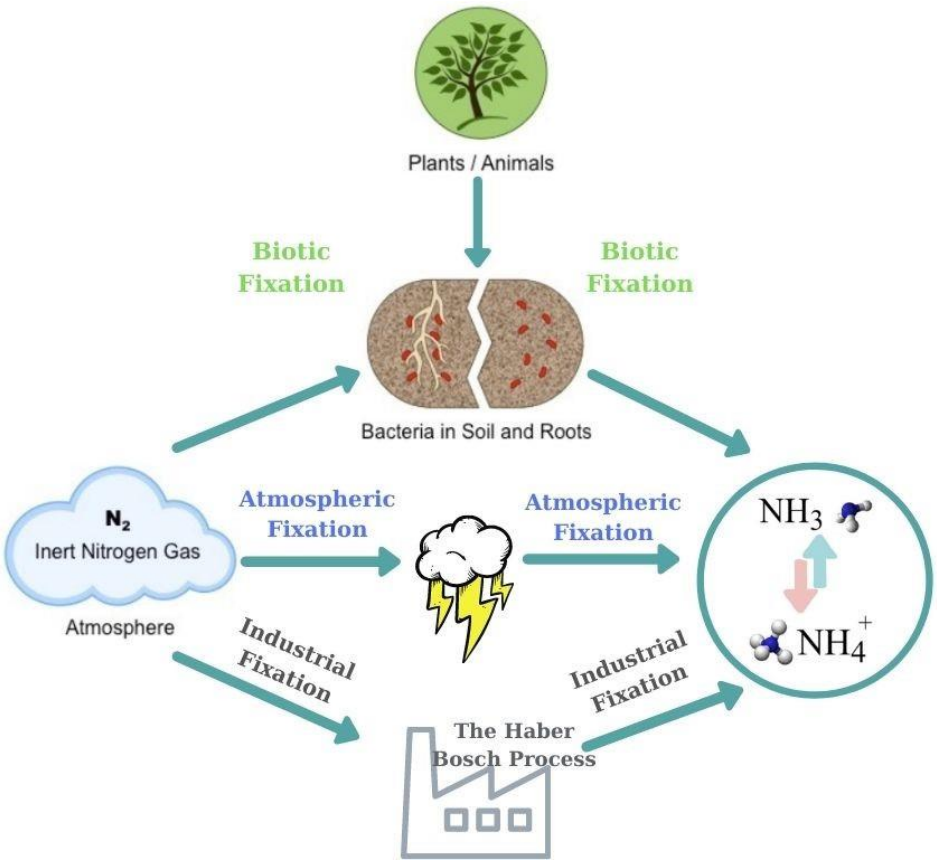


Figure 1. 1. Various ways of nitrogen fixation

The nature establishes its delicate balance and makes nitrogen a limited resource, in the meantime most organisms cannot access it directly, even though atmosphere is made up of a considerable amount of N_2 gas. So, this somehow appears as limiting primary productivity. Nitrogen in soil is present in three general forms: organic nitrogen compounds, ammonium (NH_4^+) ions and nitrate (NO_3^-) ions (Myrold, 1999). Mainly soil offers abundantly both organic particles and negatively charged (anionic) minerals to plants. However, organic nitrogen form, for instance existing in fertilizer or manure

structure, must be mineralized to inorganic nitrogen minerals in order for plants to use. Nitrate is easily moved by water as it is highly soluble. Most of the nitrogen is taken up as nitrate. It moves freely toward plant roots as they absorb water. While plants get inorganic nitrogen (NH_4^+, NO_3^-) from the soil or water, they can uptake only a small fraction of phosphorus from soils in the dissolved anionic form of PO_4^{-3} so that is generally denoted to be the growth-limiting nutrient in terrestrial ecosystems (Göran et al., 2012, Schlesinger and Bernhardt, 2013, Vitousek and Howarth, 1991).

1.1.2. Phosphorus cycle

The atmosphere does not act as a phosphorus reservoir in the phosphorus cycle. The movement of phosphorus takes place among rocks, water, soil and sediments, and organisms because almost all phosphorus in the environment tends to be concentrated in organic and inorganic solid or aqueous phases. Therefore, there is no phosphorus in the gas phase (Daneshgar et al., 2018, Mackey and Paytan, 2009), but only can it be found as tiny dust particles in air.

The global phosphorus source is primarily based in Earth's crust, and its cycle can be examined as geological (long term) and biological (short term). The reason of its long-term occurrence as geologically is due to weathering of phosphorus from phosphate rocks, which can take a thousand or even millions of years (Daneshgar et al., 2018). Phosphate is the salt of phosphoric acid (H_3PO_4). Rocks containing phosphate minerals of sufficient purity and amount are called as "phosphate". After it emerges geologically, phosphate is presented to organisms by reaching the ocean or land (Hartmann et al., 2014). Phosphate, which is found in nature in mineral form (e.g. $Ca(PO_4)_2$, etc.) can also be found in organic bound form (nucleic acids, ATP, phospholipids, etc.). However, the free PO_4^{-3}, that is the fraction suitable for plant use, is released after the organic-bound phosphors are decomposed by biological methods. The concentration of the free phosphate form in the soil is quite low because its mostly low solubility compounds (apatite and other metal complexes) can be found in the soil (Pierrou, 1976). In other words, phosphorus easily transforms into its insoluble form (even more than nitrogen does) so that makes it difficult for plants to uptake/absorb. If there are elements such as iron, aluminum, calcium and magnesium in the soil, it causes insoluble compounds to form with them to a large extent and remains immobile. Therefore, this situation restricts

the use of plants, which makes them difficult to mature. However, the conveyance of phosphorus from the soil is mainly carried out by the uptake of plants. It's conveyed from the soil by runoff, erosion or leaching as well. But this happens relatively slow. Phosphorus forms that the plant can reach, and use will be used directly by animals, and eventually, the journey of phosphorus will end in soil or water due to the decomposition of plant and animal remains. Phosphorus is finally released back to the environment either by decomposition of living beings (plant, animals etc.) or weathering process of phosphate rocks (Figure 1.2).

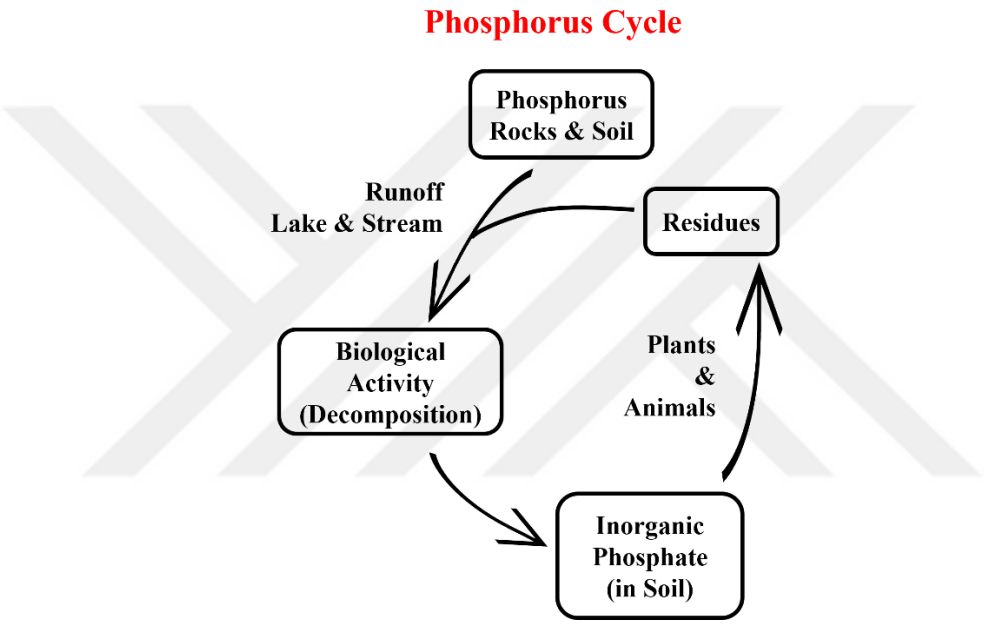


Figure 1. 2. Phosphorus Cycle

On the other hand, in case of the existence of soluble forms of phosphorus in various aquatic environments, even their relatively lower concentrations make the mobility of phosphorus easier. This is very critical for eutrophication. Because when phosphorus is found in high concentrations in the aquatic environment, it is used very quickly by aquatic plants and plankton, and this uncontrolled excessive growth in water results in eutrophication. As a result, the balance of nitrogen and phosphorus cycles that nature provides by itself is in regular basis if there is no intervention.

1.2. Impacts of Heavy Nitrogen and Phosphorus Loads in Water Bodies

Nitrogen and phosphorus are natural constituents of aquatic ecosystems, and both are monitored as part of water quality testing. Because their excessive amounts can cause significant water quality problems. Nitrogen and phosphorus forms that are conveyed to the water in various ways (Figure 1.3) are mostly in reactive inorganic structure and this nutrient enrichment is defined as eutrophication (rapid nutrient enrichment) that occurs with increasing their concentrations in natural waters.

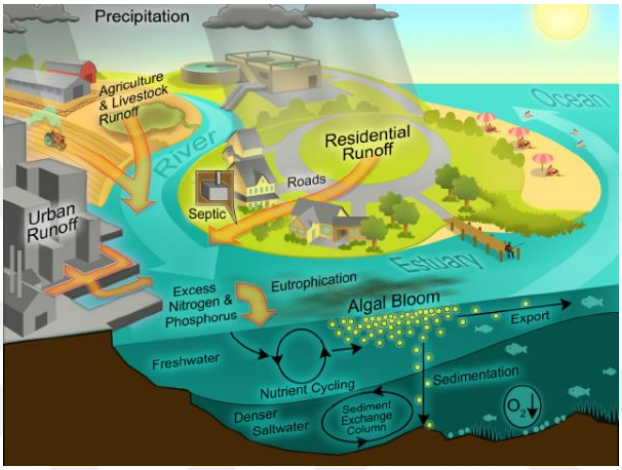


Figure 1. 3. Various pathways of nutrient deposition linked between hydrology, anthropogenic nutrient inputs, eutrophication (Paerl, 2006)

1.2.1. Eutrophication

Excessive N and P loads in natural waters can cause algal bloom and favour the aquatic plants to grow fast, that is challenging for ecosystems to handle (Smith et al., 1999). This situation results with disruption of the light, temperature, odour, and coloration which leads to problems in recreational and aesthetic meanings, as well as seriously reduction the oxygen levels in the water which leads to deterioration of biological activity of fish and other aquatic life. Due to the presence of heavy nutrient in water body, phytoplankton and macrophytes that are excessively grown are sooner or later die and settle down through the bottom of the water body. The growth of anaerobes and algal blooms is thus accelerated under anaerobic conditions (Foree and McCarty, 1970). Hence, fish and other aquatic organisms begin to suffocate. Besides, this situation may not only be limited with aquatic life, but there are also harmful effects on human life as a result of exposure to

nutrient pollution by consuming tainted fish or shellfish or drinking polluted water (Ashforth and Calvin, 1973).

Various sources or nonpoint sources such as agriculture, aquaculture, septic tanks, urban sewage, urban stormwater runoff, industry, and fossil fuel combustion cause excessive N and P release, in other words nutrient polution (Carpenter et al., 1998). Therefore, nonpoint nutrient sources are among the factors that trigger eutrophication. The main source of nutrient pollution may vary from region to region. For example, in the United States and the European Union, agricultural resources, commercial fertilizers and animal manure are typically the main sources of nutrient pollution in water streams, while the countries having lower income and prospering-economies they are sourced from urban wastewater (Mateo-Sagasta et al., 2017). Specific to nutrient types, nitrogen pollutants are resulted from agricultural lands' streams in general, while most of the phosphorus pollution originates from households and industry, especially due to phosphorus-based detergents (Weiner and Matthews, 2003). Therefore, this problem can be directly related to the increasing population and developing industry as a result of human activity.

The roles of both nitrogen and phosphorus in controlling a possible eutrophication is very critical (Carpenter, 2008). To control the eutrophication risk in lakes, the total phosphorus concentration should be less than 0.8 mg /L and the total nitrogen concentration should be less than 0.05 mg/L (Qi et al., 2022). Keeping nitrogen and phosphorus concentration lower than the others will have a limiting effect on the growth of algal bloom. Therefore, it is important to understand the causes of water pollution and to take appropriate actions for its solution.

1.3. Controlling the Water Contamination Caused by Heavy Nutrient Loads

It is necessary to implement many strategies such as the application of effective treatment methods and the promotion of phosphorus-free detergents in order to prevent pollution caused by the discharge of insufficiently treated wastewater, as well as it is necessary to develop agricultural practices in order to minimize the effect of nitrogen and phosphorus pollution caused by fertilizers in natural waters.

Compared to nitrogen concentration, it is known that phosphorus is the key factor determining especially phytoplankton growth, and that total phytoplankton biomass is

mainly determined by the actual total phosphorus, not by the total nitrogen concentrations. It was reported that by a long-term whole lake experiment from North America, nitrogen control did not not reduce phytoplankton biomass (Schindler et al., 2016). To reduce the eutrophication, it was necessary to reduce the concentration of phosphorus rather than nitrogen, unless the nitrogen concentration is so high that it does not cause direct toxic effects on humans or other organisms.

1.3.1. Ammonia and phosphate removal techniques

There are specific discharge standards of each nutrient regulated by many countries. Numerous techniques have been investigated to remove or recover various nutrient-rich wastewater.

1.3.1.1. Current ammonia removal techniques

Ammonia can be removed either physical, chemical, or biological approaches. Specifically, a wide range of ammonia removal techniques such as air stripping, membrane separation, ion exchange, vacuum distillation, precipitation as struvite, adsorption and biological oxidation etc. are available (Tchobanoglous et al., 2003). Ammonia stripping is applied by evaporating ammonia nitrogen in the gas phase by aeration of wastewater, that is a simple method applied to reduce the amount of ammonia in wastewater, but some disadvantages increase maintenance and operating costs. At pH=7, only ammonium ions are present in the water. Ammonia exists in the dissolved gas phase in solution at pH=10.5-11.5 range. When the pH is increased from 7 to 11.5, the concentration of ammonia in the gas phase increases and can be removed by aeration. Therefore, while the pH in water is increased, ammonium ion (NH_4^+) turns into ammonia (NH_3) (shown in Equations 1.1-1.2). Caustic lime $Ca(OH)_2$ is generally used to raise the pH value.

$$NH_4 + H_2O \leftrightarrow NH_4OH + H^+ \quad (1.1)$$

$$NH_4OH + H_2O \rightarrow NH_3 + H_2O \quad (1.2)$$

Ammonia is able to be removed through membrane separation distillation techniques (Ding et al., 2006, Duong et al., 2013, Yang et al., 2019a). The selectivity of ion-selective

membranes under the influence of an electric field ensures that cationic ions such as ammonium are separated from the water (Xu, 2005). Membrane distillation is a separation process resulting from simultaneous mass and heat transfer across a hydrophobic microporous membrane. Due to the partial vapor pressure difference between the hot and cold side of the mass transfer membrane a flux occurs (Yarlagadda et al., 2011).

Ammonia can be effectively removed from wastewater using the ion exchange process (Ding and Sartaj, 2016, Dryden, 1984, Jorgensen and Weatherley, 2003). Ion exchange is a reversible chemical reaction in which an ion bounding to a solid is exchanged.

In wastewater treatment plants, ammonia removal is generally conducted through biological processes. The processes used for the removal of ammonia nitrogen are:

1. **Assimilation (assimilating, digesting):** As nitrogen is a nutrient, microorganisms in the treatment assimilate (i.e., digest) nitrogen and incorporate it into them. Some of this nitrogen is returned to the wastewater as a result of cell death and lysis.
2. **Nitrification-denitrification:** Ammonia turns into nitrite, then nitrate, and then nitrogen gas.
3. **Deammonification (Anommox):** Anammox process discovered by Mulder et al. in 1995 is realized by a special bacteria group converting ammonium under anaerobic conditions directly N_2 gas by employing the nitrite as the electron acceptor without any organic carbon source (Mulder et al., 1995).

Adsorption method is another way to remove ammonia. With a classical approach of adsorption method, ammonia removal can be achieved by keeping it molecules in the liquid on the solid surface. Adsorption studies of ammonia-nitrogen has been based on a variety of adsorbents such as zeolite minerals (Liu et al., 2013a), modified powdered activated carbon (Godini et al., 2017), Iron loaded activated carbon (Ren et al., 2021), bamboo charcoal (Asada et al., 2006), coconut shell-activated carbon (Boopathy et al., 2013), magnetically modified excess sludge (Zhang et al., 2018), chemically activated biochar (Hsu et al., 2019) etc. These studies indicated that ammonia removal by adsorption process is promising method.

1.3.2. Current phosphate removal techniques

Currently, a variety of techniques that are physical, chemical, and biological methods is available to remove phosphates from wastewater. While the physical methods specifically involve filtration and membrane technologies, they can be also combined with other removal approaches/methods. As a typical chemically removal of phosphates, precipitation with the addition of calcium and some metal salts is commonly implemented (Li et al., 2009, Tchobanoglous et al., 2003). In addition to this, phosphates are precipitated in the struvite form by adding ammonium and magnesium salts. The biological removal of phosphorus is based on the binding of orthophosphate, polyphosphate, and organically bound phosphorus with the microorganism cell tissue.

1.3.2.1. Phosphate removal by physico-chemical processes

Some of these methods can be listed as reverse osmosis, electrolysis, filtration, ion exchange, precipitation, and adsorption. Reverse osmosis is a process in which pollutants are removed from wastewater by means of high pressure and semi-permeable membrane. On the other hand, electrochemical removal can be achieved by electro-coagulation or electro-oxidation, separating the coagulated and flocculated phosphorus with eluted ions from electrodes (Akyeva et al., 2008, Rotta et al., 2019, Tian et al., 2018, Zhang et al., 2013).

The basis of chemical phosphorus removal is the removal of dissolved phosphorus from the environment by converting it into solid particle form. Mainly, the chemical removal of phosphate compounds is based on precipitation with lime, iron salts, aluminum salts. These cations then somehow precipitate with orthophosphate in insoluble form. Besides the ferric chloride and aluminum sulphate as the most used metal salts in phosphorus removal, polymers are also widely used. Precipitation is pH dependent. The pH value should be between 8-11.

1.3.2.2. Phosphate removal by biological processes

In biological phosphorus removal, microorganisms remain under anaerobic or aerobic conditions. Changing conditions create a pressure on the microorganism and they take in excess phosphorus from the environment. Especially thanks to the treatment systems

configured with the Enhanced Biological Phosphate Removal system (A/O, A2/O, Bardenpho, University of Cape Town (UCT) etc.), the treatment of wastewater containing low concentrations of phosphorus can be achieved. This system is basically based on culturing polyphosphate-accumulating organisms (PAOs) in activated sludge by providing a suitable environment (anaerobic and aerobic) (Grady Jr et al., 2011). These specific bacteria absorb the carbon source in the anaerobic environment and excessive amounts of phosphate in the aerobic environment. Subsequently, through the configurations provided, carbon, nitrogen and phosphorus removal from wastewater can be performed.

1.3.3. Simultaneous ammonia and phosphate recovery

1.3.3.1. Struvite precipitation

Struvite was first introduced by H.C.G Struve and is an inorganic mineral with the chemical structure of $MgNH_4PO_4.6H_2O$ (Stratful et al., 2001). Mg^{2+}, NH_4^+ and PO_4^{3-} ions combine at a molar ratio of 1:1:1 to form a solid phase, resulting in the formation of Magnesium Ammonium Phosphate (Kumar and Pal, 2015), that is also referred to by the abbreviation MAP (Magnesium ammonium phosphate). It actually exists as hexahydrate white crystalline MAP structure (Sidorczuk et al., 2020). Chemically, the formation of magnesium ammonium phosphate is seen in Equation 1.3.

$$Mg^{2+} + NH4^+ + HPO4^{2-} + 6H_2O \rightarrow MgNH_4PO_4.6H_2O + H^+ \qquad (1.3)$$

Parameters such as initial pH value, ionic strength, presence of complex species, temperature, reaction time, and Mg, N and P molar ratio affect the formation of struvite (Hanhoun et al., 2011, Le Corre et al., 2009, Tansel et al., 2018). MAP solid phase occurs in alkaline medium and dissolves in acidic medium. The minimum pH for MAP formation should be 7 (Burns and Finlayson, 1982). In order to obtain high nitrogen and phosphorus removal efficiencies in struvite precipitation, it should be operated in the pH range where the solubility of struvite solid phase is minimal. This pH range may change according to the conditions of the aqueous media and be produced in a wide range from 7 to 11.5, but efficiently it is obtained at pH between 8-9.5 (Kim et al., 2017). Another important factor in struvite precipitation is ionic strength and formation of complex species. Complex formation increases the solubility of struvite and decreases the efficiency of the system.

Similarly, ionic strength increases the solubility of struvite and negatively affects the yield depending on the solute concentration in the environment (Doyle and Parsons, 2002).

The struvite causes operational problems in wastewater treatment plants (Mohajit et al., 1989, Ohlinger et al., 1998) as it is difficult to remove from where it is formed, thus bringing additional costs. Struvite crystals accumulate in mechanical equipment and pipes, causing pollution, clogging, and thus reducing the capacity of the equipment. On the other hand, struvite stands out in some researches on alternative and economical raw material sources of fertilizer for vegetables and plants growth. For example, sewage sludge (Thant Zin and Kim, 2021) and human urine (Wei et al., 2018) are alternative sources for struvite. Besides, struvite can be obtained from many industrial wastewaters especially including textile industries consisting of leather process (Tünay et al., 1997), slaughter-house wastewater (Kabdaşlı et al., 2009) garbage/landfill leachate (Warmadewanthi et al., 2021) as well as anaerobic treatment effluent (Ryu et al., 2020).

1.3.3.2. Adsorption process

Due to tightened regulations set for preventing nutrient pollution from natural water bodies, adsorption process has been attracted much attention in environmental studies. In the literature, in addition to the separate adsorption of ammonia and phosphate species, simultaneous adsorption of them with various adsorbent materials was also performed from either synthetic solutions or real wastewater (Gulyás et al., 2021). It is necessary to provide suitable conditions for the adsorption of these nutrient species, especially their affinity to the materials is one of the critical points. Recently, adsorption experiments for the recovery/removal of ammonia and phosphate have been extensively studied, and the adsorbents used are such as bentonite, biochar, iron oxide nanoparticles, zeolite. The different types of the adsorbents and their surface modified composites are especially investigated in order to understand the effects on adsorption efficiency (Cheng et al., 2017, Guaya et al., 2015, Hermassi et al., 2018, Li et al., 2017, Marcińczyk et al., 2022, Pesendorfer and Ellersdorfer, 2021, Sun et al., 2021, Wu et al., 2019, Xu et al., 2020, Zamparas et al., 2021).

1.4. Adsorption Theory

Adsorption, which has been investigated by many scientists at various interfaces, was first defined by German physicist Heinrich Kayser in 1881. It's mainly physical and/or chemical reaction occurring through mass transfer of species (i.e: atom, ions, and molecules) from either liquid or gas form attaching to a solid interface. Adsorption process has importance in reducing environmental pollution by keeping the pollutants (ions or molecules) on the solid adsorbent surface. While the pollutants that adhere to the surface are called adsorbate, and the surface which they adhere is called adsorbent. Adsorbent can be solid or liquid, as well as natural or artificial. In Figure 1.4, adsorption of ions or molecules adhered to the active centers as well as the separation/desorption of the adsorbates from the surface are demonstrated. The release of adsorbed species from the surface (i.e., to be transferred back to the liquid phase) by changing the properties of the liquid phase (e.g., concentration, temperature, pH) is called desorption.

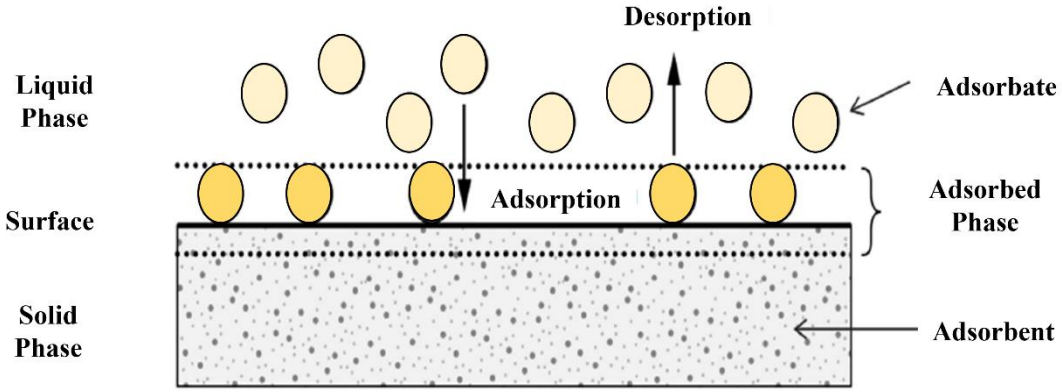


Figure 1. 4. Fundamentals terms of adsorption theory (Worch, 2012)

Considering the adsorption of an adsorbate in the liquid phase to the solid adsorbent surface (as shown in Figure 1.5), there is a four-stage system. The first stage of this system is called "Bulk Diffusion", that is known as the diffusion of adsorbate molecules in the liquid phase towards the liquid-solid interface. In the second stage, through the "Film Diffusion" or "Film Transport", the adsorbate molecules pass through the stationary part at the liquid-solid interface and move towards the pores of the adsorbent. In the third stage, the "Pore Diffusion" takes place, which is the transport of adsorbates into pores with diameters appropriate for their size. In the fourth stage, the adsorption process is

exactly completed as the “Surface Diffusion” (adhesion) of the transported adsorbate molecules to the pores of appropriate sizes takes place.

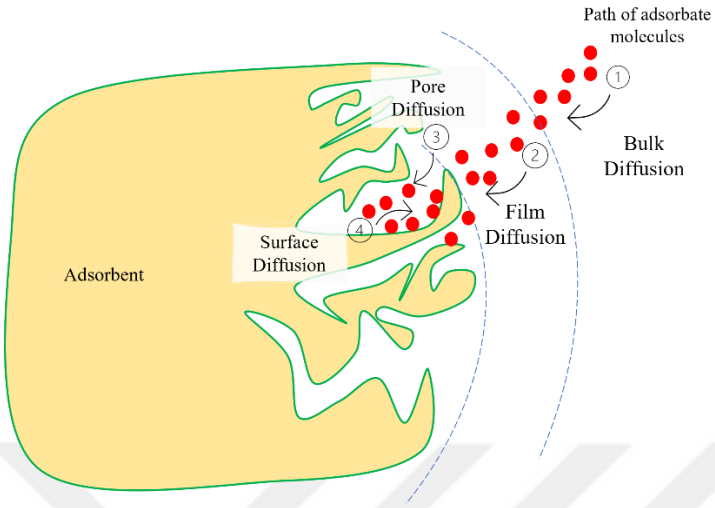


Figure 1. 5. Steps of adsorption process (adapted from Benmahdi et al., 2019)

According to the adsorption theory, the amount of adsorbed substances (mg/g) is calculated according to the mass balance equation given below (Gulyás et al., 2021):

$$q = \frac{(C_0 - Ceq) \times V}{w} \quad (1.4)$$

where, q represents the adsorbent capacity (mg/g); C0 is the initial concentration of substances in solution (mg/L); Ceq represents the final or equilibrium concentration of substances in solution (mg/L); V is the volume of experimental solution (L); and W is the weight of adsorbent (g). Removal efficiency will be calculated as:

$$R\% = \frac{(C_0 - Ce)}{C_0} \times 100 \quad (1.5)$$

where, C0 is the initial adsorbed substances concentration and Ce is the final adsorbed substances’ concentration (mg/L).

On the other hand, desorption efficiency is also calculated based on the mass balance equation given below:

$$D\% = \left(\frac{qd}{q_a}\right) \times 100 \quad (1.6)$$

where, qd represents the desorbed ion's concentration (mg/g) and qa the amount of initial adsorbed substances (mg/g).

1.5. Types of Adsorptions

The absorption is classified into three types: namely physisorption, chemisorption, and exchange (ion) adsorption, which rely on nature of the force present resulting the interaction and formation mechanism of molecules among the adsorbate and adsorbent.

1.5.1. Physisorption

In physisorption, five types of interfaces are formed: solid-solid, liquid-liquid, liquid-gas, solid-liquid and solid-gas. Physisorption/Physical adsorption occurs when adsorbed species/molecules are not attached to a specific place on the solid surface, is generally in a mobile state on the surface, and the intermolecular attraction force is small (or van der Walls' forces are active) (Pourhakkak et al., 2021). Since physisorption occurs on polar and non-polar surfaces, the bonds formed are much weaker than chemical adsorption. Because the weak layer on the solid adsorbent surface that remain mobile, the process is reversible. Thus, after the adsorption process, the adsorbent is regenerated with the desorption process, making it ready for the next use, and it is also possible to recover the molecules removed from medium.

1.5.2. Chemisorption

It's the type of adsorption of which the chemical interaction is dominant between the functional groups on adsorbent and adsorbate. Mostly, chemisorption/chemical adsorption does not occur on the entire surface of the adsorbent, but on active sites on the surface of the adsorbent. In determining chemical adsorption, it is important to detect the active sites on the surface and to perform surface reaction kinetics studies. Different from physical adsorption, molecules are attached to the adsorbent surface in chemical adsorption by the effect of ionic or covalent bonds, which are more effective/stronger forces than van der Walls'. During this process, the electronic configuration of the

adsorbate changes significantly and a monomolecular layer is formed on the adsorbent surface. Molecules are not mobile on this layer. When the entire surface of the adsorbent is covered with this monomolecular layer, the capacity of the adsorbent is almost full. Chemical adsorption is an irreversible process since it takes place with chemical reactions, changes the chemical structures of its molecules, and binds to the adsorbent with strong bonds. For this reason, regeneration of the used adsorbent or recover the molecules from medium are very difficult (Baylan, 2013). A large amount of energy, that is higher than 30 kj/mol (Helfferich, 1985), is required to separate the chemically adsorbed molecules from surface, i.e the activation energy is high. This separation process may cause deformation or deterioration of adsorbent. Generally, physical adsorption takes place much faster than chemical adsorption. The reason for this is that the reaction occurs at temperatures above a certain minimum value in chemical sorption (Baylan, 2013). Finally, while physical adsorption has an uncharacteristic property, chemisorption has quite characteristic property since the probability of reaction depends on the nature of the substances and occurs only if a chemical bond is formed. Figure 1.6 represents the demonstration of the differences between physisorption and chemisorption.

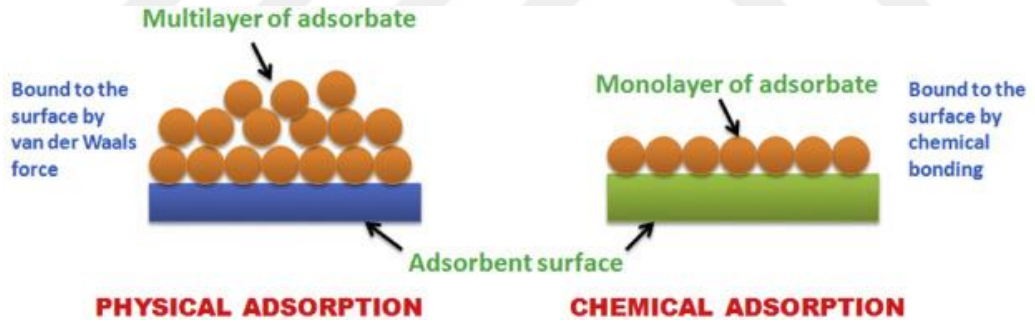


Figure 1. 6. Demonstration of differences between physisorption and chemisorption (Sarkar and Paul, 2016)

A summary table (in Table 1.1) is presented below for distinctive properties between physical and chemical adsorption.

Table 1.1. Comparison of physical and chemical adsorption

Parameter	Physical Adsorption	Chemical Adsorption
Adsorbent	All solid materials	Some of solid materials
Adsorbate	All dissolved sorbate molecules (all gases and liquids under critical temperature)	More specific than the physical sorption
Temperature	Low	Higher
Effective Bond Forces	Van der Waals forces are effective between molecules.	Chemical bonds are effective between sorbate and adsorbent surface.
Reaction Reversibility	Reversible	Irreversible
Entalphy Effect	Always at the exothermic reaction range	Mostly at the exothermic reaction range, but endothermic range possible
Velocity - Activation Energy, Ea	Very fast (Low Ea)	Non-active, low Ea Active, high Ea
Desorption Rate	High rate	Very low rate or Absent
Adsorption Layer	Monolayer or multilayer	Monolayer
Adsorption Heat	Low about 5-10 kcal per mol	Higher about 10-100 kcal per mol
Remark	For determination of surface area and pore size	For determination of active center area, surface reaction and kinetics

1.5.3. Ion (exchange) adsorption

Exchange adsorption is based on the principle that ions adsorbed by the effect of electrostatic attraction forces adhere to the charged regions on the adsorbent surface. The ion exchange reaction can be included in this type of adsorption. It is important that the adsorbent surface and the adsorbent surface, which have opposite electrical charges, attract each other. Among the ions with the opposite electric charge to the adsorbent, those with higher charge and smaller ion diameter are better adsorbed. If the charges of

ions are the same in the medium, molecules with smaller ion diameters are preferred by the surface (Baylan, 2013). It is very difficult to explain the adsorption process with only one of the other adsorption types. In many adsorption processes, different types of adsorptions can be seen together or sequentially (Baylan, 2013).

1.6. Factors Affecting Adsorption

Adsorption has been one of the effective methods conducted for separation of various contaminant species from wastewater. The adsorption process is affected by adsorbent amount and properties, adsorbed material, and ambient conditions.

Materials employed as adsorbent can be many different types and, both chemical properties and physical properties of an adsorbent are the parameters that directly affect the adsorption. While surface area, particle size and pore distribution are evaluated within the scope of physical properties, functional groups type and their distributions on adsorbent and adsorbents' acidic, basic or neutral conditions are associated with the chemical properties. Adsorption performance generally increases in direct proportion to the increase of surface area of the material. The surface area is also proportional to the amount of adsorbent matter, and the amount of substance to be adsorbed. Porosity of materials with high pore volume has also a positive effect on adsorption but the pore diameter must be compatible with the diameter of the molecules of the adsorbed substance. On the other hand, if the adsorption rate is determined by pore diffusion, too much porosity may increase resistance and thus may limit the performance. Another important property of the adsorbent is the particle size. Many studies indicate that the adsorption capacity increases with the decrease in particle size (Hou et al., 2020, Huang et al., 2017, Suresh Kumar et al., 2019, Tsai et al., 2003, Wang and Shadman, 2013). In other words, when adsorbent particle is in smaller sizes, the adsorbed number of molecules will increase. Considering the chemical characteristic of an adsorbent, the type of functional groups on the surface, and whether the adsorbent is acidic, basic or neutral are important (Li et al., 2012). Their roles help determine the forces capturing the adsorbate onto the surface.

Another important parameter affecting the adsorption process is species to be adsorbed - i.e., adsorbate. Solubility of adsorbate affects the adsorption capacity and a controlling factor for the adsorption process. Before the adsorption process takes place, the bonds

between solute and solvent must be broken (Keleş, 2008). According to this, there is the "Lundelius" rule, which explains that there is an inversely proportional relationship between the solubility of the solute in the liquid phase and its adsorption (Jørgensen, 1979, Keleş, 2008). While adsorption capacity gets stronger because of the decrease in the solvent-solute bond as the solubility decreases, it becomes weak with respect to increase in the solvent-solute bond as the solubility increases (i.e., when the substance to be adsorbed is hydrophilic). In addition, the molecular structure/size of the adsorbate also affects the adsorption. The rule is also supported by another one called "Traube" rule (Jørgensen, 1979). In this case, a hydrophilic substance will be adsorbed less than a hydrophobic substance such as long-chained hydrocarbon in the same solution. Because the hydrocarbon structure predominates, the hydrophobic property of the solute increases. Referring to this, adsorption of a molecule containing different groups on the adsorbent surface means that it can only be achieved by the hydrophobic ends of the molecule (Bansal and Goyal, 2005). If adsorbate molecules are large compared to the pore structure of an adsorbent, some of the pores may become clogged and the active centers in these pores cannot function. As a result, the adsorption capacity decreases. The ionization of adsorbate also affects the adsorption capacity, that results less adsorption of ionic-characterized adsorbates than neutral adsorbates. Therefore, it can imply that the rate of adsorption will increase in pH ranges where the substances are neutral.

Ambient conditions such as temperature, pH, and presence of substances/ions during the adsorption process are also the factors affecting the equilibrium adsorption capacity. pH value of the ambient determines the form in which the adsorbate will be in the solution. While substances dissolve in a solvent within a certain pH range, they can precipitate out of that determined range. Surface functional groups of the adsorbent are influenced by pH so that affects the adsorption capacity by increasing or decreasing its affinity of adsorbate species (Nouri, 2003, Xie et al., 2017, Yang et al., 2019b). The effect of temperature on adsorption can be different depending on endothermic or exothermic situations. However, the temperature encountered practically in water and wastewater is not at a considerable level that affects the adsorption equilibrium, small changes in temperature do not significantly change the adsorption process. Another factor that is among the ambient conditions affecting the adsorption is the competition of species/ions forming the adsorption media that is important especially in determining the adsorption

mechanism. A specie in a multi-component adsorption media can be lesser adsorbed than when it is in pure media. The reason is that some species unintended to be adsorbed go towards the adsorbent surface and occupy large area, that causes a smaller number of centers is left for the target species/ions intended to be adsorbed. On the contrary, there are some studies stating that other species in the adsorption media can facilitate the target substance to be adsorbed (Lee and Kim, 2019). As a result, in real applications for adsorption processes, it is important to determine the composition of the media beforehand and to choose the appropriate adsorbent.

1.7. Engineered Nanoparticles

Nanomaterials are simply defined as particles that are reduced in size and engineered in the range of 1-100 nm. Apart from the known liquid, solid, gas and plasma states of a matter, in fact, it has been stated that nanoparticles can be another state of matter (Buzea et al., 2007). They exist in amorphous or crystalline forms. They are developed at atomic or molecular level (below 100 nm) and having favorable physical, chemical, and biological properties. As the size of a material gets smaller, the surface interaction, increase in the number of molecules, and surface tension between the surfaces of the particles get bigger; as well as a quantum confinement results from electronic wave due to the physical dimensions of the particles (Campos et al., 2015, Gupta and Gupta, 2005). Some interesting and superior properties such as mechanical, optical, electrical, magnetic properties and chemical reactivity on the nanomaterial stand out (Rane et al., 2018), whereas the physical properties of a bulk material are present regardless of size. Thanks to these properties, the attractiveness of nanomaterials in different disciplines such as medicine, astronomy, and the environmental engineering etc. has been increasing, particularly in the last two decades (Kumar et al., 2020). Especially, in wastewater treatment they are found to be very promising adsorbents allowing the effective separation of organic, dye, and heavy metal contaminants (Do et al., 2011, Lompe et al., 2017, Luciano et al., 2013). The variety of adsorbents at nanoscale used for separation of pollutants from water are shown in Figure 1.7.

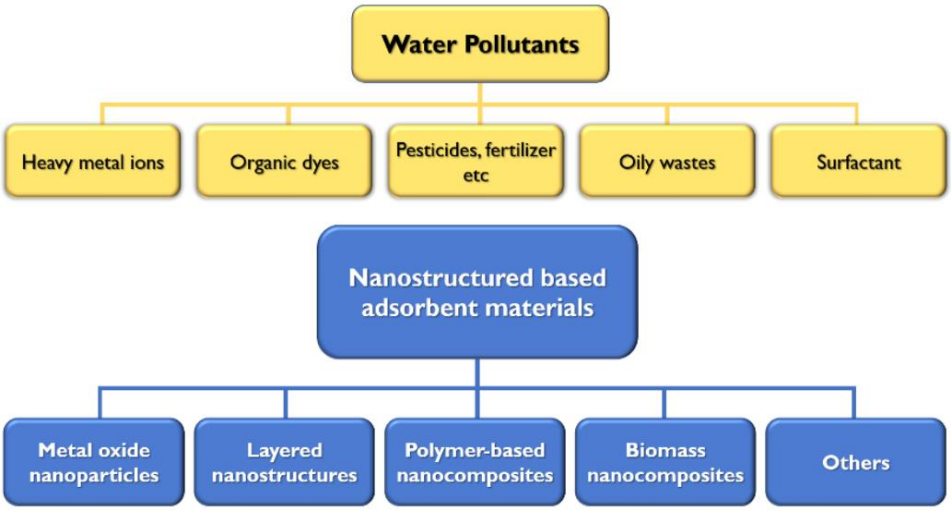


Figure 1. 7. Various water pollutants and nanostructured materials used for the removal of pollutants (Choi and Lee, 2022)

Nanoparticles synthesized from carbon-, metal-, polymer-, clay-based materials are commonly used in the adsorption of wastewater pollutants. These are synthesized with various methods. The preparation processes of nanoparticles have been grouped under six ways: 1) sol-gel processes; 2) solid-state reactions; 3) liquid-solid reactions; 4) evaporation and condensation processes; 5) plasma processes; 6) flame hydrolysis. The precipitation method, which is commonly performed in the synthesis of nanoparticles, is also defined under liquid-solid reactions. In addition, nanoparticles that can be produced by engineering methods are also formed under natural conditions. These conditions may could be resulted from forest fires, volcanic eruptions, mineral dust from the deser, and soil erosion (Turan et al., 2019).

Carbon-based adsorbents such as activated carbon, graphene, carbon nanotubes have gained interests in various studies thanks to their favourable electrical conductivity, structural arrangement, chemical properties, biocompatibility, mechanical and thermal stability (Dresselhaus et al., 2001). Carbon-based nanomaterials have a cylindrical structure. They can be classified under two groups as single-walled or multi-walled nanomaterials according to their synthesis processes. They have a high specific surface area (Ruoff and Lorents, 1996). As an important advantage in conventional disinfection processes (chlorination, ozonation, etc.), the use of carbon-based nanomaterials after chemical oxidation do not cause toxic by-products to be formed (Liu et al., 2013b).

Polymeric nanomaterials have been employed for the decontamination of various pollutants (e.g., organic substances, heavy metals, dye and microorganisms) from wastewater (Adeola and Nomngongo, 2022, Gehrke et al., 2015, Pandey et al., 2017). Both natural and synthetic polymers are available. While natural polymers (or biopolymers) are those that are found in nature as plant- and microbe-derived (such as polysaccharides, polypeptides, fungus-derived chitin, animal-produced silk, and mammal-derived collagen etc.) (Choi and Lee, 2022), synthetic polymers contain nylon, polyethylene, polyester, teflon, and epoxy, etc (Adeola and Nomngongo, 2022). Especially many structural abilities such as forming film, dimensional variability and functionalities in their composite forms draws attention as they have high surface area in the polymer matrix (Jordan et al., 2005, Lofrano et al., 2016).

Clay-based adsorbents have stood out with bentonite, montmorillonite, kaolinite, and zeolite as they possess favorable properties in the structure of materials and adsorption performances (Salek Gilani et al., 2022). Among them, nanozeolites, which are crystalline aluminosilicate abundant in sedimentary rocks (Kianfar 2019) have wide application in filtration, ion exchange and adsorption processes (Rahman et al 2022). Nanozeolites are of a rigid - three-dimensional (Kianfar, 2019) crystal structure with greater control over excitation of molecules. They have been investigated in removing organic pollutant (Pham et al., 2016), ionic nutrients (Chen et al., 2012).

Metal-based nanoparticles (e.g., Al_2O_3, ZnO, Fe_3O_4, $NiO.Fe_2O_3$, $CaO.Fe_2O_3$, TiO_2 and MgO etc.) have electrical conductivity, photocatalytic ability, high adsorption capacity (Kodama, 1999, Oliveira et al., 2018). Metals that show naturally magnetic properties in nature are such as iron, nickel and cobalt. They are mainly involved in research topics of many disciplines such as environment, medicine, materials physics, biology, and geology (Kodama, 1999). Among them, iron with various oxidation states is very reactive metal. Iron oxides appear to be promising adsorbents in removing metal ions, dyes, organic and inorganic pollutants from wastewater, and are known as the most common metal-based adsorbents. They have also magnetic behaviours at nano sizes, which is an important point to overcome the challenge of removal of target species attached to nanoparticles' surface and adsorbent separation from media. Regarding on wastewater treatment, the use of magnetic nanoparticles in adsorption processes has been very critical in terms of ease of

separation and reusability. So, they can be readily taken out the reaction media after adsorption completed through a simple magnet (Kharissova et al., 2015).

1.7.1. Engineered magnetic iron oxide nanoparticles

Magnetic Iron Oxide Nanoparticles (IONPs) with a wide range of fields of use can be synthesized in different sizes ranging from 10 to 100 nm as well as found abundantly in nature including soils, aquifers, and sediments. They can be moved by applying an external magnetic field, and easily separated from their environment. IONPs consist of different chemical components and are less sensitive to oxidation so that maintains their stable magnetic properties. They can mostly exist in nature in the form of Magnetite (Fe3O4), Hematite (α-Fe2O3) and Maghemite (γ-Fe2O3) (Saharan et al., 2014) depending on the coordination of the elements. While hematite has the structure corresponding *"Corundum"*, both magnetite and maghemite are structured as *"Spinel"* (Saharan et al., 2014). However, magnetite and maghemite are the commonly studied iron oxides. The reason may be attributed that they exhibit better magnetic characteristics in small enough particles sizes (Gutierrez et al., 2017). They can possess superparamagnetic characteristic at the diameters small enough like 20 nm (Luciano et al., 2013). Although they have almost the same physical properties, magnetite has a stronger magnetic property.

Magnetite is a black, ferrimagnetic mineral, that is known as "permanent magnet" (Kumar et al., 2010). Magnetite has a cubic geometric structure composed of Fe^{3+} and Fe^{2+} ions in a molar ratio of 2:1 ($FeO.Fe_2O_3$), and oxygen molecules placed in a regular basis along all three axes. It can also turn into a tetrahedral geometric structure by its oxidation named gamma iron oxide (γ–Fe2O3-maghemite) (Equation 1.7).

$$4\ Fe_3O_4 + O_2 \rightarrow 6\ Fe_2O_3 \qquad (1.7)$$

As maghemite is formed from the oxidized magnetite, its color appears red or brown. In the crystal structure of maghemite, which consists only of Fe^{3+} ions, half of the Fe^{3+} ions are tetrahedral, and the other half is octahedral (Scheinost, 2005). While half of the Fe^{+3} ions in magnetite are tetrahedral and the other half are octahedral geometry, all the Fe^{+2} ions are octahedral geometric structure (Scheinost, 2005, Wu et al., 2015). Another

derivative of magnetite is hematite, which is also called alpha iron oxide (α-Fe2O3), forming at high temperatures (>400˚C) and tends to antiferromagnetic structure (Jiles, 1998). Besides its geometric structure is hexagonal (Wu et al., 2015). The geometric structure of all iron oxides is shown in Figure 1.8.

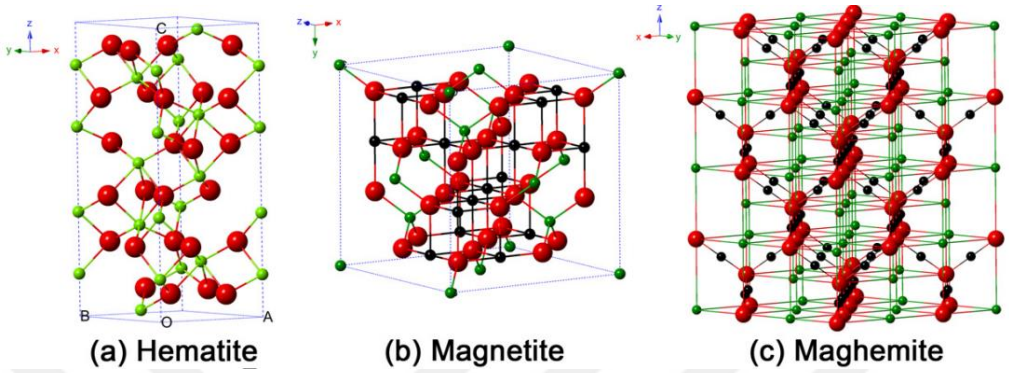


Figure 1. 8. The crystal structure of (a) hematite, (b) magnetite ve (c) maghemite kristal (the black ball is Fe^{2+}, the green ball is Fe^{3+}, and the red ball is O^{2-}) (Wu et al., 2015)

Recently, studies on various synthesis processes to improve the physical and chemical properties of IONPs have been increasing and actively researched (Ganapathe et al., 2020, Luciano et al., 2013, Nguyen et al., 2021). Besides being widely available in nature, they can be synthesized under the laboratory conditions. There are mainly several synthesis methods implemented for producing IONPs such as co-precipitation, thermal degradation, microemulsion, hydrothermal synthesis. By using these methods, some studies conducted for synthesis of magnetite, maghemite and hematite nanoparticles for various purposes were followingly compiled.

Biocompatible-maghemite nanoparticles, which have been used especially in biomedical fields, were synthesized by co-precipitation method in a study of Ramos et al.2015 carried out for the treatment of hyperthermia (cancerous cell). Magnetite nanoparticles initially obtained by co-precipitation were oxidized to form maghemite by treating with air heated at 200, 250 and 300 °C for 3, 5 and 8 hours (Múzquiz-Ramos et al., 2015). Oliveira et al.2018 has synthesized magnetite nanoparticles through thermal degradation method by mixing of Poly (vinyl alcohol) (PVA) and iron nitrate and obtaining polymer-metal (PVA/Fe^{3+}) complexes films (Oliveira et al., 2018). Bozkurt 2020 has synthesized hematite (α-Fe2O3) nanoparticles by microemulsion method consisting of n-heptane as oil phase, anionic surfactant of AOT, co-surfactant of 1-butanol. Compared to the

literature, it was noted that the hematite has been obtained with a very low particle size, approximately 13.1 nm (Bozkurt, 2020). Ahmadi et al. (2012) synthesized magnetite nanoparticles by conducting hydrothermal method. $FeCl_2$, $FeCl_3$ and NaOH that had a mole ratio of 1:2:8 respectively were placed into autoclave followed by heat treatment at high temperatures (100, 150 and 200 °C). The results showed that nanoparticles were of superparamagnetic behavior. Also the mean crystallite and physical size of the synthesized magnetite nanoparticles increased with hydrothermal temperature (Ahmadi et al., 2012).

1.7.2. Engineered magnetite nanoparticles

There is some information in various sources about the origin of the term "Magnetite". While some sources attribute it to the name of the mythological hero lived in ancient Greek, "Magnes" or "Magnetis", some sources attribute it to the origin of the name "Magnesia", a region where it was discovered in large quantities in Anatolia (Asia Minor) (Ganapathe et al., 2020, Melfos et al., 2011).

Magnetite (Fe_3O_4) contains both divalent (Fe^{2+}) and trivalent (Fe^{3+}) iron ions. By reason of the electron transfer between these ions, magnetite exhibits remarkable electrical and magnetic characteristics (Oliveira et al., 2018) depending on its size. The size of the magnetite particles is the key point for magnetism. Under a magnetic field, their magnetic properties in the bulk structure are not the same as at nanoscale. Magnetite nanoparticles can possess either ferrimagnetic (FM) or superparamagnetic (SPM) magnetisation properties (Nguyen et al., 2021). Under the absence of external magnetic field, magnetite nanoparticles having ferrimagnetic properties still exhibit magnetisation to a certain value, however they do not respond magnetically when having superparamagnetic properties considering the same situation. That is, they are not permanently magnetized without an external magnetic field needed for triggering the superparamagnetic properties (Luciano et al., 2013). There are some advantages in both of the magnetisation properties: 1) superparamagnetism ensures to decrease tendency to aggregation of nanoparticles as well as it behaves very sensitive to reach the magnetic field controlly, 2) ferrimagnetism bears strong magnetic properties that could be potentially needed intense magnetization applications.

The efficiency of the magnetite during the adsorption of water pollutants is so important, hovewer it is just as important in the process after the adsorption. At this point, the importance of the effectiveness of magnetism of magnetite nanoparticles emerges. Because at the end of the adsorption process, magnetite is captured by a magnetic field and the pollutant species that are held on it are desorbed that is very important for the sustainability of the process.

1.7.3. Engineered magnetic activated carbon (PAC-MNP) composite nanoparticles

Considering limitations encountered with various engineering nanoparticles such as filtration, dispersion, creating turbidity and high cost of reduction, nanocomposites defined as the materials of 21st century have revealed that they can overcome the challenges with their advanced and superior properties (Pandey et al., 2017). So, the possible opportunities appear in terms of efficiently use of energy, their role in wastewater treatment and biochemical medicine fields (Luo et al., 2015). Nanocomposites are of a structure having at least two components of which one is in nanoscale, with superior and desired physical and chemical properties. The effectiveness of each adsorbent material that makes up the composite is thus increased, and its best properties are featured. The sizes of composites at nanoscale can ensure more accessibility in terms of structural and electronic degrees of freedom compared to bare form (Calandra et al., 2013), and the phase interfaces can greatly be improved.

Nanocomposite materials can be made up of various matrixes (Camargo et al., 2009) consisting of metals, polymer, ceramic, clay, etc. Magnetic nanoparticles with high surface area and magnetisation property could be one of the best adsorbents against the water pollutants, and they can be functionalized fabricated/coated with activated carbon, clay, zeolite, polymer, as well.

For the combination of adsorbents in composite formation, it is essential to choose adsorbents with recoverability, availability and low cost. As mentioned in the previous sections, adsorbents can be natural and artificial. Natural adsorbents have advantages such as being low cost and causing less waste production, as well as disadvantages such as limited selectivity. While natural adsorbents are mostly preferred in industrial applications, the development of artificial adsorbents that can perform more economically

in wider application areas is also a matter of research. Among these adsorbents, *Activated Carbon* is one of the artificial adsorbents widely used in adsorption processes, and having large surface area (500–2000 m^2 g^{-1}) (Mehrabi et al., 2015) and unique pore structure obtained from materials with high carbon content, and tendency to capture various pollutants as well as not causing to form of dangerous species, like as ozone and free radicals (Al-Ghouti et al., 2010, Iram et al., 2010). However, due to its high recovery cost, the preference of activated carbon appears as limiting factor. After adsorption process, activated carbon is generally separated from media by filtration or centrifugation, which are taking a lot of time or more expensive, respectively. Some blockages may occur in filters which results the loss of activated carbon in filtration method, while centrifugation is not reasonable method as it is not economical for the separation (Gu et al., 2019). As one of the prerequisite ways for coming over the limitation of high recovery cost, it can be created a new hybrid adsorbent (Zhou et al., 2012) with the synthesis or combination of activated carbon with the magnetic properties of iron oxides nanoparticles (composite). Because nanocomposites composed of iron oxide nanoparticles exhibit specific magnetic properties so that ensure an easy operation. On the other hand, magnetic nanoparticles are also the materials that tend to be easily oxidized and agglomerated in air due to their structural properties. To control this, an idea is that activated carbon particles coated/modified with magnetic nanoparticles can ensure their stability (Jain et al., 2018, Zhou et al., 2012).

Many researchers have focused on coating/combining/doping magnetic iron oxide nanoparticles into activated carbon for good interaction with contaminants in effluents and promoting high surface reactivity. Shahrashoub and Bakhtiari, (2021) synthesized coated-magnetite composites with both powdered activated carbon (PAC) and granular activated carbon (GAC) using green tea extract as reducing agent during the synthesis process. They achieved copper removal with the maximum adsorption capacities of 23.61 mg/g and 13.37 mg/g, respectively. As MNP-PAC exhibited a higher adsorption performance compared to MNP-GAC, it was especially recommended for the removal of copper (Shahrashoub and Bakhtiari, 2021). In another copper removal study, Gu et al. (2019) prepared magnetic activated carbon particles (MACP) synthesized by doping Fe_3O_4 magnetite into the activated carbon matrix by precipitation method. The MACP properly carried out the removal of Cu^{2+} ions from the aqueous solution. A significant

increase was observed in the adsorption capacity of the composite material formed by the MACP components with Fe_3O_4 nanoparticles. It was also emphasized that the superior magnetic property provided to the adsorbent highly increased the separation efficiency and regeneration of the adsorbent from the solution (Gu et al., 2019). Amornwutiroj et al. (2019) carried out controllable synthesis of mesoporous magneticte nanoparticles impregnated with activated carbon to form two types of Fe_3O_4/AC composites for the efficient removal of hexavalent chromium. It was underlined that a high saturation of magnetization values was obtained for the adsorption and desorption processes. The adsorption performance results of Fe_3O_4/AC (w) and Fe_3O_4/AC (e) were obtained as 178.57 mg/g and 147.06 mg/g, respectively. (Amornwutiroj et al., 2019). Jain et al. (2018) studied the removal of heavy metals (Cr(VI), Cu(II) and Cd(II)) from aqueous solution with both bare magnetite nanoparticles and its composite form which is Fe_3O_4/AC synthesized by co-precipitation method). It was also recorded that the desorption and regeneration studies of these nanoparticles were effectively performed without any mass loss (Jain et al., 2018).

Liu et al. (2019) synthesized functionalized Fe_3O_4/AC which consist of abundant surface functional groups, increased specific surface area, and respond sensitively to magnetic field. Through the composite nanoparticles, fast and effective removing of rhodamine B (RhB) and methyl orange (MO) were realized with a maximum adsorption capacity of 182.48 mg g^{-1} and 150.35 mg g^{-1}, respectively (Liu et al., 2019). Juang et al. (2018) fabricated nanocomposite by chemical binding of magnetite on activated carbon to conduct the adsorption of methyl orange (MO) from aqueous solution as well. The results indicated that the nanocomposite effectively performed the adsorption with the highest capacity of 324 mg/g as well as the nanocomposite were able to be easily recovered (Juang et al., 2018).

1.7.3.1. Adsorption studies conducted with PAC-MNPs for adsorption of ammonium and phosphate ions

Magnetic activated carbon composite nanoparticles could exhibit much tendency to grab any negative ions (Mehrabi et al., 2015) such as phosphate owing to providing porous structure that is charged with positive ions. These iron-based composites were focused on various studies that were compiled. Shi et al. (2011) studied phosphate adsorption on

activated carbon impregnated with Fe (III) oxide in batch experiments. Both activated carbon and the composite performance on adsorption was compared through batch experiments. The experiments performed at low pH 3.0 concluded that phosphate adsorption performance of the composite nanoparticles was 98.3 mg/g and for activated carbon was 78.90 mg/g (Shi et al., 2011). Zach-Maor et al. (2011) studied on synthesis, performance, and modeling of granular activated carbon impregnated with iron oxide nanoparticles, having a nanocomposite layer with a large surface area and a porous structure as well as revealing a high efficiency phosphate removal with a capacity of 435 mg PO_4/g Fe (corresponding to 1.1 mol PO_4/mol Fe_3O_4) (Zach-Maor et al., 2011). Wang et al. (2012) tested phosphate removal by two series of iron-doped activated carbons modified by Fe (II) and Fe (III), respectively. According to the results it was revealed that the Fe (II)-based composite exhibited better adsorption performance with 14.12 mg/g compared to the Fe (III)-based composite with 8.73 mg/g (Wang et al., 2012). Khodadadi et al. (2017) achieved phosphate removal with 100% removal efficiency at the conditions of pH=4, t=90 min by using powdered activated carbon doped with iron oxide nanoparticles considered as superparamagnetic feature sorbent (Khodadadi et al., 2017). Suresh Kumar et al. (2017) searched on iron oxide nanoparticles doped with granular activated carbon (Fe-GACs) and examined the importance of their porous structure on phosphate removal. They reported that, due to the difficulty of coating micropores of GACs with iron oxide nanoparticles, phosphate adsorption was able to be realized in the high-fraction mesopores present in Fe-GACs (Suresh Kumar et al., 2017). Braun et al. (2019) conducted phosphate adsorption on coconuts shells-based granular activated carbon doped with iron oxides (GAC-Fe) by synthesis method of chemical precipitation. The results emphasized that pH of the solution had remarkable effect on adsorption process, which causes the surface charge of the composite to be positively charged when pH lower than 3.5. So, it was performed the best adsorption capacity at pH=3.0, and qmax reached to 2.874 mg/g (Braun et al., 2019).

To date, according to our knowledge, there is limited number of studies in the literature based on the adsorption of ammonia with iron-based nanoparticles (Drenkova-Tuhtan et al., 2017, Gulyás et al., 2021, Liu et al., 2013a, Zare et al., 2016). As well, there is only one study in the literature based on the adsorption of ammonia with magnetic activated carbon composite, which belongs to (Ren et al., 2021). They modified activated carbon

(Fe-AC) doped with Fe $(NO_3)_3$ and calcined at high temperature. Then the Fe-AC was introduced to low temperature (at 10, 15, and 25 C°) artificial wastewater. The adsorption capacity was approximately 0.14 mg/g obtained from different low temperature conditions. They also specified that the adsorption mechanisms were physical adsorption and chemical adsorption.

1.8. Importance of Crucial Nitrogen and Phosphorus Nutrients' Recovery

Phoshorus, as an essential element, is among the other prominent elements of life such as oxygen, hydrogen, potassium, nitrogen and carbon. Phosphorus is one of the limiting nutrients for plants, that should be in the form of orthophosphate, which can be used biologically, and the lack of this form creates a need for fertilizer that is mostly produced from finite phosphate reserves. In 2020, the European commission included phosphate rocks in the list of 30 critical raw materials, and phosphate is associated with agricultural and food safety on this list (EU, 2020). The estimations on the reserves of phosphate rocks are towards decreasing within the next 100 years (Tercero et al., 2018). Phosphate rocks, as non-renewable resources, are predicted that after 2035, the need for phosphorus will exceed phosphorus resources (Elser and Bennett, 2011). While the formation of phosphate rocks, takes 10-15 million years, their consumption takes place within a century (Havukainen et al., 2016). For this reason, the use of secondary phosphorus sources is gaining importance day by day.

In the early 20th century, increasing the necessity of food production due to growth of world’s population resulted in the advancement of fertilizer industry. As another essential nutrient, ammonia, although it is not among the critical raw materials, its role in fertilizer production is critical. Both of N and P nutrient ions are crucial substances for struvite production which can substitute with easily soluble industrial fertilizers. Ammonia synthesized from atmospheric nitrogen mostly through an old industrial Haber-Bosch process (Liu, 2014) has an importance of being the second most produced industrial chemical across the world. According to the statistics, the generation of reactive nitrogen has risen up more than 20 times over the years from 1860 to 2005. Recently, it is estimated as 187 tonnes annually, which corresponds about 1.5-2 times more than the planet generates naturally. It's also estimated that about half of the amount generated annually of reactive nitrogen ends up in the oceans (Aloe et al., 2014). So, the production of

ammonia by artificial means may cause disruption of the natural balance as a result of intervention in the nitrogen cycle in nature as well as the concern of the release of greenhouse gases (e.g carbon dioxide emissions) during the synthesis processes. In especial, in 2018, USA caused 13.5 million tons of carbon dioxide emissions by itself as a result of industrial ammonia synthesis (EPA, 2020). Thus, seeking safer, sustainable, and also economical approaches and sources should be assessed for reliable struvite-like fertilizers' production. At this point, the issues of nutrient management and resource efficiency gain great importance.

2. MATERIALS AND METHODS

2.1. Materials

2.1.1. Preparation of synthetic wastewater

Simultaneous N-P containing solution (1000 mg/L) was prepared by taking 3.8 g and 4.25 g from NH_4Cl and K_2HPO_4 respectively, so that 1 L of synthetic wastewater was obtained. It was actually intended to simulate the effluents obtained from B-stage of High Rate Activated Sludge systems. All used chemicals with analytical grade were mixed with deionized water to obtain desired synthetic solution.

2.2. Methods

2.2.1. Synthesis of bare and composite magnetic nanoparticles

The co-precipitation method was used in the synthesis of both bare magnetite (Fe_3O_4 - MNPs) and magnetic activated carbon nanoparticles (Composite / PAC-MNPs). While Bare MNPs were synthesized with the molar ratio 2:1 of Fe^{+3} and Fe^{+2} salts, the Composite MNPs were formed with the molar ratio 2:1 of the synthesized Fe_3O_4 powders and $Functionalized_{HCl}$ Powdered Activated Carbon (PAC), respectively. In the synthesis Bare MNPs, it was followed the previous study conducted by Gulyas et al. (2021). On the other hand, in the synthesis of PAC-MNPs, the procedure studied by Gu et al. (2019) was followed, but applying some minor modifications. In the modified procedure, 1 L of HCl (4N) was used as an activation agent in order for commercial powdered activated carbon (PAC) to be chemically oxidized or functionalized. During the activation process of PAC, the occurrence of various functional groups such as carbonyl, carboxylic and hydroxyl groups was provided onto the PACs' surfaces. The $Functionalized_{HCl}$ - PACs were finally introduced to the iron-based solution with a ratio of PAC:Fe_3O_4 = 2:1 (as optimal ratio in the study of Gu et al. (2019)). The PAC-MNPs slurry stirred at ambient temperature for 4 h, then NaOH (5 M) solution was added rapidly till the pH reached to ~11. The slurry was then washed several times, and right after it was left dehydrated in a vacuum oven at 100 °C. After that, the dried and functionalized PAC was deposited on the bare MNPs. In the Figure 2.1, it demonstrates PAC-MNPs synthesis procedure. As seen, the orange color

initially formed due to the iron ions, then converted to black precipitates that were realized right after the addition of the previously produced funtionalized$_{HCl}$ – PACs.

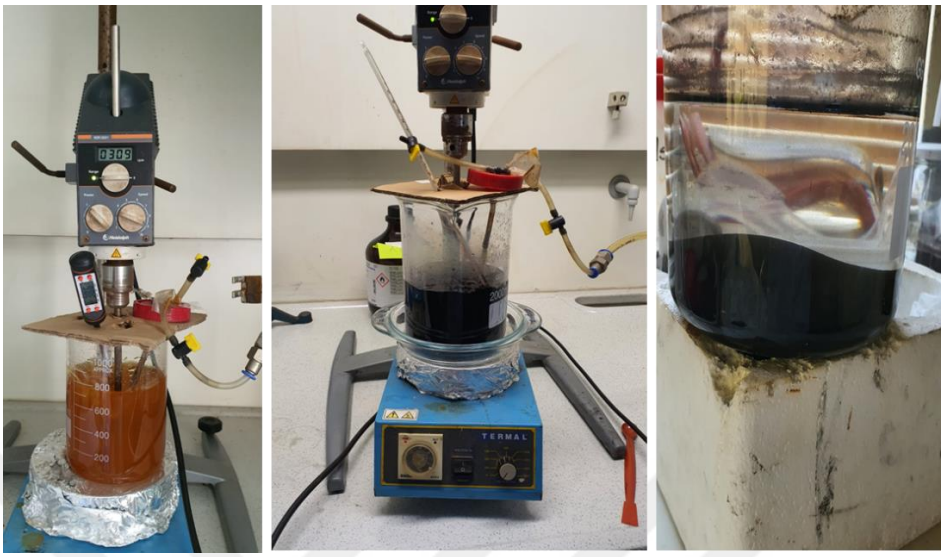


Figure 2. 1. PAC-MNPs synthesis

As mentioned in the followed studies, washing process was carried out several times with deionized water and/or ethanol after the formation of black precipitates. The washed nanoparticles were left to settle with the help of magnet. Afterwards, they were spread on porcelain plates and placed in an electric oven for drying (see in Figure 2.2).

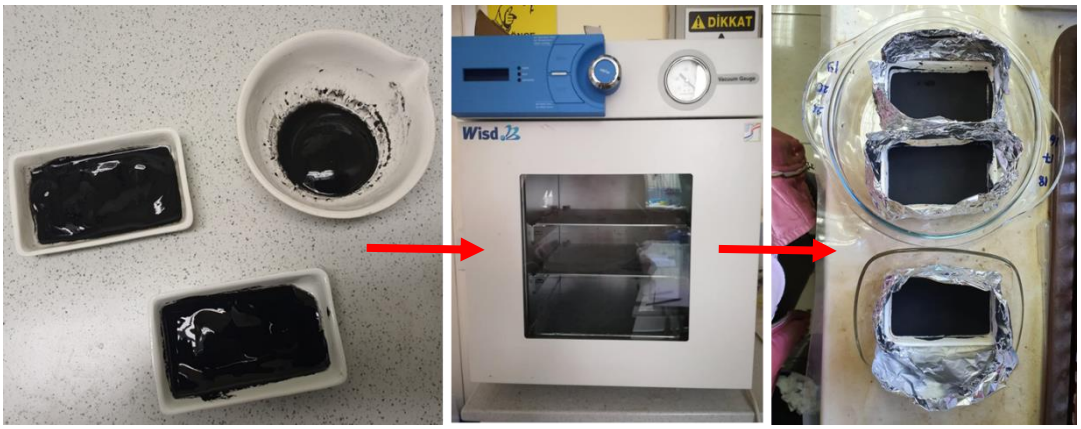


Figure 2. 2. Drying process of the composite nanoparticles

By using a mortar and pestle, the dried nanoparticles were crushed and smashed till obtaining powder form as possible, then they were grounded by beat beater with 0.5 mm grinding media. Finally, the beats were separated from the smooth powdered nanoparticles for ready-to-use (see in Figure 2.3).

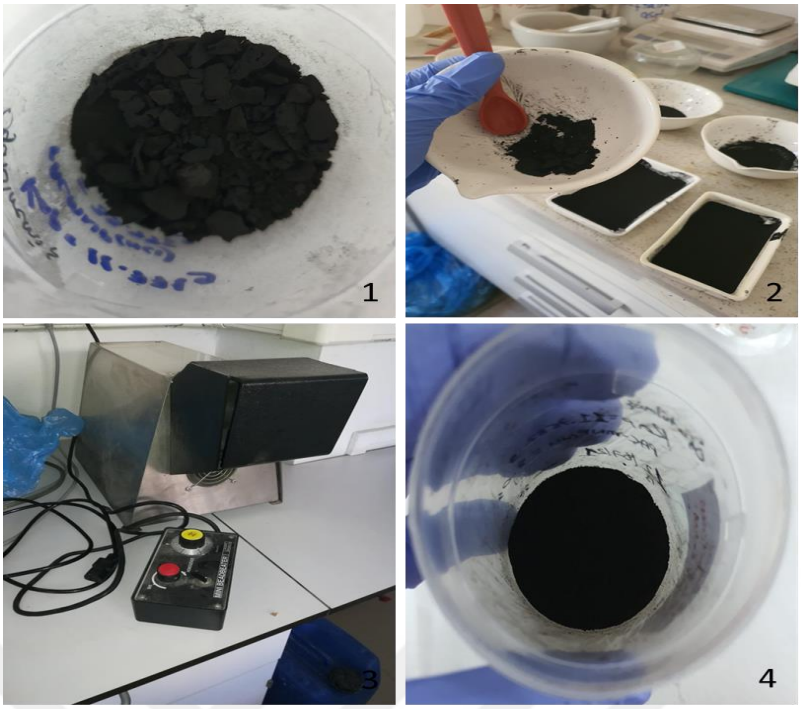


Figure 2. 3. Grinding process of dried composite nanoparticles

2.2.2. Physicochemical characterization of PAC-MNPs

Zeta Potential (IEP), Point of Zero Charge (pHpzc), SEM, EDX, FTIR and BET measurements were investigated in order to characterize the structural and morphological properties of magnetic activated carbon (PAC-MNPs) as well as the adsorption mechanisms of ammonia and phosphate species.

The relationship of pH versus surface active centers of PAC-MNPs was clarified by the two significant terms: pHpzc and IEP. While the pHpzc value was obtained from the well-known batch equilibration technique which is potentiometric titration, the IEP was detected by Zeta Potential Measurement. During the point of zero charge and zeta potential measurements, inert electrolyte solutions such as 0.1 M NaNO3 and 0.01 M NaCl were used respectively, in order to obtain a stable point that the surface charge density would not affect from ionic strength. In order for pHpzc of PAC-MNP to be detected, a 40 mL of 0.1 M $NaNO_3$ inert solution was added into the beakers. The initial pH of solutions was adjusted from 3 to 11 using either 0.5 M HCl or 0.5 M NaOH by Hach HQ40D-PHC201 pH-meter. 0.02 g of PAC-MNPs were added in 100 mL Erlenmeyer flasks, and right after pH adjustment of the solutions were done. All the flasks

were shaken in an orbital shaker at 150 rpm and room temperature for 24 hours. Then the final pH was measured of the solutions for the pHpzc measurement, the study of Shah et al. (2015) was followed (Shah et al., 2015). In order for IEP of PAC-MNP to be detected, it was measured with Zetasizer 3000 HSa (Malvern Ltd), similarly by adjusting the pH of the suspensions between 2 and 11 using either by 0.5 M HCl and 0.5 M NaOH. 0.01 g of PAC-MNP was added into 50 mL of 0.01 M NaCl solution. the study of Zhang et al. (2018) was followed (Zhang et al., 2018).

The functionalized PAC, the incorporation of raw Fe_3O_4 into modified PAC, and the adsorption of N and P species onto composite PAC-MNP have been confirmed from Fourier transform infrared spectroscopy (FT-IR; Jasco FT/IR-4700) spectra. FT-IR (Figure 2.4) was conducted through KBr method with an area of 4 cm^{-1} under atmospheric air and vacuum conditions to investigate the ammonia and phosphate adsorption relationship on PAC-MNP. The range of the measurement were between 4000-400 cm^{-1} for all samples.

Scanning electron microscopy (SEM) was used for $Functionalized_{HCl}$ PAC and PAC-MNPs to investigate their surface morphology, while Energy dispersive X-ray spectrometry (EDX) was performed to determine the elemental composition of them. Both of the analysis was conducted with a FEI-Philips XL30 ESEM-FEG (U.S.) (Figure 2.4). The results obtained with EDX analyzes were plotted as elemental ratio (%) of each component.



Figure 2. 4. FT-IR (left) and SEM (right)

The surface areas of both bare magnetite nanoparticles (MNPs) and magnetite activated carbon nanocomposites (PAC-MNPs) were measured with the help of BET analysis.

2.2.3. Adsorption experiments

Adsorption of ammonia and phosphate synthetic solution (N-P solution) conducted on PAC-MNPs was performed using batch experiments in a temperature-controlled shaking incubator (IKA, Germany) at room temperature and 220 rpm (Figure 2.5).



Figure 2. 5. Batch experiments (Gulyás et al., 2021)

The desired initial pH adjustment and control were then done with 1M HCl and NaOH solution. PAC-MNPs were put into a 20 mL volume of N-P solution, then introduced to an ultrasonic bath (Bandelin SONOREX digital 10p) for 10 minutes to allow the PAC-MNPs to be distributed well. After all the preparation of adsorption process done, the samples were left shaking as described above. Before the experimental measurements carried out to investigate the amount of the species adsorbed, PAC-MNPs were separated with the help of a magnet. The solution phase then filtered with membrane filters having the size of 0.45. The process was briefly illustrated as in Figure 2.6.

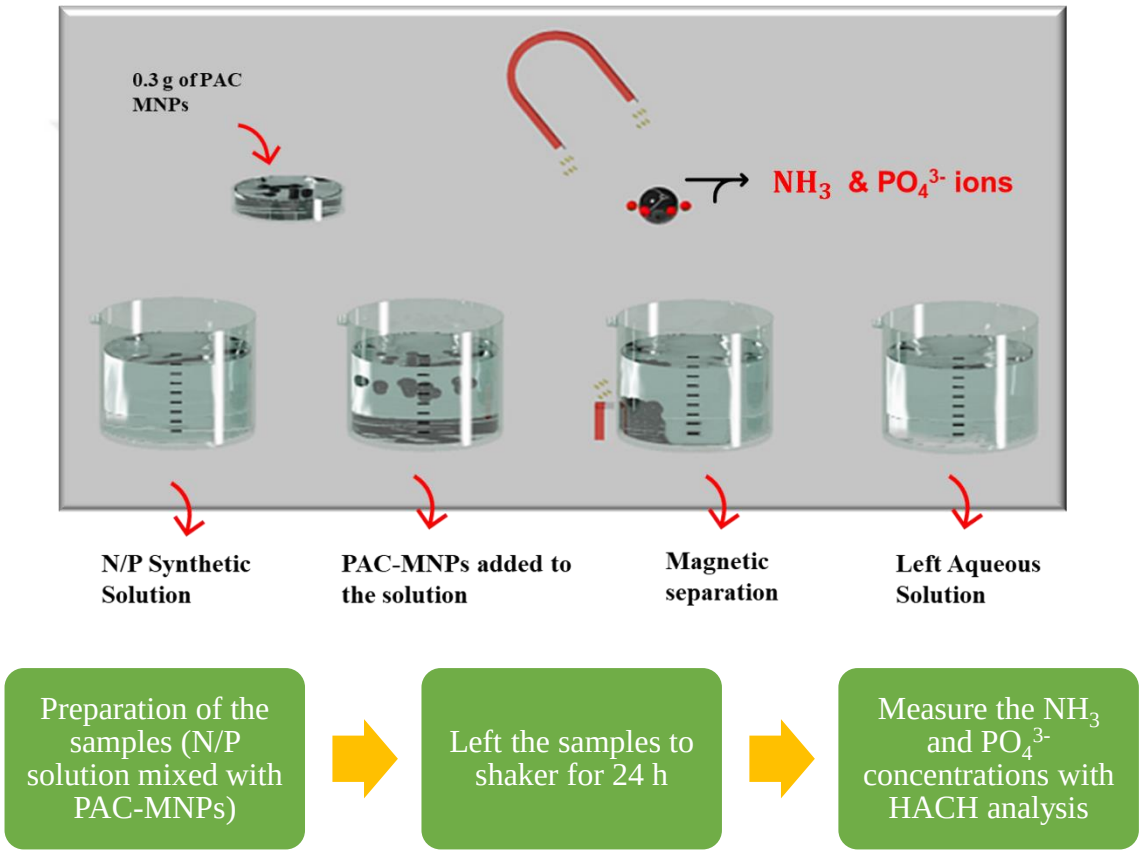


Figure 2. 6. Flow diagram of adsorption experiments

Initial set of the adsorption tests was based on the understanding the function of the initial ammonia and phosphate concentration in the synthetic N-P solution. Firstly, N-P solutions with different concentration values varying from 50 to 1000 mg/L have been studied. In this experiment, pH was initially set to ~3. Followingly, in order to understand the effect of initial pH species to be adsorbed, the various pH values were also studied (e.g., at pH 3, 4.5, 9, 10). In the equilibrium experiments, 0.3 g of PAC-MNPs were used

for the synthetic N-P solution, and other conditions are as described in the previous section.

In the second set of the adsorption studies, the kinetic experiments of the N-P solution (~500 mg/L initial P; pH ~9) were performed with 0.3 g of PAC-MNPs for different contact times (0, 120, 240, 360, 480, 600, 720, 840, 960, 1080, 1200, 1320 and 1440 minutes), and other conditions are as described at the first section.

In the third set of the adsorption studies, the effect of adsorbent dosage/amount on ammonia and phosphate adsorption was studied for 0.3, 0.5 and 1 g. The tests were conducted with the conditions of the initial N-P concentration which was ~1000 mg/L and pH reached to ~4.5, and other conditions were the same as described in the first section.

2.2.4. Desorption experiments

Desorption experiments were performed to recover ammonia and phosphate rich solution, also to verify the potential reusability of PAC-MNPs. The appropriate contact time of the desorption process was considered as 1 hour and left shaking for 250 rpm, with reference to the study of Gulyás et al., (2021). Desorption of N and P species from PAC-MNPs was carried out at room temperature, and two different types of desorption solutes were used such as HCl and NaOH solutions (20ml), which were of various molarities (0.5 M and 0.1 M, respectively), and compared their effects on desorption capability. Experimental conditions for adsorption were 15 g/L of PAC-MNP with initial pH = 10, and initial N-P concentration: ~500 mg/L. A simple flow scheme of the desorption experiments which clarify the cycls was demonstrated in Figure 2.7. The adsorption-desorption cycles were performed 4 times. Both adsorption and desorption performances were experimentally measured after each cycle.

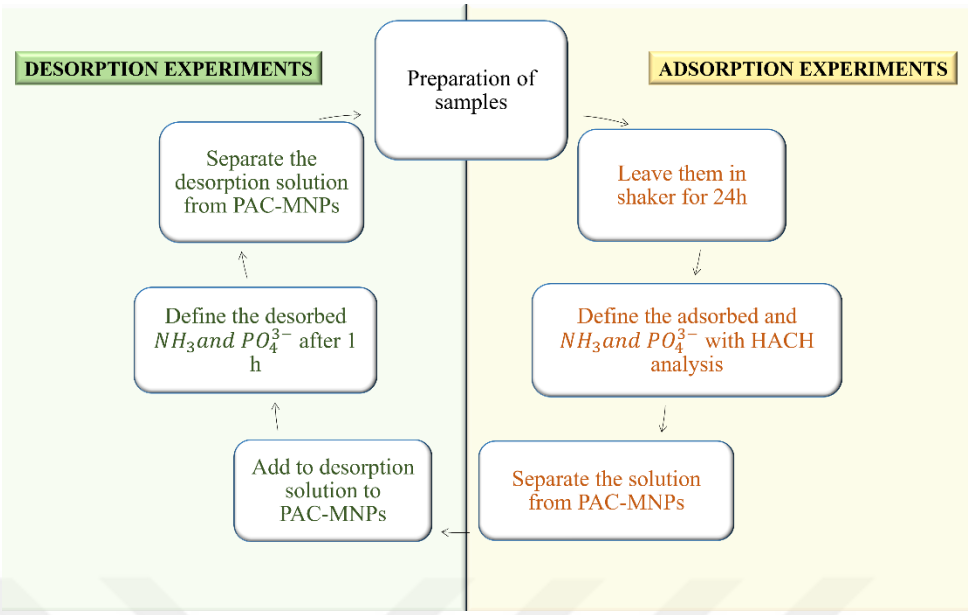


Figure 2. 7. Flow diagram of the cycles of adsorption-desorption experiments

2.2.5. Analytical - experimental measurements

Phosphate species in the solutions were measured with the Amino Acid Method (Method 8178), which is a fast and reliable colorimetric measurement method. As a result of the reaction occurring among the phosphate and reagents (1 mL Amino Acid and 1 mL Molybdate Reagents), blue color appears in the sample solution, and phosphate value in the range of 0.0 to 30,0 mg/L results. Phosphate concentration was measured with a HACH DR2500 Spectrophotometer at a wavelength of 880 nm.

Similarly, Nesslerization Method was used for the measurement of ammonia as a fast and reliable measurement method. Three different reagents, namely Mineral Stabilizer, Polyvinyl Alcohol and Nessler reagent were used. As a result of the reaction between the ammonia and them, a yellow color is formed in the sample solution. Ammonia concentration was measured at 380 nm wavelength with HACH Spectrophotometer.

2.2.6. Conducting the studies of kinetics and isotherm models

It is important to determine the appropriate time for the adsorption reaction reaching the equilibrium as well as to obtain information about the adsorption mechanism. Adsorption kinetics and isotherm studies help understand such these information. The kinetic and isotherm models were formed with Microsoft Office Excel software. The batch

experiments were performed for these tests. Initial concentration of the synthetic N-P solution in test flasks was ~500 mg/L and adjusted for at pH 9-10. From the beginning of the kinetic test, a flask was taken from the shaker at different predetermined time intervals, and the concentration of ammonia and phosphate in the sample solution was determined by analytical measurements. Before the measurement, the liquid phase which consists of remaining N and P species was separated from the adsorbent with a magnet placed at the bottom of the sample flask, and then the liquid phase was passed through a 0.45 μm membrane filter.

In this study, three kinetic models, which are widely studied in the literature were used. These are the pseudo-first-order (PFO), pseudo-second-order (PSO) and Elowich models, which are expressed in Equations (2.1), (2.2) and (2.3), respectively.

$$Q_t = Q_e(1 - e^{-k1t}) \tag{2.1}$$

$$Q_t = \frac{(t \times k2 \times Qe^2)}{(1 + k2 \times Q_e \times t)} \tag{2.2}$$

$$Q_t = \frac{\frac{1}{\beta}}{\ln(1 + \alpha \times \beta \times t)} \tag{2.3}$$

where Qe (mg/g) is the equilibrium amount of NH_3-N and PO_4^{-3}-P adsorbed by the PAC-MNPs, Qt (mg/g) is the amount of NH_3-N and PO_4^{-3}-P adsorbed by the PAC-MNPs at time t (min), and k1 (1/min) and k2 (g/(mg.min)) are the rate constants of the pseudo-first-order model and the pseudo-second-order model, respectively. The plots of Qt against t, and their fitting curves indicated the most appropriate model for this study.

Besides, the determination of the adsorption isotherm is very important to specify the maximum adsorbed ammonia and phosphate molecules on PAC-MNPs' surface. Various adsorption isotherms have been investigated in the adsorption phenomenon (Foo and Hameed, 2010). In this study, the four most common isotherm models which are Langmuir, Freundlich, Sips and Redlich–Peterson isotherms were studied.

The equations in which the parameters used in determining the isotherm model were calculated with the Chi-square (x^2), correlation coefficient (R^2) and normalized root mean square error (NRMSE) (Table 2.1).

Table 2. 1. Isotherms parameters used for model determination (Gulyás et al., 2021)

Parameter	Equation
Chi square	$x^2 = \sum_{i=1}^{n} \frac{(q_{exp} - q_{calc})^2}{q_{calc}}$
Correlation coefficient	$R^2 = 1 - \frac{\sum_{i=1}^{n}(q_{exp} - q_{calc})^2}{\sum_{i=1}^{n}(q_{exp} - q_{exp,mean})^2}$
Normalized root mean square error	$NRMSE = \frac{\sqrt{\frac{\sum_{i=1}^{n}(q_{exp} - q_{calc})^2}{n}}}{q_{exp,max} - q_{exp,min}}$

where n is the data points number; q_{exp} represents the amount of adsorbed species obtained from the experiments; q_{calc}; represents the amount of adsorbed species calculated by models; $q_{exp,max}$ and $q_{exp,min}$, $q_{exp,mean}$ represent the maximum, minimum and mean values of the adsorbed species obtained from the experiments (Gulyás et al., 2021).

3. RESULTS AND DISCUSSION

3.1. Characterization of The PAC-MNPs

Various characterization measurements are carried out to determine the physical, chemical and magnetic properties of PAC-MNPs as well as their structural and surface properties. In this study, Fourier transform infrared (FTIR) spectroscopy, scanning electron microscopy (SEM), energy dispersive X-ray spectrometry (EDX), Brauner-Emmet-Teller and (BET) characterization methods were performed.

3.1.1. Point of zero charge (pHpzc) and zeta potential (IEP) results

The relationship of pH versus surface active centers of PAC-MNPs was clarified by the two significant terms: pHpzc and IEP. While the pHpzc value was obtained from the well-known batch equilibration technique which is potentiometric titration, the IEP was detected by Zeta Potential Measurement. The common definition of the point of zero charge (pHpzc) corresponds to the pH value at which the surface charge density or electrical state of an adsorbent is neutral. The result was obtained from a stable point occurred during the PAC-MNPs contacted with the inert electrolyte solution (salt solution), in other words from a point at which surface charge density is not affected from ionic strength. This point is clearly observed when the initial pH (pHinitial) and ΔpH (pHfinal- pHinitial) values intersected at the ΔpH equals zero. The pHpzc was around 6.54 for PAC-MNP as clearly observed from the Figure 3.1.a. The similar result was also obtained from other studies investigated with such similar composite adsorbents (e.g., iron based activated carbon composites) (Barbosa et al., 2020, Braun et al., 2019, Fayazi et al., 2015, Kakavandi et al., 2015, Liu et al., 2010, Mehrabi et al., 2015, Muñiz et al., 2009, Shah et al., 2015). At this pHpzc, 6.54, the total positive charges on the surface of PAC-MNPs equals to the total negative charges, which is generally interpreted as the surface charge of the PAC-MNP being positive when the solution pH is kept lower than pHpzc and vice versa.

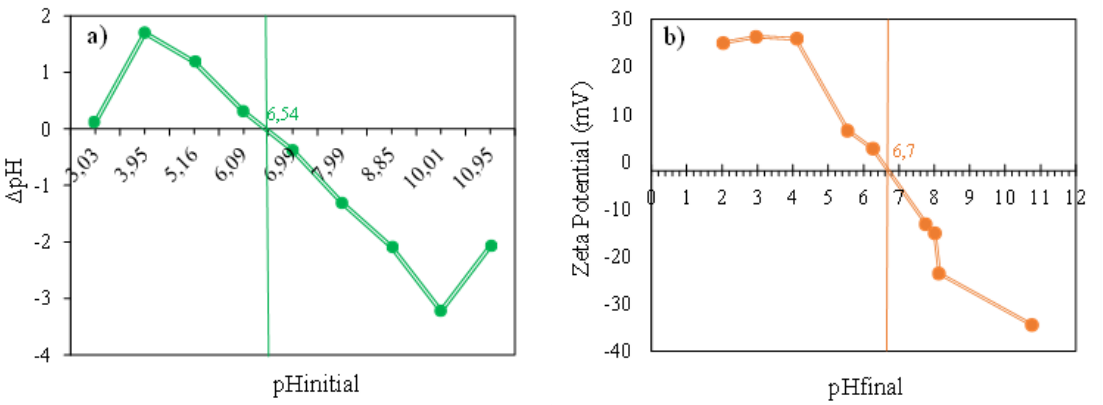


Figure 3. 1. a) pHpzc value of PAC-MNPs b) IEP value of PAC-MNPs

Moreover, another term that is similarly used to determine the electrical state of the surface of an adsorbent in solution is isoelectic point (IEP) which is obtained from Zeta Potential Measurement. The IEP was around 6,7 for PAC-MNP as demonstrated in the Figure 3.1.b. The thing that differs the IEP from PZC is dealt with the external surface charge of particles in solution is to have the neutral charge at the external surface, which means no movement under that electric field. Thereby, the external part (or shear plane) at which the electrokinetic potential becomes zero conceived as IEP value. On the other hand, PZC varies in response to both external and internal (net total) surface charge of the particles in an inert solution (Menéndez et al., 1995). As a result of the 24-hour potentiometric titration experiment, the tendency of H^+ protons to be retained by the material decreased until pH<6.5, and so that the internal charge turned from negative to positive. As well, after pH> 6.5, the tendency of OH^- groups to be retained by the material increased this time, which indicates that the internal charge changed from negative to positive. The resulted values obtained from Zeta Potential and potentiometric titration measurement were very close to each other. This fact about the close results is emphasized in a study of Tran et al. (2017), which gives information about the surface charge distribution, and accordingly, it can be said that the surface charge has a homogeneous distribution, since the difference (PZC - IEP) obtained for the PAC-MNP is close to zero (Tran et al., 2017). Starting from this point, the most suitable pH value was tried to be determined for efficient adsorption of ammonia and phosphorus species at the same time. It is clear from the graphs in Figure 3.1 that regions where IEP is negative coincide with regions where PZC values are also negative. Therefore, there is no region in the material where one is negative and the another

is positive. Therefore, a solution containing ammonia and phosphorus species was studied at both acidic (3) and basic (10) pH values. The findings obtained were consistent with the PZC and IEP values of the material and provided the clarification of the adsorption mechanism. In addition, the effect created by the difference caused by the internal and external charges after adsorption (as seen in the graph in Figure 3.1.a) can be interpreted in accordance with the definition of pHpzc. In fact, in adsorption experiments performed at pH> 6.5 (e.g., at pH 9 -10), the tendency to retain OH^- or PO_4^{-3} anionic groups has increased while the internal charge is positive, and this situation is reflected as negative on the external charge. Because the zeta potential is negative at pH>10. It is considered that the inner surface complexation might have been the reason of the simultaneous adsorption of ammonia that was captured at pH>6.5 while the internal charge was positive. That is, the chemical bonds and/or electrostatic attraction between the nutrient ions and the main functional groups of PAC-MNP may have caused the ammonia adsorption.

3.1.2. BET results

The BET analysis was carried out for both the bare MNPs and its composite form (PAC-MNP). It has been determined that both adsorbent materials had a very high surface area. While the surface area of the bare MNPs is approximately ~100 m^2/g, the PAC-MNPs have much higher value of 682 m^2/g. In the literature, it has been reported that nano-sized magnetite adsorbents have a high surface area of approximately 100 m^2/g (Cornell and Schwertmann, 1997, Ficai et al., 2012, Hou et al., 2020, Iconaru et al., 2016, Lee and Kim, 2019, Liu et al., 2018), that contributes abundant surface functional groups for better adsorption performance. In this study, as the surface area of magnetite is compatible with the literature, it was supported that the sizes of the bare magnetite particles were in nanoscale. The surface area of PAC-MNP is also compatible with the literature (Gu et al., 2019, Panneerselvam et al., 2012, Saharan et al., 2014, Yang et al., 2008). According to the synthesis procedure, PAC-MNPs was fabricated with the molar ratio of 2:1 of Fe_3O_4 powders and $Functionalized_{HCl}$ Powdered Activated Carbon (PAC). Gu et al. (2019) similarly synthesized magnetic granular activated carbon adsorbent (MAPs) with various composition ratios. Among them, AF3 had the same composition ratio - 2:1 just as PAC-MNPs and its surface area was 202 m^2/g. The results revealed that all the MACPs showed better adsorption performance compared to bare AC samples for Cu ions removal (Gu et

al., 2019). Panneerselvam et al. (2012) synthesized three different adsorbents, which are activated carbon from palm kernel shell (PKSAC), magnetite nanoparticles, the composite PKSAC-Fe3O4. Comparison of the adsorption performance of these three adsorbents for dye removal showed that the composite form was the most efficient one (Panneerselvam et al., 2012). Yang et al. (2008) have also fabricated magnetite activated carbon from rice husk (RHC) to remove of MB. Comparing the efficiency of both the bare activated carbon with magnetite-RHC showed that a better adsorption performance was observed through magnetite-RHC as it is of high surface area and large pore size (Yang et al., 2008).

3.1.3. FT-IR results

The FTIR analysis carried out for both the functionalized$_{HCl}$-PAC and its composite form (PAC-MNP before adsorption) was demonstrated in the Figure 3.2. The adsorption peaks of functionalized$_{HCl}$-PAC and raw PAC-MNPs stayed at similar positions, however the intensities of their peaks showed differences. The IR spectrum for raw-functionalized PAC exhibits C=C stretching vibrations at 1608 (Rodrigues et al., 2020), and C-O stretching vibrations at 1287, which are typical vibrations present in carbonaceous materials. On the other hand, the IR spectrum of the PAC-MNP shows the presence of COOH groups; –C=O stretching vibration is at 1623 cm^{-1}, while –OH stretching vibration is in carboxy group in the region of 3415 cm^{-1}. Moreover, two new peaks were observed for PAC-MNPs. One is at 743 that can be ascribed to Fe-O-H bending vibration, the other one is at 539 cm^{-1} directly corresponding to Fe-O vibrations directly confirming the presence of Fe_3O_4 particles that were successfully impregnated on the surface of PAC, which is also manifested with the presence of the iron particles from the EDX results explained in detail later.

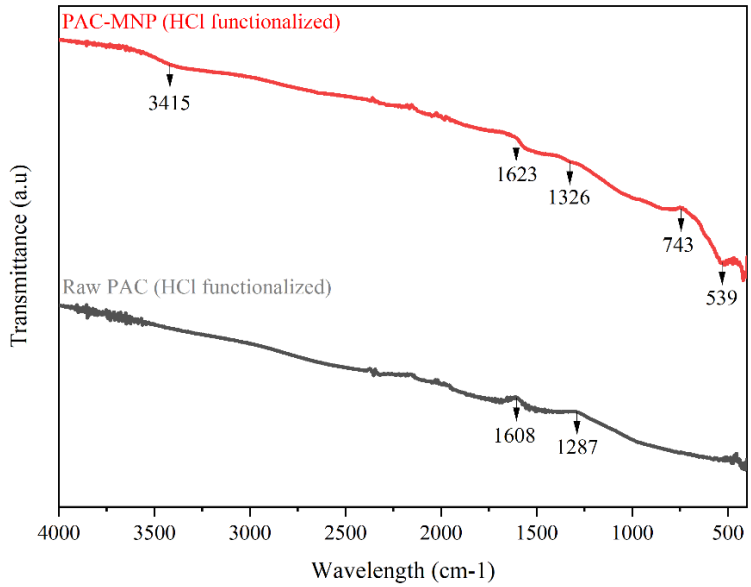


Figure 3. 2. IR spektrum of 1) functionalized$_{HCl}$-PAC, 2) PAC-MNP (HCl modification)

In the Figure 3.3, the FTIR spectrum belongs to the Composite/PAC-MNP, but this time, one spectrum is its raw form and the other is the form after introduced to the N-P synthetic 1000 ppm solution at pH 10 for adsorption process.

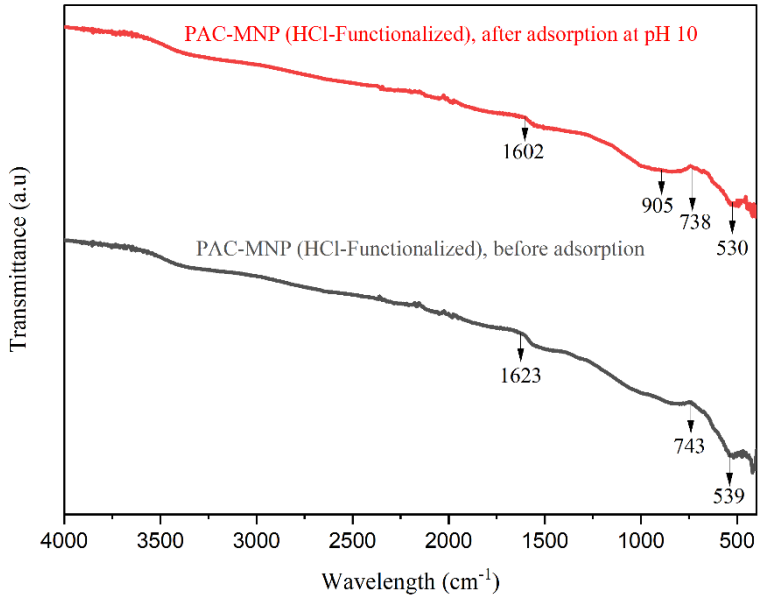


Figure 3. 3. IR spektrum of 1) Raw PAC-MNP 2) PAC-MNP after Adsorption at pH=10

After the adsorption process, vibrations of 1623, 743 and 539 cm^{-1} slightly shifted, that the complexation between -OH groups and ammonia or phosphate species may have formed. Furthermore, the new peaks at 905 cm^{-1} attributed to P=O or P-O vibration could be observed (Amornwutiroj et al., 2019). Besides these, N and P species were captured on the surface of PAC-MNPs at pH 10, and it was also obtained through the EDX results explained in detail later.

3.1.4. SEM results

The surface morphology of the Functionalized $_{(HCl)}$ -PAC and the PAC-MNPs (before and after adsorption) was characterized by SEM. This was especially important in order to distinguish between the surface form of Functionalized PAC, and the structural difference after it was combined with MNP. As seen in the Figure 3.4.a, the functionalized PAC's external surface is rough and of irregular shapes and some cavities distributed in different sizes and shapes, and having approx. several micrometers similar to the study of Yegane Badi et al. (2018) (Yegane Badi et al., 2018). Similar to the study of Chen and Wu (2004), the reason of some cavities and eroded cleavages that were generated could be expressed with acidic treatment during the functionalization $_{(HCl)}$ process (Chen and Wu, 2004). On the other hand, as can be clearly seen in Figure 3.4.b, a rough and heterogeneous surface also appears on the PAC-MNP (before adsorption); the polygonal small particles are Fe_3O_4 nanoparticles of about <75–100 nm dispersed on the Functionalized $_{(HCl)}$-PAC powders, this result is similarly referred to the study of (Yegane Badi et al., 2018). Therefore, this can be interpreted as magnetite nanoparticles impregnated on the surface of the functionalized $_{(HCl)}$ - PAC powder. These results showed that Fe_3O_4 nanoparticles were properly synthesized on the Functionalized $_{(HCl)}$ -PAC surface (Yegane Badi et al., 2018).

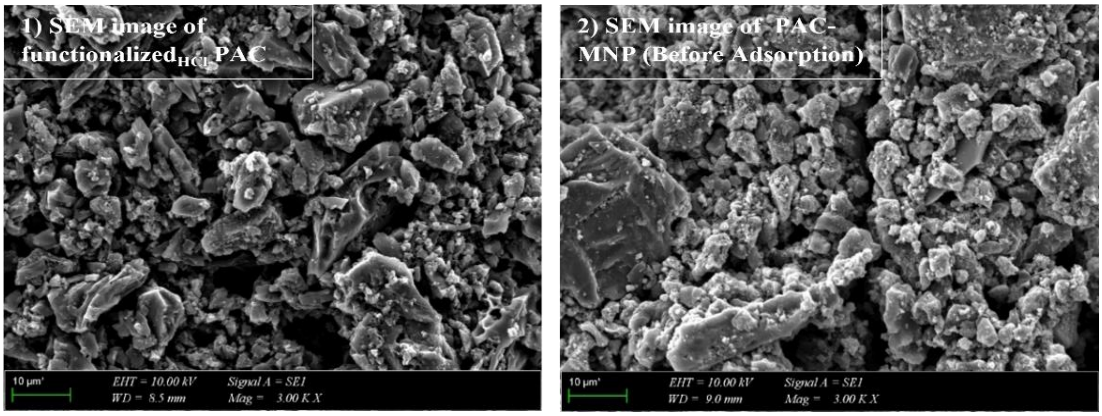


Figure 3. 4. SEM images of 1) functionalized$_{HCl}$-PAC, 2) PAC-MNP (before adsorption)

The SEM images of the PAC-MNP after adsorption process, shown in Figure 3.5, is observed that the surface gains a more homogeneous appearance. This can be interpreted that N and P species partially interact with the pores of the adsorbent and adhere to the particles. The result indicates that the adsorption was able to be properly performed.

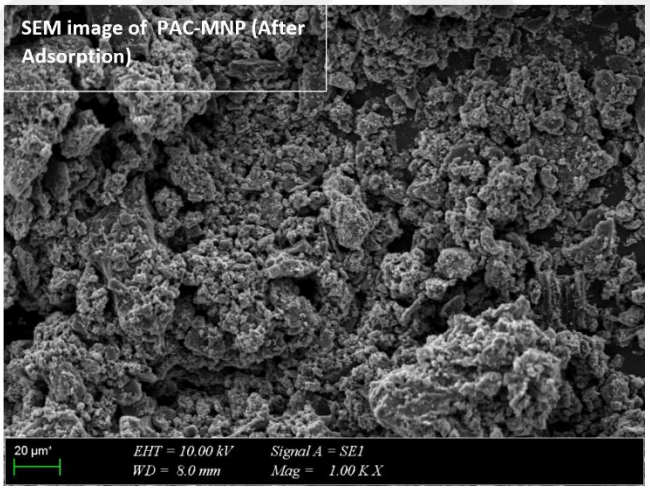


Figure 3. 5. SEM image of PAC-MNP (after adsorption)

3.1.5. EDX results

The elemental analysis was determined according to EDX measurements. It should be noted that these measurements were performed by taking different points/spots from the sample composition.

The EDX images obtained from Functionalized $_{(HCl)-}$ -PAC and PAC-MNPs (before and after adsorption forms) were characterized in the following Figure 3.6 As seen in the

Figure 3.6. Functionalized $_{(HCl)}$ -PAC sorbent consists of oxygen and chloride elements, which means the PAC powders were well-functionalized with HCl activation agent.

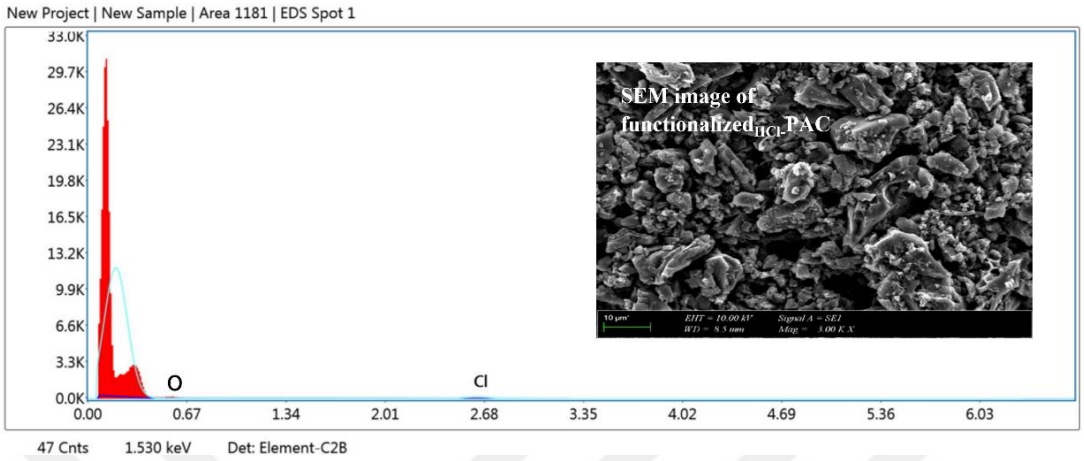


Figure 3. 6. The EDX results obtained from FunctionalizedHCl -PAC

In addtion, the EDX results (Figure 3.7) of PAC-MNPs (before adsorption) imply that the adsorbent consists of Carbon, Oxygen and Iron elements, as expected. The elements distributed on the surface of PAC-MNP before adsorption according to their weight percentage were also demonstrated in the Figure 3.7.

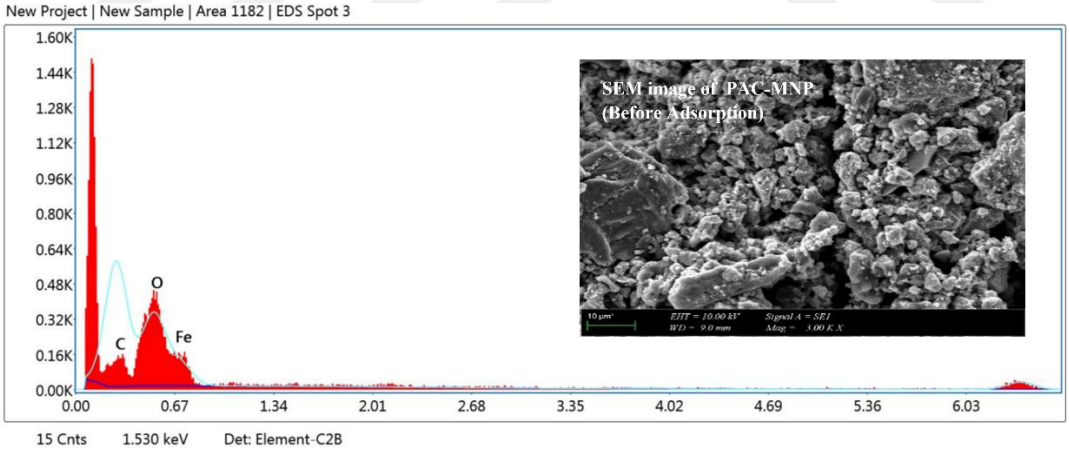


Figure 3. 7. The EDX results obtained from of PAC-MNPs (before adsorption)

In the final EDX result (Figure 3.8) of PAC-MNPs (after adsorption) indicate that the adsorbent consists of Carbon Oxygen, Iron, Nitrogen and Phosphorus elements as intended.

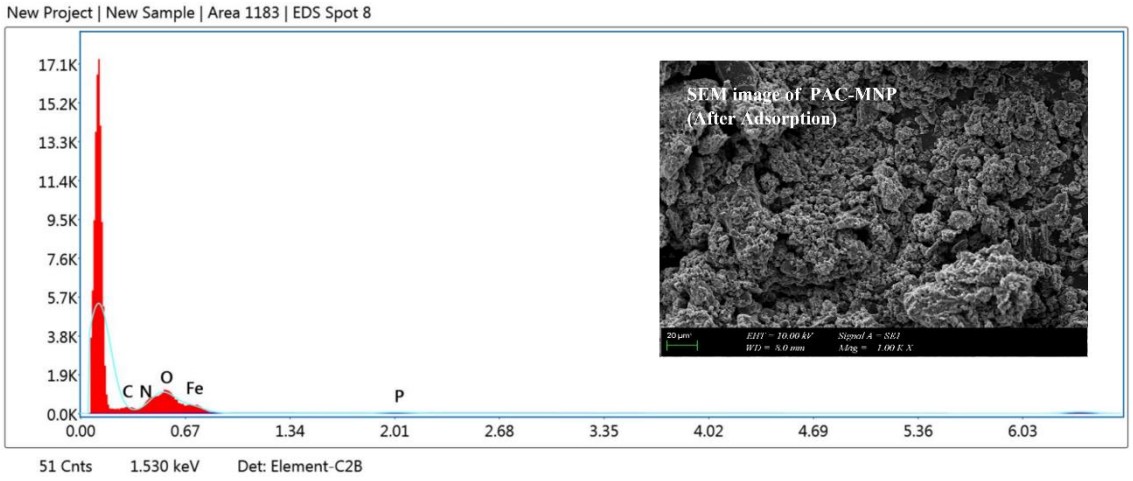


Figure 3. 8. The EDX results obtained from of PAC-MNPs (after adsorption)

After the adsorption with synthetic N-P solution, it was confirmed that the PAC-MNP has the capability for adsorbing of both ammonia and phosphate species that was also confirmed through weight percentage results obtained with EDX analysis (Figure 3.9).

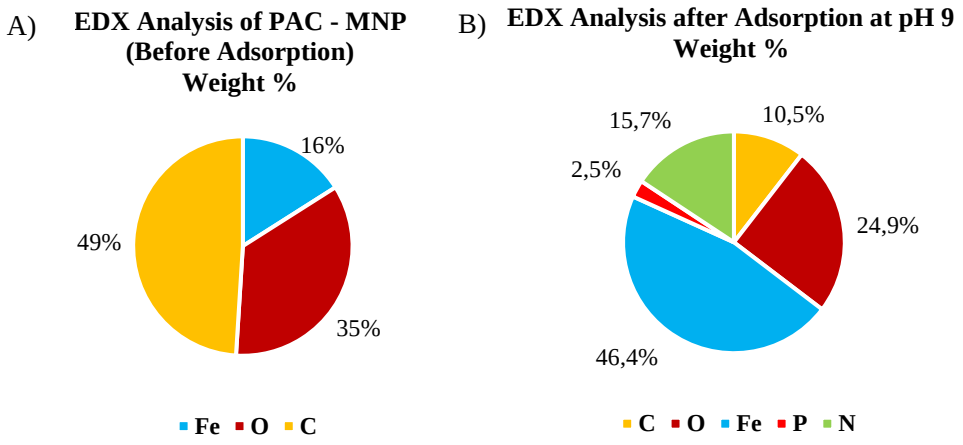


Figure 3. 9. The EDX results A) obtained from PAC-MNPs (before adsorption) as weight percentage B) PAC-MNPs (after adsorption) as weight percentage

3.2. Adsorption Performance

3.2.1. Adsorption isotherm experiment – equilibrium tests

Four isotherm models were assessed for PAC-MNPs adsorption mechanism by the nonlinear fitting of the results including Langmuir, Freundlich, Sips and Redlich–Peterson isotherms, and their parameters and coefficients are summarized in Table 3.1. According

to the data, while the Freundlich Model had a stronger correlation ($R^2 > 0.999$) than the other equations for ammonia species, Redlich-Peterson model was among the most fitted ($R^2 > 0.999$) model for describing the adsorption of phosphate species.

Table 3. 1. Theoretical parameters of kinetic and isotherm studies

Model	Parameters	Phosphate	Ammonia
Langmuir	q_m	3000	65
	K_L	0	0,000356
	$\chi 2$	3,8182	0,2207
	R_2	0,9523	0,9916
Freundlich	K_F	0,003	0,016
	$1/n$	1,305	1,025
	$\chi 2$	16,4374	0,000080
	R^2	0,96265	0,999
Sips	Q^s_m	1993,9	73,6
	K_S	0	0,001
	n_S	0,859	1,12
	$\chi 2$	8,7016	0,6222
	R_2	0,98223	0,99075
Redlich-Peterson	K_R	0,135	0,093
	α_R	6,187	2,957
	β_R	0	0,044
	$\chi 2$	0,0103	0,0518
	R^2	0,99986	0,99895

While the Langmuir suggests homogeneous and monolayer adsorption model, the Freundlich suggests multilayer and heterogeneous adsorption model for substances (Abukhadra et al., 2020). These heterogenous structures might be the main indication to clarify the adsorption mechanism of ammonia and phosphate species on PAC-MNPs. The Chi-squared (χ^2) coefficient also reflected that Freundlich model strong agreement with ammonia adsorption as it was of very low value almost close to zero (Table 3.1). On the other hand, the reported good fitness of with Redlich-Peterson isotherm model of

phosphate adsorption coexisting with ammonia species could be attributed the model properties. Becuase this model connects the specific features of both Langmuir and Freundlich isotherms. Thus, both monolayer and multilayer heterogeneous structure features (Mangwandi et al., 2014) can be subjected for the mechanism of the phosphate adsorption onto PAC-MNPs. However, it has been evaluated that the multilayer heterogeneous structure features of Redlich-Peterson isotherm were dominated on the adsorption mechanism due to the data obtained from kinetic studies. The inner surface complexation process was actually leading in the adsorption mechanism and there was probably the formation of chemical bonds and/or electrostatic attraction between the adsorbed ammonia and phosphate and the main functional groups of PAC-MNP (Mangwandi et al., 2014).

3.2.2. Adsorption kinetics tests

The adsorption process was further fitted using the pseudo-first-order, pseudo-second-order and Elowich models. The plots of Qt against t are presented in Figure 3.10, and their fitting curves using the two models are also given.

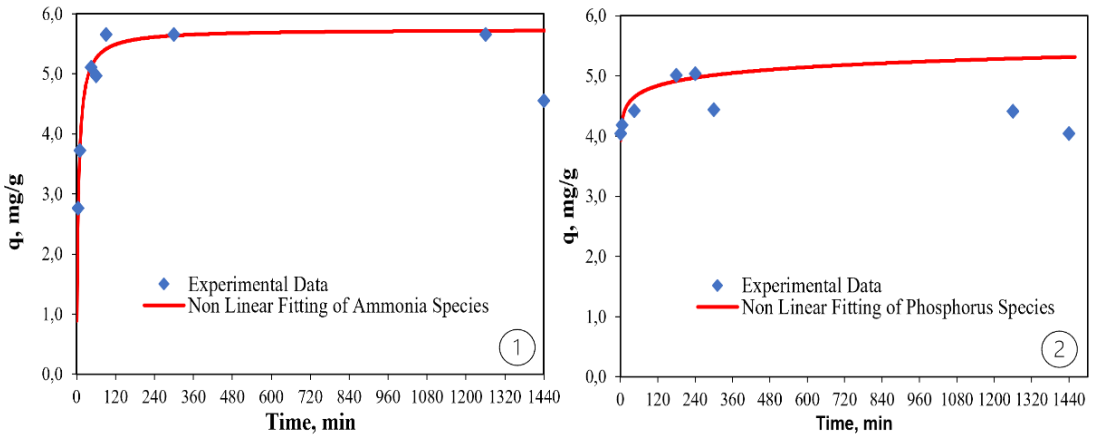


Figure 3. 10. Kinetic model plots for NH_3 (1) and PO_4^{-3} (2) adsorption (Adsorption conditions: N-P solution, 500 mg/L, pH ~9).

Kinetic model parameters for PFO, PSO and Elowich models for each species are provided Table 3.2 and shows the results of the nonlinear regression analysis of each model. The pseudo-second-order kinetics model for ammonia had generally higher correlation coefficient value (R^2) than the pseudo-first-order model while the Elowich kinetics model

for P species had generally higher correlation coefficient value. The adsorption amount of ammonia and phosphate species by PAC-MNPs remained basically unchanged after 180 min adsorption reaction, indicating that the adsorption had reached equilibrium.

Table 3. 2. Kinetic model parameters for NH_3 and PO_4^{-3} adsorption on PAC-MNPs at pH 10

Model	**Model Constant**	**R2**	**X2**	**NRMSE**
PFO, N	k_1,N= 0.1	0.942	0.0694	0.0692
PSO, N	k_2,N= 0.032	0.983	0.0279	0.0469
EWH,N	α=3.898 β=1.056	0.973	0.0347	0.0467
PFO, P	k_1,P=2	0.359	0.1190	0.2633
PSO, P	k_2,P=1.167	0.581	0.1034	0.2443
EWH,P	α=147,612,910.48 β=5.219	0.904	0.0184	0.1020

The pseudo-second-order kinetic model suggested the chemical affinity-based mechanisms which might consist of the electron-sharing and exchange reactions, surface complexation, and internal diffusion (Abukhadra et al., 2020). The reported well-fitness with Elovich model indicates the energetic heterogeneity available on the PAC-MNP throughout adsorption reactions. This stituation can be associated with estimated result from the pseudo-second-order model (Abukhadra et al., 2020). Thus, the resulting mechanism is dominated by a complex adsorption process or by surface complexation and/or ion exchange. The isotherm models supported this estimation for the adsorption reactions.

3.2.3. Effect of pH

One of the studies dealing with the ammonia adsorption from aqueous solution in the literature have been investigated by Hsu et al. (2019), and they employed “Chemically Activated Biochar” with two type base activators (NaOH and KOH) as the adsorbent (Hsu et al., 2019). They reported that the pH of ammonium-nitrogen solution is critical on the formation of surface charge distribution affecting the electrostatic and molecular interactions between the adsorbent and the solution, especially adsorption capacity increased due to increasing pH value from 3.0 to 9.0. However, they also emphasized that further increase of the pH, e.g. at pH 10, caused a sharp decrease in adsorption capacity, which was attributed that the electrostatic attraction mechanism was not effective at that pH value (10). Ren et al. (2021) also studied ammonia-nitrogen adsorption on iron-loaded activated carbon, and reported that the optimum adsorption performance of ammonia-nitrogen was achieved at pH 7 (Ren et al., 2021). They noted that over the pH 7 condition, the ammonia nitrogen adsorption capacity of Fe-AC began to decrease. In our study, ammonia adsorption was quite high at high pH values too (Figure 3.11.a), but unlike the aforementioned studies, it had the highest adsorption value at pH 10 simultaneously N-P containing solutions (Figure 3.11 demonstrates the results of 500 ppm N-P solution). Simultaneously presence of PO_4^{-3} species in the aqueous solution may be one of the reasons affecting the ammonia adsorption mechanism.

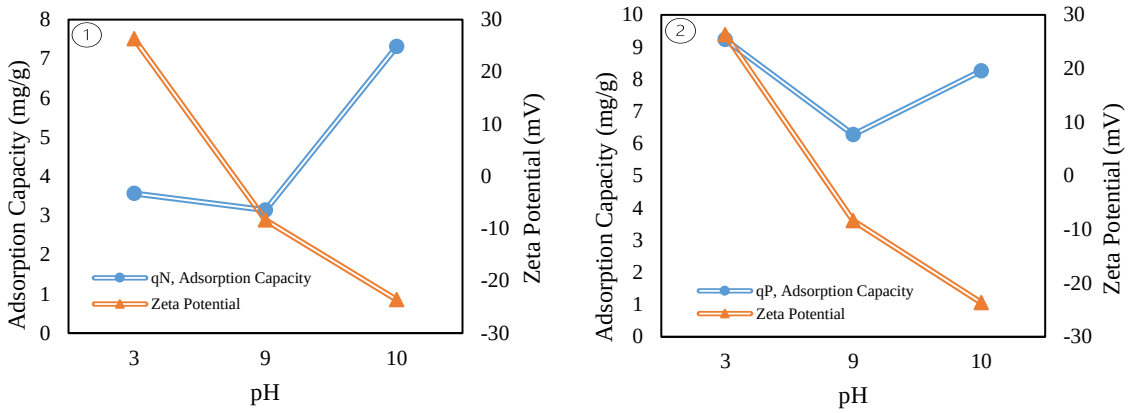


Figure 3. 11. Effect of solution pH on NH_3 (1) and PO_4^{3-} (2) adsorption and the zeta potential of PAC-MNPs (adsorption conditions: N-P simultaneous solution, 500 mg/L; PAC-MNPS dosage; temperature, 20 °C).

There are several studies investigating the simultaneous adsorption of N and P species in the literature. Wu at al. (2019) fabricated a granular composite adsorbent consisting of zeolite powders and Al–Mn binary oxide, they reported that, during the simultaneous of NH_3 and P adsorption process, the adsorption rate of NH_3 was barely influenced by the addition of P, and vice versa (Wu et al., 2019). They interpreted that coexisting ammonia-nitrogen and phosphate species did almost not compete for the same functional groups. They also observed the effect of the solution pH on the adsorption process and noted that while the removal efficiency of NH_3 could be ensured the most at pH 10, at alkali conditions P adsorption was insufficient as the adsorbent was already positively charged at high pH < 8.53. On the other hand, Xu et. al. (2020) studied the simultaneous adsorption of ammonia and phosphate by employing green synthesized iron oxide nanoparticles dispersed onto zeolite (ELMNP@zeolite) and emphasized that there were various parameters affecting the adsorption of co-existing NH_4^+-PO_4^{3-}. However, interms of the effect of pH, the optimum adsorption of NH_3-N remained stable at the pH range of 4-10, while PO_4^{3-} removal efficiency significantly decreased when the pH was < 8.00. Lastly, in the study of Wang et al. (2021), Fe_3O_4 magnetic nanocomposites coated with fulvic acid (Fe_3O_4/FA) were employed as an adsorbent for the adsorption of simulated wastewater containing Ni(II), Pb(II), NH_4^+, PO_4^{3-} and Basic Blue 3 (BB3) (Wang et al., 2021). The result showed that at solution pH 5, the removal efficiency of ammonia-nitrogen and phosphorus were quite high about 75% and 85%, respectively.

In order to understand the effect of the highest and lowest pH values on adsorption capacity of especially phosphate species, at different initial concentrations, the batch trials were performed, and the results are demonstrated in the Figure 3.12. When the adsorption was operated at low pH value which was at 3, the competition between high concentration of NH_3-N and PO_4-P species for the adsorptive sites on oxidized PAC-MNPs intensifies, inducing weak adsorption achieved to be 6.57 mg/g and 13.28 mg/g, respectively. The increase in the pH value tends to increase OH^- amount in the aqueous solution, that imparts the chance of its ionically exchange with phosphate species due to high concentration difference, so that is facilitating to increase in the adsorption of phosphate species achieved to be 21.74 mg/g. Addition to this, ammonia-nitrogen adsorption performance was also increased to 15.05 mg/g.

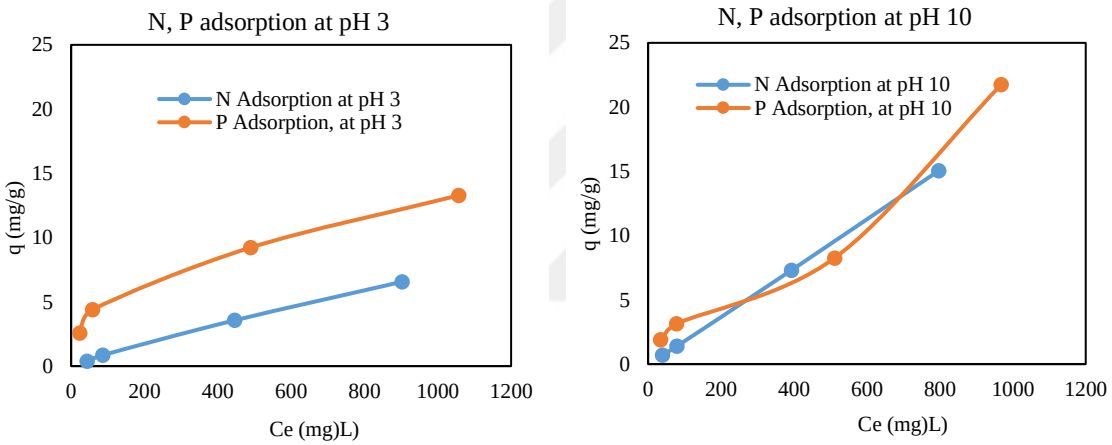


Figure 3. 12. Effect of solution pH on NH_3 (1) and PO_4^{-3} (2) adsorption (adsorption conditions: N-P simultaneous solution, 1000 mg/L; PAC-MNPS dosage; temperature, 20 °C).

The adsorption performance of PAC-MNPs (i.e., qe) demonstrates an increasing trend with the equilibrium concentration (Ce) for phosphate species.

3.2.4. Effect of adsorbent dosage

The consequence of PAC-MNPs dose for the adsorption of NH_3 and PO_4^{3-} species was examined under batch adsorption experiments (as shown in Figure 3.13) using different amounts of the adsorbent (as 5-50 g/L) while keeping the other parameters constant, like pH (4.5), temperature (20^{o}C) and the initial as concentration (1000 mg/L). On gradual rise

in the quantity of PAC-MNPs from 5 to 50 g/L, the increase in phosphae adsorption capacity was observed from 24.8 to 8.45 mg/g, while 10 to 3.73 mg/g ammonia adsorption capacity was noticed, respectively. In terms of removal efficiency from the Figure 3.13, the enhanced NH_3 and PO_4^{3-} removal efficiency could be ascribed to the available vacant sites (or surface area) and the number of ion-exchange sites for the uptake of these nutrient species on increasing the PAC-MNPs dose.

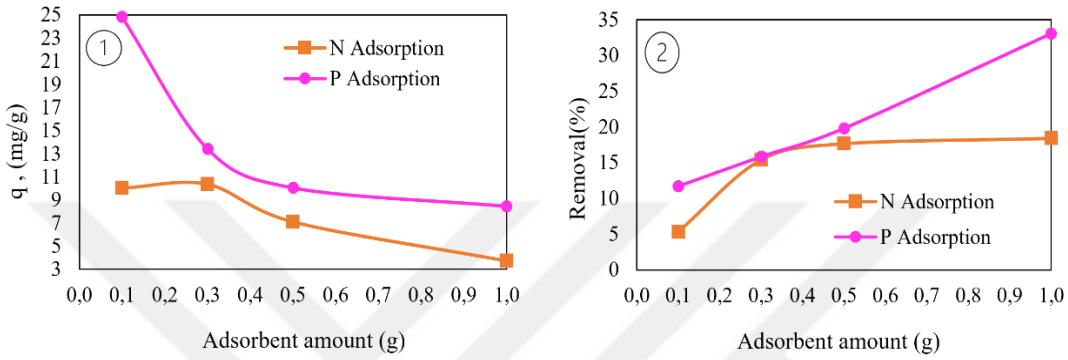


Figure 3. 13. Effect of adsorbent dosage on NH_3 (1) and PO_4^{-3} (2) adsorption (adsorption conditions: N-P simultaneous solution, 1000 mg/L; PAC-MNPS dosage; temperature, 20 °C).

3.2.5. Comparing the adsorption performance of Functionalized$_{HCl}$-PAC and PAC-MNPs

The adsorption performance of both raw functionalized powdered activated carbon (Functionalized$_{HCl}$-PAC) and its composite form (PAC-MNPs) were investigated in N-P simultaneous solution. The results clearly show that the composite PAC-MNPs showed the best adsorption performance in capturing simultaneously both ammonia and phosphate species in 500 mg/L concentration, at two different pH values (3 and 10), respectively. Furthermore, while the adsorption of PO_4^{-3} species through Functionalized$_{HCl}$-PAC were almost zero at the highest pH (10), they were adsorbed much more through PAC MNPs which was about 8-9 times of that raw form, at two different pH values.

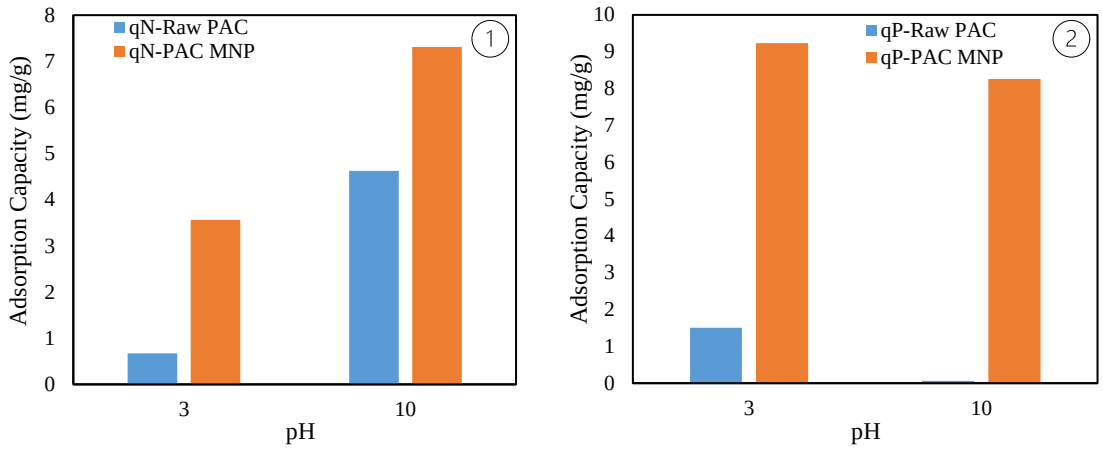


Figure 3. 14. Comparison of adsorbent performance of Functionalized$_{HCl}$-PAC and PAC-MNPs on N (1) and P (2) species, respectively shown on graphs (adsorption conditions: N-P simultaneous solution, 500 mg/L; PAC-MNPS dosage; temperature, 20 °C)

3.3. Desorption Experiments

3.3.1. Desorption of N and P

One of the important parameters to determine the potential and sustainability of an adsorbent is its reusability. The regeneration of the PAC-MNPs was studied with different desorption solution such as Distilled Water (DW), and HCl and NaOH solutions. By the way, in order for ammonia and phosphorus to be concentrated, especially the same distille water desorption solution was used in through desorption cycles. Hence, it will help recover phosphorus and ammonia through precipitation with required amounts of chemical addition in following steps. In this regard, the distilled water desorption of the composite was investigated during the four cycles of adsorption and desorption of NH_3 and PO_4^{-3} species from 500 mg/L N-P simultaneous solutions at pH 3 and 10 for 1 hr conditions (shown in Figure 3.15). As the cycles increased, the color of the material began to turn orange, and after the 4th cycle, separation with the magnet began to take more time.

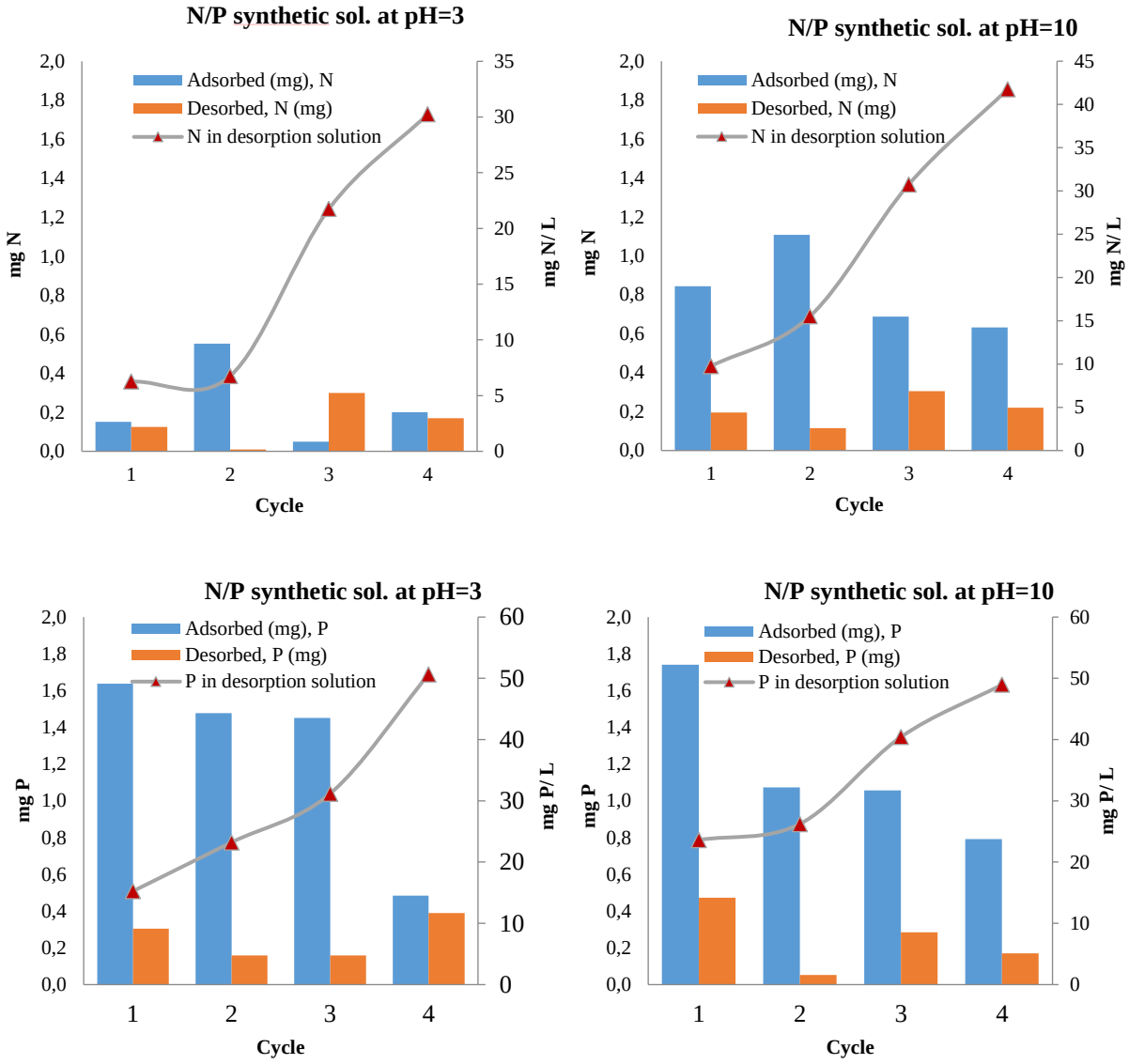


Figure 3. 15. Reusability of magnetic nanoparticles for phosphate recovery from synthetic N-P solution (Experimental conditions for desorption; distille water, 1 h contact time. Experimental conditions for adsorption; for synthetic N-P solution: 15 g/L MNP, initial N-P: ~500 mg/L)

In order to understand the behavior of only ammonia species on PAC-MNP, it was introduced to an ammonia synthetic solution that was prepared for ~500 mg/L, so that helped understand the effect of coexistence with phosphate species in terms of competition for the composite. The results shown in Figure 3.16 indicate that simultaneous PO_4^{3-} species almost doesn't affect the NH_3 adsorption on PAC-MNPs.

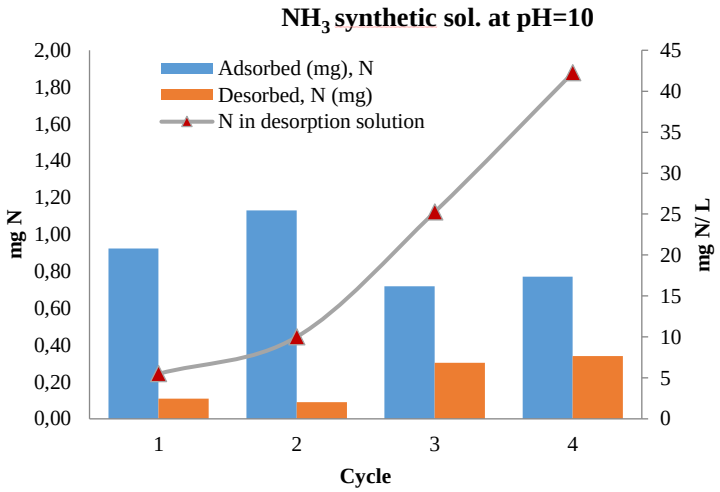


Figure 3. 16. Adsorption performance of PAC-MNPs for ammonia species recovery from synthetic NH_3 solution (Experimental conditions for desorption; distille water, 1 h contact time. Experimental conditions for adsorption; for synthetic N solution: 15 g/L MNP, initial pH = 10, initial N: ~500 mg/L)

Moreover, to determine the appropriate desorption solution and the mechanism of ammonia and phosphate species, the four cycles adsorption-desorption could be carried out with different concentrations of HCl (0.1 M, 0.5 M, and 1 M) and NaOH (1 M) solutions, and the adsorption conditions were performed at only pH 10, in 500 mg/L N-P simultaneous solutions. The adsorption-desorption cycles of each specie were demonstrated in Figure 3.17 and Figure 3.18, respectively. Interestingly, ammonia species were able to be the most recovered as 88.5 mg/L and 81 mg/L through 0,1M HCl and 0,5 M HCl desorption solutions, respectively. On the other hand, 1M HCl and 1M NaOH solutions desorbed them slightly lesser, that are 75.4 mg/L and 77 mg/L, respectively.

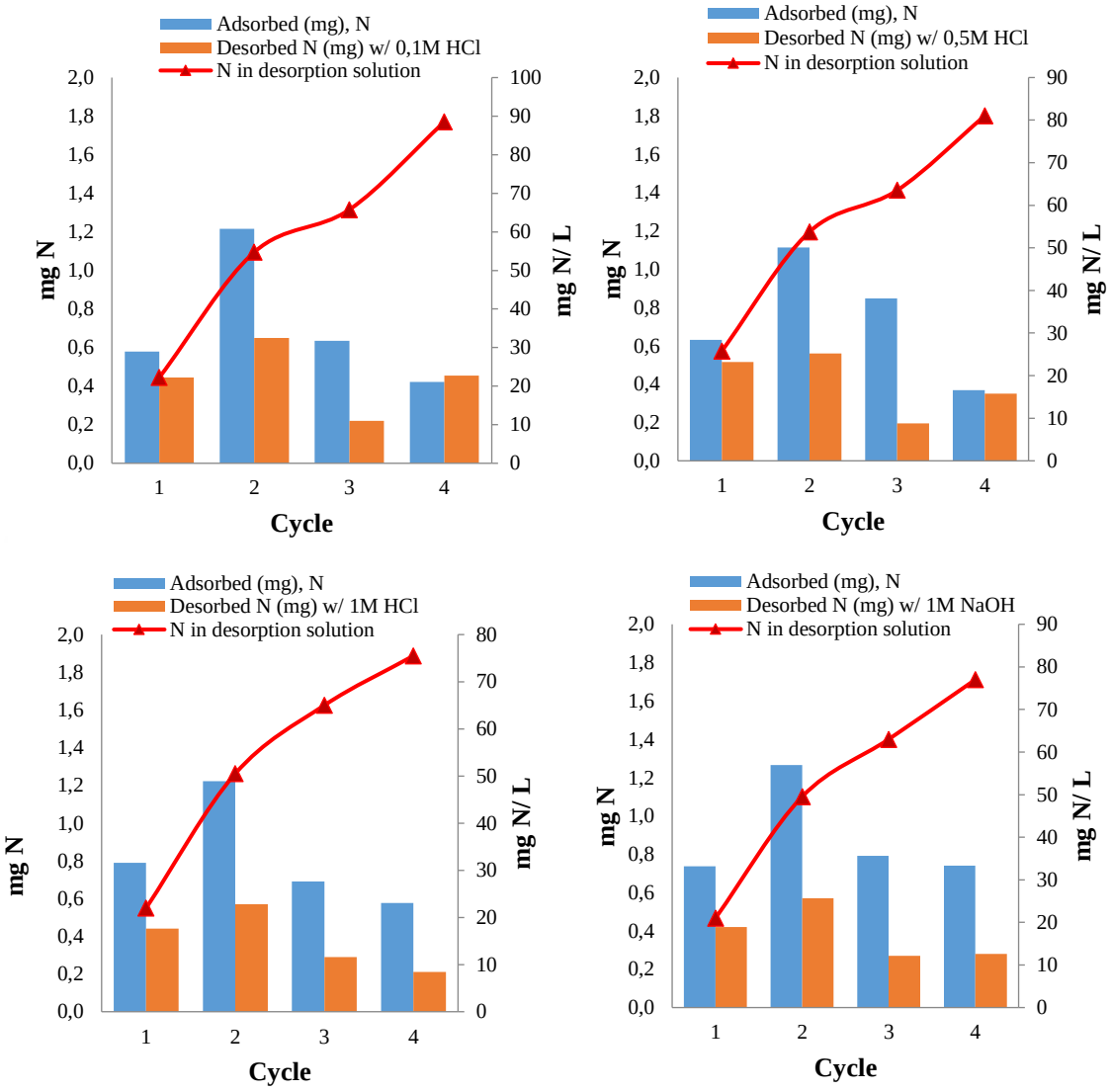


Figure 3. 17. Reusability of magnetic nanoparticles for ammonia recovery from synthetic N-P solution through 0.1 M HCl, 0.5 M HCl, 1 M HCl, 1 M NaOH desporption solutions (Experimental conditions for desorption; distille water, 1 h contact time. Experimental conditions for adsorption; for synthetic N-P solution: 15 g/L MNP, initial pH = 10, initial N-P: ~500 mg/L).

In respect to desorption of phosphorus species, 1M NaOH provided the highest desorption that recovered ~135 mg/L at the end of the 4th adsorption-desorption cycles while 0.1 M, 0.5 M and 1 M HCl acidic solutions could desorbed 19 mg/L, 64.75 mg/L and 106.42 mg/L, respectively.

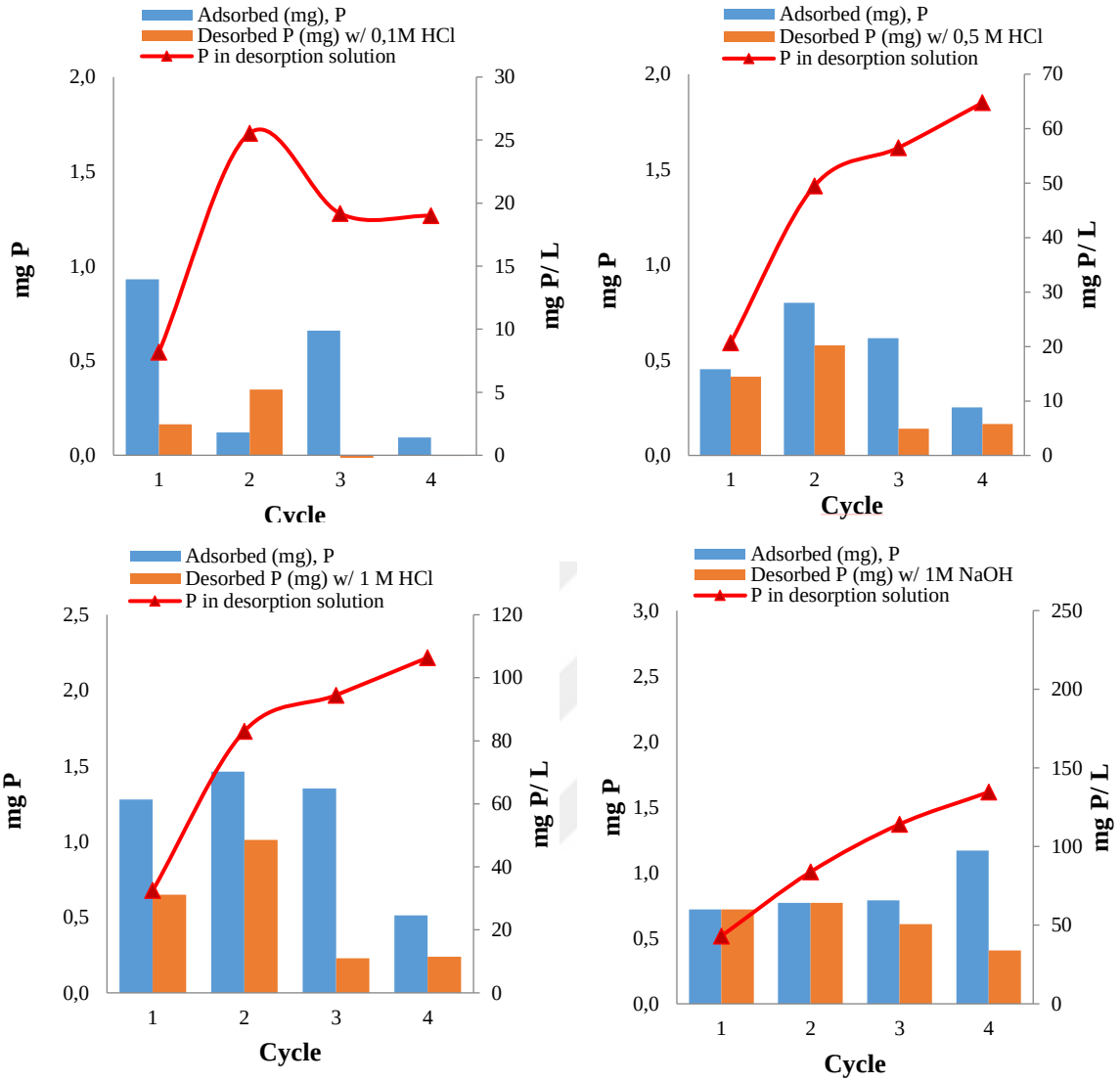


Figure 3. 18. Reusability of magnetic nanoparticles for phosphorus recovery from synthetic N-P solution through 0.1 M HCl, 0.5 M HCl, 1 M HCl, 1 M NaOH desporption solutions (Experimental conditions for desorption; distille water, 1 h contact time. Experimental conditions for adsorption; for synthetic N-P solution: 15 g/L MNP, initial pH = 10, initial N-P: ~500 mg/L)

During the adsorption-desorption cycles, changes in the color of the material were observed. Especially in the last cycle, the color of the liquid started turning orangeish (shown in Figure 3.19). This means that the material started to oxidize. In addition, the magnet separation process was even slower during each cycle. The reason of this situation

may be due to the adsorption mechanism. It is known that the chemical structures of molecules change during chemical adsorption and bind to the adsorbent with strong bonds. For this reason, the regeneration of the adsorbent used or the recovery of molecules from the solution becomes very difficult. Therefore, this separation process may have caused deformation or deterioration of the adsorbent.

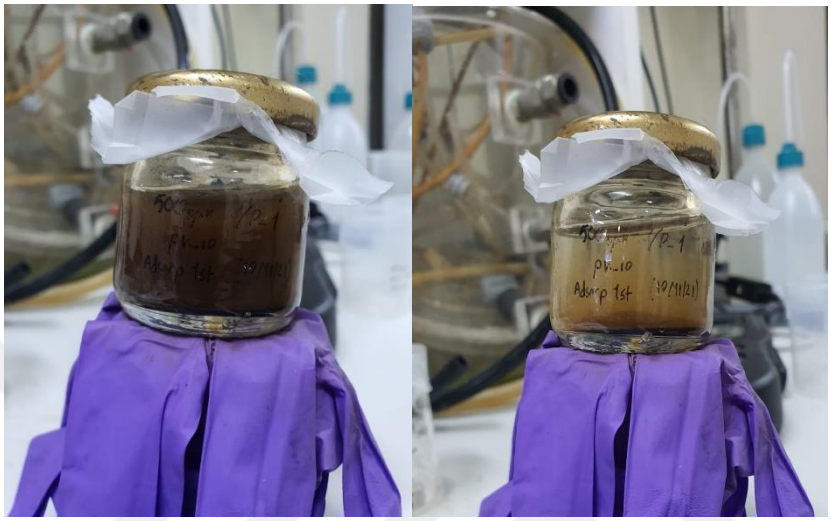


Figure 3. 19. Color changing during the adsorption-desorption cycles

Lastly, it was observed that the material gradually released a yellow-greenish color to the solution (see in Figure 3.20) after the desorption cycles especially with 0.5 M and 1 M HCl solutions. This can be attributed to the similarly occurring mechanism or high acid concentration.

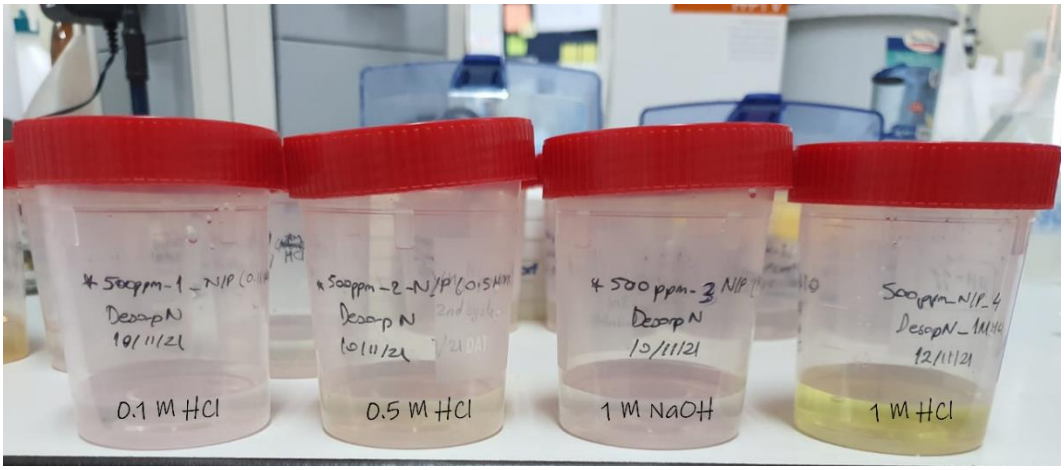


Figure 3. 20. Effect of 0.5 M and 1 M HCl desorption solutions on the PAC-MNPs (changing color)

4. CONCLUSIONS

In this study, it is aimed to develop a novel-functionalized powdered activated carbon (PAC) coated with magnetite (MNPs) nanoparticles (PAC-MNPs) for enhanced removal and recovery of ammonia and phosphate species from aqueous solution. For this reason, PAC-MNPs were tested in different conditions to detect optimum adsorption process, which was conducted with batch experiments. In order to both increase the adsorption capacity of powdered activated carbon and facilitate its separation from the solution by ensuring a magnetic property; 1) functionalization of activated carbon with strong HCl acid 2) co-precipitation synthesis process with magnetite nanoparticles were carried out.

The characterization studies of PAC-MNP composites were conducted with Potentiometric titration, Zeta Potential, SEM, EDX, FT-IR, and BET. The analyzes revealed that the PAC-MNPs were successfully synthesized and were able to adsorb simultaneously ammonia-nitrogen and phosphate species through electrostatic attraction and ion exchange reactions with the possible contribution of functionalized outer and inner sphere surface complexes under the strong basic conditions. The pHpzc and IEP values obtained from potentiometric titration and zeta potential measurements being as 6.54 and 6.71, respectively were very close to each other. This result gives the information about the surface charge distribution which was homogeneously dis-tributed. From this information, it was tried to determine the most suitable pH value and adsorbent dosage for optimum simultaneous adsorption study. The optimum conditions were determined to be pH=10. Through the SEM images, the structural difference between the functionalized$_{(HCl)}$ - PAC and the PAC-MNPs were clearly observed. While there were some cavities formed on the functionalized$_{(HCl)}$ – PAC that is an indication of acidic treatment during the functionalization process, a rough and heterogeneous surface formed on PAC-MNP that indicates also the Fe_3O_4 nano-particles appropriately dispersed. Following to this, with the SEM images of PAC-MNPs after adsorption process, it was understood that the surface turned a more homogeneous appearance so that ammonia-nitrogen and phosphate species adhered to the adsorbent. The elemental analysis obtained from EDX measurement confirmed that the functionalization with HCl of the PACs was achieved as well impregnation of magnetite nanoparticles on functionalized$_{(HCl)}$ - PACs was proved. Following to this, with the EDX results of PAC-MNPs after adsorption process, it was

confirmed that both ammonia and phosphate species were able to be simultaneously adsorbed. These results were also supported with FT-IR measurements, confirmed with the related peaks of the elements. BET results revealed that both the bare magnetite nanoparticles and the composite forms had high surface area that were able to enhance the adsorption performance.

In order to determine adsorption kinetics and adsorption equilibrium, the experimental data were applied to Pseudo-first-order, Pseudo-second-order, Elowich kinetic models and Langmuir, Freundlich, Sips and Redlich–Peterson isotherm models. The pseudo-second-order kinetics model for ammonia-nitrogen suggested that the adsorption of the ammonia followed Pseudo-second-order kinetics model while phosphate followed Elowich kinetics model on PAC-MNPs. On the other hand, Freundlich Model fitted well to the equilibrium data for ammonia-nitrogen, while Redlich-Peterson fitted best for phosphate ions.

Batch experiments were conducted to understand the simultaneous adsorption effect of ammonia-nitrogen and phosphate species of the lowest (3) and highest (10) pH values at different initial concentrations. It was observed that the high pH value enhaced the simultaneous adsorption of ammonia-nitrogen and phosphate species. The reason was attributed to high concentration of OH^- functional group resulted in high pH high so that causes ionic exchange of phosphate species due to high concentration difference between them. It has been also suggested that the adsorption of ammonia-nitrogen was facilitated by this functional group formed due to high pH. The optimum adsorbent dosages of PAC-MNPs were studied and found that it was 5 g/L on synthetic nutrient rich wastewater.

Desorption tests were performed as 4 adsorption/desorption experiment on the synthetic nutrient rich wastewater (at pH=10, and C_0=500ppm) with various desorption solution. The results showed that, while the maximum ammonia desorption was obtained via 0.5 M HCl solution recovered ~88.5 mg N/L, the maximum phosphate desorption was performed with 1 M NaOH solution recovered ~135 mg P/L. Furthermore, Struvite was produced by adding suffient amount of Mg to the ammonia-nitrogen and phosphate rich nutrient solution obtained from the last (4th) desorption cycle with 1 M NaOH.

This study proved that PAC-MNP could be a very promising adsorbent that is able to be reused several times in removing and recovering of crucial ammonia-nitrogen and

phosphate species from wastewater, even enabling the conversion of crucial N and P species into struvite as an excellent nutrient source.

REFERENCES

Abukhadra, M.R., Ali, S.M., Nasr, E.A., Mahmoud, H.A.A.,Awwad, E.M. (2020) Effective Sequestration of Phosphate and Ammonium Ions by the Bentonite/Zeolite Na-P Composite as a Simple Technique to Control the Eutrophication Phenomenon: Realistic Studies. ACS Omega, 5(24), 14656-14668.

Adeola, A.O.,Nomngongo, P.N. (2022) Advanced Polymeric Nanocomposites for Water Treatment Applications: A Holistic Perspective. Polymers, 14(12), 2462.

Ahmadi, S., Chia, C.-H., Zakaria, S., Saeedfar, K.,Asim, N. (2012) Synthesis of Fe3O4 nanocrystals using hydrothermal approach. Journal of Magnetism and Magnetic Materials, 324(24), 4147-4150.

Akyeva, S.C., Berkelieva, L.K.,Evzhanov, K.N. (2008) Wastewater treatment of phosphate ions by the electrodialysis method. Journal of Water Chemistry and Technology, 30(4), 246-250.

Al-Ghouti, M.A., Li, J., Salamh, Y., Al-Laqtah, N., Walker, G.,Ahmad, M.N. (2010) Adsorption mechanisms of removing heavy metals and dyes from aqueous solution using date pits solid adsorbent. J Hazard Mater, 176(1-3), 510-520.

Aloe, K.A., Bouraoui, F., Grizzetti, B., Bidoglio, G.,Pistocchi, A. (2014)Managing Nitrogen and Phosphorus Loads to Water Bodies: Characterisation and Solutions. Commission, E. (ed), Institute for Environment and Sustainability, Luxembourg.

Amornwutiroj, S., Manpetch, P., Singhapong, W., Srinophakun, P.,Jaroenworaluck, A. (2019) Controllable synthesis of mesoporous magnetite/activated carbon composites as efficient adsorbents for hexavalent chromium removal. Journal of Dispersion Science and Technology, 41(10), 1427-1444.

Asada, T., Ohkubo, T., Kawata, K.,Oikawa, K. (2006) Ammonia Adsorption on Bamboo Charcoal with Acid Treatment. Journal of Health Science, 52(5), 585-589.

Ashforth, G.K.,Calvin, G. (1973) Phosphorus in Fresh Water and the Marine Environment. Jenkins, S.H. and Ives, K.J. (eds), pp. 309-320, Pergamon.

Bansal, R.C.,Goyal, M. (2005) Activated Carbon Adsorption, CRC Press.

Barbosa, J.A., Labuto, G.,Carrilho, E.N.V.M. (2020) Magnetic nanomodified activated carbon: characterization and use for organic acids sorption in aqueous medium. Chemical Engineering Communications, 208(10), 1450-1463.

Baylan, N. (2013) Bentonit Ve Üzüm Çekirdeği Aktif Karbonunun Tekli Ve Çoklu İyon Sistemlerindeki Adsorpsiyon Özelliklerinin İncelenmesi. Master of Science Thesis, İstanbul Teknik Üniversitesi.

Benmahdi, F., Semra, S., Haddad, D., Mandin, P., Kolli, M.,Bouhelassa, M. (2019) Breakthrough Curves Analysis and Statistical Design of Phenol Adsorption on Activated Carbon. Chemical Engineering & Technology, 42(2), 355-369.

Boopathy, R., Karthikeyan, S., Mandal, A.B.,Sekaran, G. (2013) Adsorption of ammonium ion by coconut shell-activated carbon from aqueous solution: kinetic, isotherm, and thermodynamic studies. Environmental Science and Pollution Research, 20(1), 533-542.

Bozkurt, G. (2020) Synthesis and Characterization of α-Fe2O3 Nanoparticles by Microemulsion Method. Erzincan University Journal of Science and Technology, 13(2), 890-897.

Braun, J.C.A., Borba, C.E., Godinho, M., Perondi, D., Schontag, J.M.,Wenzel, B.M. (2019) Phosphorus adsorption in Fe-loaded activated carbon: Two-site monolayer equilibrium model and phenomenological kinetic description. Chemical Engineering Journal, 361, 751-763.

Burns, J.R.,Finlayson, B. (1982) Solubility product of magnesium ammonium phosphate hexahydrate at various temperatures. J Urol, 128(2), 426-428.

Buzea, C., Pacheco, II,Robbie, K. (2007) Nanomaterials and nanoparticles: sources and toxicity. Biointerphases, 2(4), Mr17-71.

Calandra, P., La Parola, V., Turco Liveri, V., Lidorikis, E.,Finocchi, F. (2013) Composite Nanoparticles. Journal of Chemistry, 2013, 536341.

Camargo, P.H.C., Satyanarayana, K.G.,Wypych, F. (2009) Nanocomposites: synthesis, structure, properties and new application opportunities. Materials Research-ibero-american Journal of Materials, 12, 1-39.

Campos, E.A., Pinto, D.V.B.S., Oliveira, J.I.S.d., Mattos, E.d.C.,Dutra, R.d.C.L. (2015) Synthesis, Characterization and Applications of Iron Oxide Nanoparticles - a Short Review. Journal of Aerospace Technology and Management, 7, 267-276.

Carpenter, S.R. (2008) Phosphorus control is critical to mitigating eutrophication. Proc Natl Acad Sci U S A, 105(32), 11039-11040.

Carpenter, S.R., Caraco, N.F., Correll, D.L., Howarth, R.W., Sharpley, A.N.,Smith, V.H. (1998) Nonpoint Pollution of Surface Waters with Phosphorus and Nitrogen. Ecological Applications, 8(3), 559-568.

Chen, J.P.,Wu (2004) Acid/Base-Treated Activated Carbons: Characterization of Functional Groups and Metal Adsorptive Properties. Langmuir, 20(6), 2233-2242.

Chen, X., Wendell, K., Zhu, J., Li, J., Yu, X.,Zhang, Z. (2012) Synthesis of nano-zeolite from coal fly ash and its potential for nutrient sequestration from anaerobically digested swine wastewater. Bioresource Technology, 110, 79-85.

Cheng, Q., Li, H., Xu, Y., Chen, S., Liao, Y., Deng, F.,Li, J. (2017) Study on the adsorption of nitrogen and phosphorus from biogas slurry by NaCl-modified zeolite. Plos One, 12(5), e0176109.

Choi, W.S.,Lee, H.-J. (2022) Nanostructured Materials for Water Purification: Adsorption of Heavy Metal Ions and Organic Dyes. Polymers, 14(11), 2183.

Cornell, M.R.,Schwertmann, U. (1997) R.M. Cornell and U. Schwertmann The Iron Oxides: Structure, Properties Reactions Occurrence and Uses. Mineralogical Magazine, 61(408), 740-741.

Daneshgar, S., Callegari, A., Capodaglio, A.G.,Vaccari, D. (2018) The Potential Phosphorus Crisis: Resource Conservation and Possible Escape Technologies: A Review. Resources, 7(2), 37.

Ding, Y.,Sartaj, M. (2016) Optimization of ammonia removal by ion-exchange resin using response surface methodology. International Journal of Environmental Science and Technology, 13(4), 985-994.

Ding, Z., Liu, L., Li, Z., Ma, R.,Yang, Z. (2006) Experimental study of ammonia removal from water by membrane distillation (MD): The comparison of three configurations. Journal of Membrane Science, 286(1), 93-103.

Do, M.H., Phan, N.H., Nguyen, T.D., Pham, T.T.S., Nguyen, V.K., Vu, T.T.T.,Nguyen, T.K.P. (2011) Activated carbon/Fe3O4 nanoparticle composite: Fabrication, methyl orange removal and regeneration by hydrogen peroxide. Chemosphere, 85(8), 1269-1276.

Doyle, J.D.,Parsons, S.A. (2002) Struvite formation, control and recovery. Water Res, 36(16), 3925-3940.

Drenkova-Tuhtan, A., Schneider, M., Franzreb, M., Meyer, C., Gellermann, C., Sextl, G., Mandel, K.,Steinmetz, H. (2017) Pilot-scale removal and recovery of dissolved phosphate from secondary wastewater effluents with reusable ZnFeZr adsorbent @ Fe3O4/SiO2 particles with magnetic harvesting. Water Research, 109, 77-87.

Dresselhaus, M.S., Smalley, R.E., Dresselhaus, G.,Avouris, P. (2001) Carbon Nanotubes: Synthesis, Structure, Properties, and Applications, Springer-Verlag, New York.

Dryden, H.T. (1984) Ammonium ion removal from dilute solutions and fish culture water by ion-exchange, Heriot-Watt University.

Duong, T., Xie, Z., Ng, D.,Hoang, M. (2013) Ammonia removal from aqueous solution by membrane distillation. Water and Environment Journal, 27(3), 425-434.

Elser, J.,Bennett, E. (2011) Phosphorus cycle: A broken biogeochemical cycle. Nature, 478(7367), 29-31.

EPA (2020)Inventory of U.S. Greenhouse Gas Emissions and Sinks (1990-2018). Agency, U.S.E.P. (ed).

EU (2020)Study on the EU's list of critical raw materials (2020) : critical raw materials factsheets. Directorate-General for Internal Market, I.E., Smes, Blengini, G., El Latunussa, C., Eynard, U., Torres De Matos, C., Wittmer, D., Georgitzikis, K., Pavel, C., Carrara, S., Mancini, L., Unguru, M., Grohol, M., Mathieux, F. and Pennington, D. (eds), Publications Office.

Falkowski, P.G. (2001) Encyclopedia of Biodiversity. Levin, S.A. (ed), pp. 437-453, Elsevier, New York.

Fayazi, M., Ghanei-Motlagh, M.,Taher, M.A. (2015) The adsorption of basic dye (Alizarin red S) from aqueous solution onto activated carbon/γ-Fe2O3 nano-composite: Kinetic and equilibrium studies. Materials Science in Semiconductor Processing, 40, 35-43.

Ficai, D., Andronescu, E., Ficai, A., Voicu, G., Vasile, B., Ionita, V.,Guran, C. (2012) Synthesis and Characterization of Mesoporous Magnetite Based Nanoparticles. Current Nanoscience, 8(6), 875-879.

Foo, K.Y.,Hameed, B.H. (2010) Insights into the modeling of adsorption isotherm systems. Chemical Engineering Journal, 156(1), 2-10.

Foree, E.G.,McCarty, P.L. (1970) Anaerobic decomposition of algae. Environmental Science & Technology, 4(10), 842-849.

Ganapathe, L.S., Mohamed, M.A., Mohamad Yunus, R.,Berhanuddin, D.D. (2020) Magnetite (Fe3O4) Nanoparticles in Biomedical Application: From Synthesis to Surface Functionalisation. Magnetochemistry, 6(4), 68.

Gehrke, I., Geiser, A.,Somborn-Schulz, A. (2015) Innovations in nanotechnology for water treatment. Nanotechnol Sci Appl, 8, 1-17.

Godini, H., Dargahi, A., Tabandeh, L., Mohammadi, M., Vaziri, Y., Hoseini Ahagh, M.M., Sharafi, K.,Jalilian, Z. (2017) The efficiency of modified powdered activated carbon for removal of ammonia nitrogen from aqueous solution: a process optimization using RSM (Response Surface Methodology), adsorption isotherm and kinetic study. Journal of Advances in Environmental Health Research, 5(3), 172-182.

Göran, I.A., Martin, W.,Magnus, F.K.B. (2012) Nutrient Limitation on Terrestrial Plant Growth - Modeling the Interaction Between Nitrogen and Phosphorus. The New Phytologist, 194(4), 953-960.

Grady Jr, C.L., Daigger, G.T., Love, N.G.,Filipe, C.D. (2011) Biological wastewater treatment, CRC press.

Gu, S.-Y., Hsieh, C.-T., Gandomi, Y.A., Yang, Z.-F., Li, L., Fu, C.-C.,Juang, R.-S. (2019) Functionalization of activated carbons with magnetic Iron oxide nanoparticles for removal of copper ions from aqueous solution. Journal of Molecular Liquids, 277, 499-505.

Guaya, D., Valderrama, C., Farran, A., Armijos, C.,Cortina, J.L. (2015) Simultaneous phosphate and ammonium removal from aqueous solution by a hydrated aluminum oxide modified natural zeolite. Chemical Engineering Journal, 271, 204-213.

Gulyás, A., Genç, S., Can, Z.S.,Semerci, N. (2021) Phosphate recovery from sewage sludge supernatants using magnetic nanoparticles. Journal of Water Process Engineering, 40.

Gupta, A.K.,Gupta, M. (2005) Synthesis and surface engineering of iron oxide nanoparticles for biomedical applications. Biomaterials, 26(18), 3995-4021.

Gutierrez, A.M., Dziubla, T.D.,Hilt, J.Z. (2017) Recent advances on iron oxide magnetic nanoparticles as sorbents of organic pollutants in water and wastewater treatment. Rev Environ Health, 32(1-2), 111-117.

Hanhoun, M., Montastruc, L., Azzaro-Pantel, C., Biscans, B., Frèche, M.,Pibouleau, L. (2011) Temperature impact assessment on struvite solubility product: A thermodynamic modeling approach. Chemical Engineering Journal, 167(1), 50-58.

Hartmann, J., Moosdorf, N., Lauerwald, R., Hinderer, M.,West, A.J. (2014) Global chemical weathering and associated P-release — The role of lithology, temperature and soil properties. Chemical Geology, 363, 145-163.

Havukainen, J., Nguyen, M.T., Hermann, L., Horttanainen, M., Mikkilä, M., Deviatkin, I.,Linnanen, L. (2016) Potential of phosphorus recovery from sewage sludge and manure ash by thermochemical treatment. Waste Management, 49, 221-229.

Helfferich, F.G. (1985) Principles of adsorption & adsorption processes, by D. M. Ruthven, John Wiley & Sons, 1984, xxiv + 433 pp. AIChE Journal, 31(3), 523-524.

Hermassi, M., Dosta, J., Valderrama, C., Licon, E., Moreno, N., Querol, X., Batis, N.H.,Cortina, J.L. (2018) Simultaneous ammonium and phosphate recovery and stabilization from urban sewage sludge anaerobic digestates using reactive sorbents. Sci Total Environ, 630, 781-789.

Holland, E.A. (1998) Geochemistry, pp. 428-431, Springer Netherlands, Dordrecht.

Hou, L., Liang, Q.,Wang, F. (2020) Mechanisms that control the adsorption–desorption behavior of phosphate on magnetite nanoparticles: the role of particle size and surface chemistry characteristics. RSC Advances, 10, 2378-2388.

Howarth, R.W. (ed) (2022) Nitrogen☆, Elsevier, Oxford.

Hsu, D., Lu, C., Pang, T., Wang, Y.,Wang, G. (2019) Adsorption of Ammonium Nitrogen from Aqueous Solution on Chemically Activated Biochar Prepared from Sorghum Distillers Grain. Applied Sciences, 9(23), 5249.

Huang, J., Rathnayake Kankanamge, N., Chow, C., Welsh, D., Li, T.,Teasdale, P. (2017) Removing ammonium from water and wastewater using cost-effective adsorbents: A review. Journal of Environmental Sciences, 63.

Iconaru, S.L., Guégan, R., Popa, C.L., Motelica-Heino, M., Ciobanu, C.S.,Predoi, D. (2016) Magnetite (Fe3O4) nanoparticles as adsorbents for As and Cu removal. Applied Clay Science, 134, 128-135.

Iram, M., Guo, C., Guan, Y., Ishfaq, A.,Liu, H. (2010) Adsorption and magnetic removal of neutral red dye from aqueous solution using Fe3O4 hollow nanospheres. Journal of hazardous materials, 181(1), 1039-1050.

Jahnke, R.A. (1992) International Geophysics. Butcher, S.S., Charlson, R.J., Orians, G.H. and Wolfe, G.V. (eds), pp. 301-315, Academic Press.

Jain, M., Yadav, M., Kohout, T., Lahtinen, M., Garg, V.K.,Sillanpää, M. (2018) Development of iron oxide/activated carbon nanoparticle composite for the removal of Cr(VI), Cu(II) and Cd(II) ions from aqueous solution. Water Resources and Industry, 20, 54-74.

Jiles, D.C. (1998) Introduction to Magnetism and Magnetic Materials, Second Edition, Taylor & Francis.

Jordan, J., Jacob, K.I., Tannenbaum, R., Sharaf, M.A.,Jasiuk, I. (2005) Experimental trends in polymer nanocomposites—a review. Materials Science and Engineering: A, 393(1), 1-11.

Jørgensen, S.E. (1979) Studies in Environmental Science. Jørgensen, S.E. (ed), pp. 61-80, Elsevier.

Jorgensen, T.C.,Weatherley, L.R. (2003) Ammonia removal from wastewater by ion exchange in the presence of organic contaminants. Water Research, 37(8), 1723-1728.

Juang, R.-S., Yei, Y.-C., Liao, C.-S., Lin, K.-S., Lu, H.-C., Wang, S.-F.,Sun, A.-C. (2018) Synthesis of magnetic Fe3O4/activated carbon nanocomposites with high surface area as recoverable adsorbents. Journal of the Taiwan Institute of Chemical Engineers, 90, 51-60.

Kabdaşlı, I., Tünay, O.,Özcan, P. (2009) Application of struvite precipitation coupled with biological treatment to slaughterhouse wastewaters. Environmental Technology, 30(10), 1095-1101.

Kakavandi, B., Kalantary, R.R., Jafari, A.J., Nasseri, S., Ameri, A., Esrafili, A.,Azari, A. (2015) Pb(II) Adsorption Onto a Magnetic Composite of Activated Carbon and Superparamagnetic Fe3O4 Nanoparticles: Experimental and Modeling Study. CLEAN – Soil, Air, Water, 43(8), 1157-1166.

Keleş, E. (2008) Kimyasal bileşimi farklı üç fosfat kayası ile kurşun (II) iyonunun adsorpsiyonu. Master's Degree Thesis, Atatürk Üniversitesi.

Kharissova, O.V., Dias, H.V.R.,Kharisov, B.I. (2015) Magnetic adsorbents based on micro- and nano-structured materials. RSC Advances, 5(9), 6695-6719.

Khodadadi, M., Hosseinnejad, A., Rafati, L., Dorri, H.,Nasseh, N. (2017) Removal Of Phosphate From Aqueous Solutions By Iron Nano-Magnetic Particle Coated With Powder Activated Carbon. JOURNAL OF HEALTH SCIENCES AND TECHNOLOGY, 1(1), -.

Kianfar, E. (2019) Nanozeolites: synthesized, properties, applications. Journal of Sol-Gel Science and Technology, 91(2), 415-429.

Kim, D., Min, K.J., Lee, K., Yu, M.S.,Park, K.Y. (2017) Effects of pH, molar ratios and pre-treatment on phosphorus recovery through struvite crystallization from effluent of anaerobically digested swine wastewater. Environmental Engineering Research, 22(1), 12-18.

Kodama, R.H. (1999) Magnetic nanoparticles. Journal of Magnetism and Magnetic Materials, 200(1), 359-372.

Kumar, M., Singh Dosanjh, H., Sonika, Singh, J., Monir, K.,Singh, H. (2020) Review on magnetic nanoferrites and their composites as alternatives in waste water treatment: synthesis, modifications and applications. Environmental Science: Water Research & Technology, 6(3), 491-514.

Kumar, R., Inbaraj, B.S.,Chen, B.H. (2010) Surface modification of superparamagnetic iron nanoparticles with calcium salt of poly(γ-glutamic acid) as coating material. Materials Research Bulletin, 45(11), 1603-1607.

Kumar, R.,Pal, P. (2015) Assessing the feasibility of N and P recovery by struvite precipitation from nutrient-rich wastewater: a review. Environ Sci Pollut Res Int, 22(22), 17453-17464.

Le Corre, K.S., Valsami-Jones, E., Hobbs, P.,Parsons, S.A. (2009) Phosphorus Recovery from Wastewater by Struvite Crystallization: A Review. Critical Reviews in Environmental Science and Technology, 39(6), 433-477.

Lee, W.-H.,Kim, J.-O. (2019) Effect of coexisting components on phosphate adsorption using magnetite particles in water. Environmental Science and Pollution Research, 26(2), 1054-1060.

Li, C., Ma, J., Shen, J.,Wang, P. (2009) Removal of phosphate from secondary effluent with Fe2+ enhanced by H2O2 at nature pH/neutral pH. J Hazard Mater, 166(2-3), 891-896.

Li, C., Yao, J., Zhang, T.C., Xing, W., Liang, Y.,Xiang, M. (2017) Simultaneous removal of nitrogen and phosphorus by cetylpyridinium bromide modified zeolite. Water Science and Technology, 76(11), 2895-2906.

Li, L., Sun, Z., Li, H.,Keener, T.C. (2012) Effects of activated carbon surface properties on the adsorption of volatile organic compounds. Journal of the Air & Waste Management Association, 62(10), 1196-1202.

Liu, H. (2014) Ammonia synthesis catalyst 100 years: Practice, enlightenment and challenge. Chinese Journal of Catalysis, 35(10), 1619-1640.

Liu, H., Peng, S., Shu, L., Chen, T., Bao, T.,Frost, R.L. (2013a) Effect of Fe3O4 addition on removal of ammonium by zeolite NaA. Journal of colloid and interface science, 390(1), 204-210.

Liu, J., Yu, Y., Zhu, S., Yang, J., Song, J., Fan, W., Yu, H., Bian, D.,Huo, M. (2018) Synthesis and characterization of a magnetic adsorbent from negatively-valued iron mud for methylene blue adsorption. Plos One, 13(2), e0191229.

Liu, X., Tian, J., Li, Y., Sun, N., Mi, S., Xie, Y.,Chen, Z. (2019) Enhanced dyes adsorption from wastewater via Fe3O4 nanoparticles functionalized activated carbon. Journal of hazardous materials, 373, 397-407.

Liu, X., Wang, M., Zhang, S.,Pan, B. (2013b) Application potential of carbon nanotubes in water treatment: A review. J Environ Sci (China), 25(7), 1263-1280.

Liu, Z., Zhang, F.-S.,Sasai, R. (2010) Arsenate removal from water using Fe3O4-loaded activated carbon prepared from waste biomass. Chemical Engineering Journal, 160(1), 57-62.

Lofrano, G., Carotenuto, M., Libralato, G., Domingos, R.F., Markus, A., Dini, L., Gautam, R.K., Baldantoni, D., Rossi, M., Sharma, S.K., Chattopadhyaya, M.C., Giugni, M.,Meric, S. (2016) Polymer functionalized nanocomposites for metals removal from water and wastewater: An overview. Water Res, 92, 22-37.

Lompe, K.M., Menard, D.,Barbeau, B. (2017) The influence of iron oxide nanoparticles upon the adsorption of organic matter on magnetic powdered activated carbon. Water Res, 123, 30-39.

Luciano, C., Fernando, S.G.a.E., Mónica, C.G.l.,Daniel, O.M.r. (2013) Waste Water. Fernando Sebastian García, E. and Luciano, C. (eds), IntechOpen, Rijeka.

Luo, G., Du, L., Wang, Y.,Wang, K. (2015) Encyclopedia of Microfluidics and Nanofluidics. Li, D. (ed), pp. 453-460, Springer New York, New York, NY.

Maathuis, F.J.M.,Diatloff, E. (2013) Roles and Functions of Plant Mineral Nutrients, Humana Press, Totowa, NJ.

Mackey, K.R.M.,Paytan, A. (2009) Encyclopedia of Microbiology (Third Edition). Schaechter, M. (ed), pp. 322-334, Academic Press, Oxford.

Mackey, K.R.M., Van Mooy, B., Cade-Menun, B.J.,Paytan, A. (2019) Encyclopedia of Microbiology (Fourth Edition). Schmidt, T.M. (ed), pp. 506-519, Academic Press, Oxford.

Mangwandi, C., Albadarin, A.B., Glocheux, Y.,Walker, G.M. (2014) Removal of ortho-phosphate from aqueous solution by adsorption onto dolomite. Journal of Environmental Chemical Engineering, 2(2), 1123-1130.

Marcińczyk, M., Ok, Y.S.,Oleszczuk, P. (2022) From waste to fertilizer: Nutrient recovery from wastewater by pristine and engineered biochars. Chemosphere, 306, 135310.

Mateo-Sagasta, J., Zadeh, S.M., Turral, H.,Burke, J.J. (2017)Water pollution from agriculture: a global review. Executive summary.

Mehrabi, N., Soleimani, M., Yeganeh, M.M.,Sharififard, H. (2015) Parameter optimization for nitrate removal from water using activated carbon and composite of activated carbon and Fe2O3 nanoparticles. RSC Advances, 5(64), 51470-51482.

Melfos, V., Helly, B.,Voudouris, P. (2011) The ancient Greek names “Magnesia” and “Magnetes” and their origin from the magnetite occurrences at the Mavrovouni mountain of Thessaly, central Greece. A mineralogical–geochemical approach. Archaeological and Anthropological Sciences, 3(2), 165-172.

Menéndez, J.A., Illán-Gómez, M.J., y León, C.A.L.,Radovic, L.R. (1995) On the difference between the isoelectric point and the point of zero charge of carbons. Carbon, 33(11), 1655-1657.

Mohajit, Bhattarai, K.K., Taiganides, E.P.,Yap, B.C. (1989) Struvite deposits in pipes and aerators. Biological Wastes, 30(2), 133-147.

Mulder, A., van de Graaf, A.A., Robertson, L.A.,Kuenen, J.G. (1995) Anaerobic ammonium oxidation discovered in a denitrifying fluidized bed reactor. FEMS Microbiology Ecology, 16(3), 177-183.

Muñiz, G., Fierro, V., Celzard, A., Furdin, G., Gonzalez-Sánchez, G.,Ballinas, M.L. (2009) Synthesis, characterization and performance in arsenic removal of iron-doped activated carbons prepared by impregnation with Fe(III) and Fe(II). Journal of hazardous materials, 165(1), 893-902.

Múzquiz-Ramos, E.M., Guerrero-Chávez, V., Macías-Martínez, B.I., López-Badillo, C.M.,García-Cerda, L.A. (2015) Synthesis and characterization of maghemite

nanoparticles for hyperthermia applications. Ceramics International, 41(1, Part A), 397-402.

Myrold, D.D. (1999) Environmental Geology, pp. 435-436, Springer Netherlands, Dordrecht.

Nguyen, M.D., Tran, H.-V., Xu, S.,Lee, T.R. (2021) Fe3O4 Nanoparticles: Structures, Synthesis, Magnetic Properties, Surface Functionalization, and Emerging Applications. Applied Sciences, 11(23), 11301.

Nieder, R., Benbi, D.K.,Reichl, F.X. (2018) Soil Components and Human Health. Nieder, R., Benbi, D.K. and Reichl, F.X. (eds), pp. 223-255, Springer Netherlands, Dordrecht.

Nouri, S. (2003) Effect of Functional Groups and pH on the Affinity and Adsorption Capacity of Activated Carbon: Comparison of Homogeneous and Binary Langmuir Model Parameters. Adsorption Science & Technology, 21, 511 - 524.

Ohlinger, K.N., Young, T.M.,Schroeder, E.D. (1998) Predicting struvite formation in digestion. Water Research, 32(12), 3607-3614.

Oliveira, P.N., Bini, R.D., Dias, G.S., Alcouffe, P., Santos, I.A., David, L.,Cótica, L.F. (2018) Magnetite nanoparticles with controlled sizes via thermal degradation of optimized PVA/Fe(III) complexes. Journal of Magnetism and Magnetic Materials, 460, 381-390.

Paerl, H.W. (2006) Assessing and managing nutrient-enhanced eutrophication in estuarine and coastal waters: Interactive effects of human and climatic perturbations. Ecological Engineering, 26(1), 40-54.

Pandey, N., Shukla, S.K.,Singh, N.B. (2017) Water purification by polymer nanocomposites: an overview. Nanocomposites, 3(2), 47-66.

Panneerselvam, P., Morad, N., Tan, K.A.,Mathiyarasi, R. (2012) Removal of Rhodamine B Dye Using Activated Carbon Prepared from Palm Kernel Shell and Coated with Iron Oxide Nanoparticles. Separation Science and Technology, 47(5), 742-752.

Pesendorfer, S.,Ellersdorfer, M. (2021) Kinetics of Simultaneous Ammonium and Phosphate Recovery by Natural Zeolite. ChemEngineering, 5(4), 68.

Pham, T.-H., Lee, B.-K.,Kim, J. (2016) Improved adsorption properties of a nano zeolite adsorbent toward toxic nitrophenols. Process Safety and Environmental Protection, 104, 314-322.

Pierrou, U. (1976) The Global Phosphorus Cycle. Ecological Bulletins, (22), 75-88.

Pourhakkak, P., Taghizadeh, A., Taghizadeh, M., Ghaedi, M.,Haghdoust, S. (2021) Interface Science and Technology. Ghaedi, M. (ed), pp. 1-70, Elsevier.

Qi, J., Deng, L., Song, Y., Qi, W.,Hu, C. (2022) Nutrient Thresholds Required to Control Eutrophication: Does It Work for Natural Alkaline Lakes? Water, 14(17), 2674.

Rane, A.V., Kanny, K., Abitha, V.K.,Thomas, S. (2018) Synthesis of Inorganic Nanomaterials. Mohan Bhagyaraj, S., Oluwafemi, O.S., Kalarikkal, N. and Thomas, S. (eds), pp. 121-139, Woodhead Publishing.

Ren, Z., Jia, B., Zhang, G., Fu, X., Wang, Z., Wang, P.,Lv, L. (2021) Study on adsorption of ammonia nitrogen by iron-loaded activated carbon from low temperature wastewater. Chemosphere, 262, 127895.

Rodrigues, S.C., Silva, M.C., Torres, J.A.,Bianchi, M.L. (2020) Use of Magnetic Activated Carbon in a Solid Phase Extraction Procedure for Analysis of 2,4-dichlorophenol in Water Samples. Water, Air, & Soil Pollution, 231(6).

Rotta, E.H., Bitencourt, C.S., Marder, L.,Bernardes, A.M. (2019) Phosphorus recovery from low phosphate-containing solution by electrodialysis. Journal of Membrane Science, 573, 293-300.

Ruoff, R.S.,Lorents, D.C. (1996) Carbon Nanotubes. Endo, M., Iijima, S. and Dresselhaus, M.S. (eds), pp. 143-148, Pergamon, Oxford.

Ryu, H.-D., Lim, D.Y., Kim, S.-J., Baek, U.-I., Chung, E.G., Kim, K.,Lee, J.K. (2020) Struvite Precipitation for Sustainable Recovery of Nitrogen and Phosphorus from Anaerobic Digestion Effluents of Swine Manure. Sustainability, 12(20), 8574.

Saharan, P., Chaudhary, G.R., Mehta, S.K.,Umar, A. (2014) Removal of water contaminants by iron oxide nanomaterials. J Nanosci Nanotechnol, 14(1), 627-643.

Salek Gilani, N., Ehsani Tilami, S.,Azizi, S.N. (2022) Adsorption properties of low-cost synthesized nanozeolite L for efficient removal of toxic methylene blue dye from aqueous solution. 2022, 69(2), 8.

Sarkar, A.,Paul, B. (2016) The global menace of arsenic and its conventional remediation - A critical review. Chemosphere, 158, 37-49.

Scheinost, A.C. (2005)Metal Oxides Hillel, D. (ed), pp. 428-438, Elsevier, Oxford.

Schindler, D.W., Carpenter, S.R., Chapra, S.C., Hecky, R.E.,Orihel, D.M. (2016) Reducing Phosphorus to Curb Lake Eutrophication is a Success. Environmental Science & Technology, 50(17), 8923-8929.

Schlesinger, W.H.,Bernhardt, E.S. (2013) Biogeochemistry: an analysis of global change, Academic press.

Shah, I., Adnan, R., Wan Ngah, W.S.,Mohamed, N. (2015) Iron Impregnated Activated Carbon as an Efficient Adsorbent for the Removal of Methylene Blue: Regeneration and Kinetics Studies. Plos One, 10(4), e0122603.

Shahrashoub, M.,Bakhtiari, S. (2021) The efficiency of activated carbon/magnetite nanoparticles composites in copper removal: Industrial waste recovery, green synthesis, characterization, and adsorption-desorption studies. Microporous and Mesoporous Materials, 311, 110692.

Shi, Z.-l., Liu, F.-m.,Yao, S.-h. (2011) Adsorptive removal of phosphate from aqueous solutions using activated carbon loaded with Fe(III) oxide. New Carbon Materials, 26(4), 299-306.

Sidorczuk, D., Kozanecki, M., Civalleri, B., Pernal, K.,Prywer, J. (2020) Structural and Optical Properties of Struvite. Elucidating Structure of Infrared Spectrum in High Frequency Range. The Journal of Physical Chemistry A, 124(42), 8668-8678.

Smith, V.H., Tilman, G.D.,Nekola, J.C. (1999) Eutrophication: impacts of excess nutrient inputs on freshwater, marine, and terrestrial ecosystems. Environmental Pollution, 100(1), 179-196.

Stratful, I., Scrimshaw, M.D.,Lester, J.N. (2001) Conditions influencing the precipitation of magnesium ammonium phosphate. Water Res, 35(17), 4191-4199.

Sun, S., Ji, G., Lv, Y., Liu, H., Hu, T., Chen, Z.,Xu, S. (2021) Simultaneous recovery of ammonium and total phosphorus from toilet tail water by modified palygorskite-bentonite clay. Water Environ Res, 93(7), 1077-1086.

Suresh Kumar, P., Korving, L., Keesman, K.J., van Loosdrecht, M.C.M.,Witkamp, G.-J. (2019) Effect of pore size distribution and particle size of porous metal oxides on phosphate adsorption capacity and kinetics. Chemical Engineering Journal, 358, 160-169.

Suresh Kumar, P., Prot, T., Korving, L., Keesman, K.J., Dugulan, I., van Loosdrecht, M.C.M.,Witkamp, G.-J. (2017) Effect of pore size distribution on iron oxide coated granular activated carbons for phosphate adsorption – Importance of mesopores. Chemical Engineering Journal, 326, 231-239.

Tansel, B., Lunn, G.,Monje, O. (2018) Struvite formation and decomposition characteristics for ammonia and phosphorus recovery: A review of magnesium-ammonia-phosphate interactions. Chemosphere, 194, 504-514.

Tchobanoglous, G., Burton, F.L., Stensel, H.D., Metcalf, Eddy, I.,Burton, F. (2003) Wastewater Engineering: Treatment and Reuse, McGraw-Hill Education.

Tercero, L., Stotz, H., Deubzer, O., Garcia, B.R., Lepe, R.G., Bilewska, K., Osadnik, M., Mazur, J., Ökvist, L.S., Eriksson, J.,Hu, X. (2018)Critical Raw Material Substitution Profiles, p. 84, SCRREEN.

Thant Zin, M.M.,Kim, D.-J. (2021) Simultaneous recovery of phosphorus and nitrogen from sewage sludge ash and food wastewater as struvite by Mg-biochar. Journal of hazardous materials, 403, 123704.

Tian, Y., He, W., Liang, D., Yang, W., Logan, B.E.,Ren, N. (2018) Effective phosphate removal for advanced water treatment using low energy, migration electric–field assisted electrocoagulation. Water Research, 138, 129-136.

Tran, H.N., You, S.-J., Hosseini-Bandegharaei, A.,Chao, H.-P. (2017) Mistakes and inconsistencies regarding adsorption of contaminants from aqueous solutions: A critical review. Water Research, 120, 88-116.

Tsai, W.T., Lai, C.W.,Hsien, K.J. (2003) Effect of particle size of activated clay on the adsorption of paraquat from aqueous solution. J Colloid Interface Sci, 263(1), 29-34.

Turan, N.B., Erkan, H.S., Engin, G.O.,Bilgili, M.S. (2019) Nanoparticles in the aquatic environment: Usage, properties, transformation and toxicity—A review. Process Safety and Environmental Protection, 130, 238-249.

Tünay, O., Kabdasli, I., Orhon, D.,Kolçak, S. (1997) Ammonia removal by magnesium ammonium phosphate precipitation in industrial wastewaters. Water Science and Technology, 36(2-3), 225-228.

Vitousek, P.M.,Howarth, R.W. (1991) Nitrogen limitation on land and in the sea: How can it occur? Biogeochemistry, 13(2), 87-115.

Wang, H.,Shadman, F. (2013) Effect of particle size on the adsorption and desorption properties of oxide nanoparticles. AIChE Journal, 59(5), 1502-1510.

Wang, M., Zheng, Y., Li, Q., Qi, Y., Liao, X.-H.,Fu, Q. (2021) The Efficiency Adsorption of Ammonia Nitrogen, Phosphate and Basic Blue 3 by Fulvic Acid Decorated Fe3O4 Magnetic Nanocomposites. Polish Journal of Environmental Studies, 30(4), 3299–3305.

Wang, Z., Nie, E., Li, J., Yang, M., Zhao, Y., Luo, X.,Zheng, Z. (2012) Equilibrium and kinetics of adsorption of phosphate onto iron-doped activated carbon. Environmental Science and Pollution Research, 19(7), 2908-2917.

Warmadewanthi, I.D.A.A., Zulkarnain, M.A., Ikhlas, N., Kurniawan, S.B.,Abdullah, S.R.S. (2021) Struvite precipitation as pretreatment method of mature landfill leachate. Bioresource Technology Reports, 15, 100792.

Wei, S.P., van Rossum, F., van de Pol, G.J.,Winkler, M.-K.H. (2018) Recovery of phosphorus and nitrogen from human urine by struvite precipitation, air stripping and acid scrubbing: A pilot study. Chemosphere, 212, 1030-1037.

Weiner, R.F.,Matthews, R.A. (2003) Environmental Engineering (Fourth Edition). Weiner, R.F. and Matthews, R.A. (eds), pp. 51-79, Butterworth-Heinemann, Burlington.

Widdison, P.E.,Burt, T.P. (2008) Encyclopedia of Ecology. Jørgensen, S.E. and Fath, B.D. (eds), pp. 2526-2533, Academic Press, Oxford.

Worch, E. (2012) Adsorption Technology in Water Treatment: Fundamentals, Processes, and Modeling, De Gruyter.

Wu, K., Li, Y., Liu, T., Zhang, N., Wang, M., Yang, S., Wang, W.,Jin, P. (2019) Evaluation of the adsorption of ammonium-nitrogen and phosphate on a granular composite adsorbent derived from zeolite. Environmental Science and Pollution Research, 26(17), 17632-17643.

Wu, W., Wu, Z., Yu, T., Jiang, C.,Kim, W.-S. (2015) Recent progress on magnetic iron oxide nanoparticles: synthesis, surface functional strategies and biomedical applications. Science and Technology of Advanced Materials, 16(2), 023501.

Xie, R., Jin, Y., Chen, Y.,Jiang, W. (2017) The importance of surface functional groups in the adsorption of copper onto walnut shell derived activated carbon. Water Science and Technology, 76(11), 3022-3034.

Xu, Q., Li, W., Ma, L., Cao, D., Owens, G.,Chen, Z. (2020) Simultaneous removal of ammonia and phosphate using green synthesized iron oxide nanoparticles dispersed onto zeolite. Science of the Total Environment, 703.

Xu, T. (2005) Ion exchange membranes: State of their development and perspective. Journal of Membrane Science, 263(1), 1-29.

Yang, N., Zhu, S., Zhang, D.,Xu, S. (2008) Synthesis and properties of magnetic Fe3O4-activated carbon nanocomposite particles for dye removal. Materials Letters, 62(4), 645-647.

Yang, X., Duke, M., Zhang, J.,Li, J.-D. (2019a) Modeling of heat and mass transfer in vacuum membrane distillation for ammonia separation. Separation and Purification Technology, 224, 121-131.

Yang, X., Wan, Y., Zheng, Y., He, F., Yu, Z., Huang, J., Wang, H., Ok, Y.S., Jiang, Y.,Gao, B. (2019b) Surface functional groups of carbon-based adsorbents and their roles in the removal of heavy metals from aqueous solutions: A critical review. Chemical Engineering Journal, 366, 608-621.

Yarlagadda, S., Gude, V.G., Camacho, L.M., Pinappu, S.,Deng, S. (2011) Potable water recovery from As, U, and F contaminated ground waters by direct contact membrane distillation process. J Hazard Mater, 192(3), 1388-1394.

Yegane Badi, M., Azari, A., Pasalari, H., Esrafili, A.,Farzadkia, M. (2018) Modification of activated carbon with magnetic Fe3O4 nanoparticle composite for removal of ceftriaxone from aquatic solutions. Journal of Molecular Liquids, 261, 146-154.

Zach-Maor, A., Semiat, R.,Shemer, H. (2011) Synthesis, performance, and modeling of immobilized nano-sized magnetite layer for phosphate removal. Journal of colloid and interface science, 357, 440-446.

Zamparas, M., Kyriakopoulos, G.L., Drosos, M.,Kapsalis, V.C. (2021) Phosphate and Ammonium Removal from Wastewaters Using Natural-Based Innovative Bentonites Impacting on Resource Recovery and Circular Economy. Molecules, 26(21), 6684.

Zare, K., Sadegh, H., Shahryari-ghoshekandi, R., Asif, M., Tyagi, I., Agarwal, S.,Gupta, V.K. (2016) Equilibrium and kinetic study of ammonium ion adsorption by Fe3O4 nanoparticles from aqueous solutions. Journal of Molecular Liquids, 213, 345-350.

Zhang, L.-J., Zhang, X., Liang, H.-F., Xie, Y.,Tao, H.-C. (2018) Ammonium removal by a novel magnetically modified excess sludge. Clean Technologies and Environmental Policy, 20(10), 2181-2189.

Zhang, Y., Desmidt, E., Van Looveren, A., Pinoy, L., Meesschaert, B.,Van der Bruggen, B. (2013) Phosphate Separation and Recovery from Wastewater by Novel Electrodialysis. Environmental Science & Technology, 47(11), 5888-5895.

Zhou, Q., Wang, X., Liu, J.,Zhang, L. (2012) Phosphorus removal from wastewater using nano-particulates of hydrated ferric oxide doped activated carbon fiber prepared by Sol–Gel method. Chemical Engineering Journal, 200-202, 619-626.

CURRICULUM VITAE

Name Surname : Büşra KARA

Education:

Degree	Department/Program	University/High School	Year
High School	Science	Oğuz Canpolat Highschool	2008-2012
Undergraduate	Environmental Engineering	Çanakkale Onsekiz Mart University	2012-2017
Postgraduate	Environmental Engineering (Special Student)	Yıldız Technical University	2018
Postgraduate	Environmental Engineering	Marmara University	2019 -

International Conference Publications:

Kara, B., Gulyás, A., Semerci, N., Genç, S., and Can, S, Z. Recovery of Crucial Nutrient Ions Through Engineered Magnetic Nanoparticles. 4th IWA Resource and Recovery Conference, 5 – 8 September 2021, online. (Oral Presentation)

Kara, B., Semerci, N., Genç, S., and Can, S, Z. Ammonium and Phosphate Removal Using Magnetic Nanoparticles. 12th Eastern European Young Water Professionals Conference, 31 March – 2 April 2021, online. (Oral Presentation)

Kara, B., Semerci, N., Genç, S., and Can, S, Z. Adsorption of Ammonium and Phosphate Ions: Comparing the Adsorption Performances of the Bare & Composite Magnetite Nanoparticles. 5th EurAsia Waste Management Symposium, 26 – 28 October 2020, online. (Oral Presentation)

Project Assignment:

TÜBİTAK - ARDEB, Project No: 118Y532, October 2019 – October 2020.